

# UC Irvine

## UC Irvine Electronic Theses and Dissertations

### Title

Mitigating Seawater Desalination Membrane Biofouling using Quorum Sensing Inhibitors

### Permalink

<https://escholarship.org/uc/item/97w156dq>

### Author

Katebian, Leda

### Publication Date

2016

Peer reviewed|Thesis/dissertation

UNIVERSITY OF CALIFORNIA,  
IRVINE

Mitigating Seawater Desalination Membrane Biofouling using Quorum Sensing Inhibitors

DISSERTATION

Submitted in partial satisfaction of the requirements  
for the degree of

DOCTOR OF PHILOSOPHY

in Engineering

by

Leda Katebian

Dissertation Committee:  
Professor Sunny Jiang, Chair  
Associate Professor Diego Rosso  
Assistant Professor Kristen Davis

2016



## TABLE OF CONTENTS

ACKNOWLEDGMENTS .....	iv
LIST OF TABLES.....	v
LIST OF FIGURES.....	vi
CURRICULUM VITAE.....	ix
ABSTRACT OF DISSERTATION.....	xiv
CHAPTER 1. INTRODUCTION.....	1
1.1. Background .....	1
1.2. Research Motivation.....	2
1.3. Hypothesis & Objectives .....	3
CHAPTER 2. LITERATURE REVIEW .....	4
2.1. The Demand for Alternative Water Treatment Processes.....	4
2.2. Current State of RO Membrane Technology.....	5
2.3. Membrane Fouling with Specific Emphasis on Organic Fouling/Biofouling .....	8
2.4. Membrane Properties Affecting the Fouling Rate .....	10
2.5. Antifouling effort with Membrane Materials.....	11
2.5.1 . Biomimetic membrane.....	11
2.5.2 Quorum Sensing and Quorum Sensing Inhibition in Biofilm .....	13
2.5.2.1. Quorum Sensing Pathways .....	13
2.5.2.2. Auto-inducer type 1 signaling system.....	14
2.5.2.3. Auto-inducer type 2 signaling system.....	16
2.5.2.4. Interfering with QS Signals .....	18
CHAPTER 3. INHIBITING QS PATHWAYS TO MITIGATE SEAWATER DESALINATION RO MEMBRANE BIOFOULING .....	20

3.1. Introduction.....	21
3.2. Materials & Methods .....	24
3.2.1. Bacterial Strains and Seawater Bacterial Community .....	24
3.2.2. Quorum Sensing Inhibitors .....	24
3.2.3. Identification of Bacterial AI-1 QS Molecule Production.....	25
3.2.4. Effect of QSI on Biofilm Production.....	26
3.2.5. RO Membrane Biofilm Reduction .....	28
3.2.6. Biofilm Quantification by Confocal Laser Scanning Microscopy (CLSM).....	29
3.3. Results.....	30
3.2.1. Bacterial AHL Production.....	30
3.2.2. Effect of QSI on Biofilm Growth .....	31
3.2.3. QSI Effect on RO Membrane Biofilm Reduction .....	35
3.4. Discussion.....	37
3.5. Conclusions.....	40
 CHAPTER 4. QSI MODIFIED RO MEMBRANES FOR BIOFOULING PREVENTION IN SEAWATER DESALINATION .....	
41	
4.1. Introduction.....	42
4.2. Methods.....	44
4.2.1. QSI Compounds .....	44
4.2.2. QSI Modified RO Membranes.....	44
4.2.3. QSI Presence on RO membranes Detected by Raman Microscopy .....	44
4.2.4. Membrane Performance and Surface Property Characterization .....	45
4.2.5. QSI-RO Membrane Anti-Biofouling Capability .....	46
4.2.6. Membrane Biofilm Characterization .....	47
4.3. Result.....	48
4.3.1. QSI Deposited RO Membranes and Stability.....	48
4.3.2. QSI-RO Membrane Performance and Surface Property.....	51

4.3.3. QSI-RO Membrane Biofilm Formation.....	52
4.4. Discussion.....	55
4.5. Conclusions.....	57
CHAPTER 5. SUMMARY, CONCLUSIONS & RECOMMENDATIONS .....	58
CHAPTER 6. REFERENCES.....	60
APPENDIX A. SUPPORTING STUDY: SUPPRESSING RO AND FO MEMBRANE BIOFOULING WITH QUORUM SENSING INHIBITORS .....	72
APPENDIX B. SUPPORTING STUDY: THE EFFECTIVENESS OF PHYSICALLY ATTACHED QUORUM SENSING INHIBITORS TO RO AND FO MEMBRANES TO REDUCE BIOFOULING .....	77

## ACKNOWLEDGMENTS

First and foremost, I would like to express my sincerest gratitude towards my committee chair, Dr. Sunny Jiang whose guidance has not only been influential in the completion of my dissertation, but my development as a researcher. Dr. Jiang encourages her students to strive for excellence in both research and academics by creating a work environment devoted to learning, creativity, and self-improvement.

I am also grateful towards my dissertation and candidacy committee members, Dr. Diego Rosso, Dr. Kristen Davis, Dr. Bill Cooper, and Dr. Hung Nguyen for providing their support and direction throughout my research and academic career. Their expertise has strengthened my understanding of environmental and chemical engineering concepts and improved the quality of my research.

The microscopy and chromatography/spectrometry analysis would not have been possible without guidance from the following directors, Dr. Adeela Syed, Dr. Dmitry Fishman, Dr. John Greaves, and Dr. Beniam Berhane at UC Irvine's Optical Biology Core, Laser Spectroscopy, and Mass Spectrometry Facilities. I owe Dr. Szu-Wen Wang's lab, Dr. Alon Gorodetsky's lab, and Dr. Albert Yee's lab at UC Irvine my gratitude for permitting me to use their laboratory instruments to complete a portion of this work. I would like to express my gratitude towards Dr. Goen Ho's lab at Murdoch University in Western Australia and Dr. Michael Hoffmann's lab at California Institute of Technology for graciously allowing me to conduct experimental studies in their groups as well.

I am truly grateful to my fellow students at UC Irvine, in particular the Jiang lab, Rosso lab, Cooper lab, and Olson lab. Through their accomplishments and attitude, these students inspired and motivated me to become a better researcher. They helped me improve my work by sharing their knowledge and research experiences and provided valuable feedback on the direction of my research. I owe my greatest appreciation towards my family, boyfriend, and friends whose continued support and encouragement provided me with the incentive to complete this dissertation.

Lastly, this work would not have been possible without the generous fellowships from UC Irvine (School of Henry Samueli's Academic Year 2014-2015 Fellowship and Graduate Research Fellowships), AWWA in partnership with CDM Smith (2014 Thomas R. Camp Scholarship), and AMTA (2014 Affordable Desalination Collaboration Fellowship) who provided me with support to conduct these experimental studies. A portion of this research was supported under the National Centre of Excellence in Desalination in Australia (Grant No. D-1-K00016) and the Dow Resnick Bridge Program between Dow Chemical and California Institute of Technology as well.

## LIST OF TABLES

<b>Table 2.1.</b> AHL Signaling System for Biofilm Regulation in Wastewater Bacterial Isolates ....	15
<b>Table 2.2.</b> AHL Signaling System for Biofilm Regulation in Marine Bacterial Isolates .....	16
<b>Table 2.3.</b> AI-2 Signaling System in Marine and Wastewater Bacterial Isolates .....	17



## LIST OF FIGURES

Figure 2.1. In reverse osmosis, the applied pressure to the concentrated feed water side (i.e. seawater) overcomes the natural osmotic pressure gradient to drive the flow of water through the semi-permeable RO membrane.....	5
Figure 2.2. RO spiral wound module.....	6
Figure 2.3. Cross-section of the thin film composite polyamide RO membrane.....	7
Figure 2.4. Scaling caused by crystalline barium sulfate on a RO membrane surface [3].....	8
Figure 2.5. Stages of biofilm formation [1].....	9
Figure 2.6. Water transport in a cell membrane with a selective protein (i.e. aquaporin).....	11
Figure 2.7. The steps occurring in the AI-1 (purple) and AI-2 (green) QS pathways responsible for $G^-$ and $G^+$ and $G^-$ bacterial communication, respectively. These pathways are branched off of the activated methyl cycle (blue), which synthesizes amino acids.....	14
Figure 2.8. Chemical structure of the AHL molecule in the AI-1 QS pathway.....	15
Figure 2.9. Chemical structure of the family of AI-2 QS molecules including S-THMF-borate, the furanosyl borate diester (A), MHF (B), and R-THMF (C)[2].....	17
Figure 3.1. RO membrane bio-monitoring schematic.....	28
Figure 3.2. UPLC-MS/MS Chromatograms of C4-HSL standard (A), and extracts from single species bacterial cultures, B1 (B) and B2 (C), B3 (D), B4 (E) and mixed culture of B1, B2, B3, and B4 (F). The shaded peak indicated the quantity of C4-HSL. ....	30
Figure 3.3. Normalized biofilm growth in samples treated with the AI-1 inhibitors, VA (A, B) and KJ (C, D) shown as the ratio of the QSI treated to control biofilm growth at different QSI concentrations. Single species marine bacterial biofilm (A, C) comprised of isolates from Carlsbad Desalination Plant, CA (B1, B2, B3, and B4) and Perth Desalination Plant, Western Australia (RO16, RO28, RO32, and C10). Mixed species biofilm (B, D) used the mixture of bacterial isolates from Carlsbad, CA or uncultured native seawater marine bacterial communities from Long Beach, Newport Beach, and Dana Point, CA.....	31
Figure 3.4. Normalized biofilm growth in samples treated with the AI-1/AI-2 inhibitors, F-30 (A, B) and CNMA (C, D) shown as the ratio of the QSI treated to control biofilm growth at different QSI concentrations. Single species marine bacterial biofilm (A, C) comprised of isolates from desalination plants in Carlsbad, CA (B1, B2, B3, and B4) and Perth, Western Australia (RO16, RO28, RO32, and C10). Mixed species biofilm (B, D) used the mixture of bacterial isolates from Carlsbad, CA or uncultured native seawater marine bacterial communities from Long Beach, Newport Beach, and Dana Point, CA.....	33
Figure 3.5. RO membrane biofilm formed from four mixed species bacterial isolates from Carlsbad, CA (B1, B2, B3 and B4). Samples were subjected to VA (top), CNMA (bottom), and their respective controls (methanol and DI water). The effectiveness of VA and CNMA to reduce marine biofilm were evaluated by comparing average biofilm thickness (A) and biomass (B) in EPS, dead cells and live cells for QSI treated samples and controls.....	34
Figure 3.6. RO membrane biofilm formed by native marine bacterial community from Dana Point, CA. Samples were treated by VA (top), CNMA, (bottom), and their respective controls (methanol and DI water). The effectiveness of CNMA and VA to reduce marine biofilm were evaluated by comparing average biofilm thickness (A) and biomass (B) in EPS, dead cells and live cells for QSI treated samples and controls.....	35
Figure 3.7. CSLM 3-D images of control (A, C) and VA treated (B, D) RO membranes that were subjected to biofouling by Dana Point natural bacterial community. Images were captured 48 hours after the initiation of the experiment. Attached live and dead bacterial cells on the control and the VA treated RO membrane are shown in image (A) and (B), respectively. EPS on the control and the VA treated RO membrane is shown in image (C) and (D), respectively. The x-axis and y-axis of the image shows EPS or live and dead cells along the membrane surface. The z-axis measures the fluorescence intensity of EPS or live and dead cells.....	36

Figure 4.1. Set-up for QSI deposition onto the thin film surface of the RO membrane.....	44
Figure 4.2. High pressure RO system schematic.....	45
Figure 4.3. Characterization of CNMA deposited Dow SW30XLE (A,B) and Hydranautics SWC5 (C,D) RO membranes. CNMA peaks associated with the CNMA RO membrane were revealed based on the Raman spectra for the CNMA modified and unmodified membranes and CNMA in its natural state as a liquid (A,C). The time period for the maximum amount of CNMA incorporated onto the membrane surface was determined based on the QSI peak areas (1000, 1253, 1627, and 1677 $\text{cm}^{-1}$ ) at 24, 48, and 72 h (B,D).....	49
Figure 4.4. Surface characterization for VA deposited Dow SW30XLE and Hydranautics SWC5 RO membrane. VA peaks were identified based on the Raman spectra for the VA modified and unmodified membranes and VA in its natural state (A,C). The time at which the maximum amount of VA was deposited onto the membrane was based on the QSI peak areas (1628 and 1677 $\text{cm}^{-1}$ ) at 24, 48, and 72 h (B,D). ....	50
Figure 4.5. QSI modified RO membrane performance. Normalized pure water permeate flux (A) and salt rejection rates (B) were calculated by the ratio of QSI RO membrane to unmodified membrane performance.....	51
Figure 4.6. Contact angle measurements for the unmodified SWC5 (Hydranautics) and SW30XLE (Dow) membranes as well as the CNMA and VA deposited SWC5 and SW30XLE membranes.....	51
Figure 4.7. Permeate flux over the biofouling period for QSI (CNMA and VA) modified and unmodified RO membranes, SWC5 (A) and SW30XLE (B).....	52
Figure 4.8. Biofilm formation on CNMA and VA modified and unmodified RO membranes (Hydranautics SWC5 and Dow SW30XLE) formed by a mixed culture of <i>Alteromonas sp.</i> and <i>Shewanella sp.</i> bacterial isolates. The effectiveness of QSI deposited RO membranes to reduce membrane biofilm formation was evaluated by comparing EPS, live and dead cell biomass (A) and thickness (B) with unmodified membranes.....	53
Figure 4.9. Raman spectra of the maximum CNMA deposited and biofouled SW30XLE (A) and SWC5 (B) membranes along with the VASW30XLE (C) and SWC5 (D) membranes before and after the biofouling event, respectively. QSI retention on the membrane surface was based on the QSI peak areas for CNMA (1000, 1253, 1627, and 1677 $\text{cm}^{-1}$ ) and VA (1628 and 1677 $\text{cm}^{-1}$ ) before and after the biofouling event. Biofouled QSI RO membranes showed minimal QSI peak formation, which could not be quantified.....	54
Figure A.1. Bench scale RO membrane system schematic.....	72
Figure A.2. The normalized flux for control and vanillin treated RO membrane biofouling systems. The normalized permeate flux was calculated as the flux over the initial flux.....	74
Figure A.3. Comparison of membrane biofilm without (A) and with vanillin treatment (B) in high pressure RO system for the lead membrane section. The 3D image is composed of multiple layers of biofilm, which are approximately 1000 $\mu\text{m}$ in height. ImageJ automatically determines the dimensions of the y- and x-axis. The y-axis represents the bottom to top layer of the biofilm and the x-axis refers to bottom biofilm layer along the horizontal center of the membrane surface. The z-axis measures the florescence intensity of the live and dead cells.....	72
Figure A.4. Normalized flux for vanillin treated and control FO membrane system. The normalized permeate flux was measured by the flux over the starting permeate flux.....	75
Figure B.1. Bench scale RO membrane system.....	77
Figure B.2. Normalized permeate flux for RO membranes with the following conditions: control, vanillin attached, and vanillin attached without bacteria present in the feed reservoir. Normalized permeate flux was calculated as the permeate flux over the initial flux.....	79
Figure B.3. 3D Comparison of single species biofilm formation on the surface of the RO membrane (A) and physically attached vanillin RO membrane (B). The 3D image is composed of multiple layers of biofilm, which are approximately 1000 $\mu\text{m}$ in height. ImageJ automatically determines the dimensions of the y- and x-axis. The y-axis represents the bottom to top layer of the biofilm and the x-axis refers to	

bottom biofilm layer along the horizontal center of the membrane surface. The z-axis measures the florescence intensity of the live and dead cells.....80

Figure B.4. Normalized flux for control and vanillin attached FO membranes. Normalized flux was measured as the permeate flux over the initial flux.....81

Figure B.5. 3D Comparison of biofilm formation on the lead FO membrane (A) and physically attached vanillin FO membrane biofilm (B). The 3D image is composed of multiple layers of biofilm, which are approximately 1000  $\mu\text{m}$  in height. ImageJ automatically determines the dimensions of the y- and x-axis. The y-axis represents the bottom to top layer of the biofilm and the x-axis refers to bottom biofilm layer along the horizontal center of the membrane surface. The z-axis measures the florescence intensity of the live and dead cells.....82

# CURRICULUM VITAE

**Leda Katebian**

---

## **Education**

---

### **University of California Irvine (UC Irvine)**

Doctor of Philosophy January 2016  
Major: Engineering  
Concentration: Environmental Engineering  
Defense Exam: January 2016  
Defense Topic: Mitigating Seawater Desalination Membrane Biofouling using Quorum Sensing Inhibitors  
Committee Chair: Dr. Sunny Jiang, Civil & Environmental Engineering Department  
Committee Members: Dr. Diego Rosso, Civil & Environmental Engineering Department  
Dr. Kristen Davis, Civil & Environmental Engineering Department  
Qualifying Exam: December 2013  
Qualifying Topic: Mitigating Seawater Desalination Membrane Biofouling using Quorum Sensing Inhibitors  
Committee Chair: Dr. Sunny Jiang, Civil & Environmental Engineering Department  
Committee Members: Dr. Diego Rosso, Civil & Environmental Engineering Department  
Dr. Kristen Davis, Civil & Environmental Engineering Department  
Dr. William Cooper, Civil & Environmental Engineering Department  
Dr. Hung Nguyen, Chemical Engineering Department  
Preliminary Exam: May 2012  
Committee Members: Dr. Sunny Jiang, Civil & Environmental Engineering Department  
Dr. Diego Rosso, Civil & Environmental Engineering Department  
Dr. Soroosh Sorooshian, Civil & Environmental Engineering Department

### **University of California Irvine**

Master of Science March 2012  
Major: Engineering  
Concentration: Environmental Engineering  
Thesis Topic: Marine Biofilm Formation and Its Responses to Periodic Hyperosmotic Shock on a Flat Sheet Membrane Surface  
Committee Chair: Dr. Sunny Jiang, Civil & Environmental Engineering Department  
Committee Members: Dr. William Cooper, Civil & Environmental Engineering Department  
Dr. Diego Rosso, Civil & Environmental Engineering Department

### **University of California Irvine**

Bachelor of Science June 2010  
Major: Chemical Engineering  
Specialization: Environmental Engineering  
Research Topic: Marine Biofilm Inhibition using Hyperosmotic Shock  
Research Advisor: Dr. Sunny Jiang, Civil & Environmental Engineering Department

## Certification

Engineering-In-Training (EIT/FE), certification number 145361

April 2012

## Research Experience

### Researcher

Feb. 2015-Jan. 2016

#### Geology and Planetary Sciences, California Institute of Technology

- Incorporated quorum sensing (QS) inhibitors, vanillin and cinnamaldehyde onto RO membrane surfaces using a chemical deposition approach in order to improve the membrane anti-biofouling potential for seawater desalination.
- This work was supported under the Dow Resnick Bridge Program.

### Laboratory Safety Representative,

Sept. 2014-Dec. 2015

#### Civil & Environmental Engineering, UC Irvine

- Worked with Environmental Health and Safety to ensure Dr. Sunny Jiang's lab was in compliance with safety regulations ranging from to hazardous chemicals and earthquake preparedness.
- Responsible for going over standard operating procedures for incoming lab members.

### 2012 Sustainability Science Team, Environmental Institute, UC Irvine

Sept. 2012-2014

- Worked in a multidisciplinary team of five doctoral students to study the Salton Sea's water quality and hydrological cycle. Investigation included determining which desalination technology will be able to restore and sustain salinity levels as well as examining the sustained profitability of desalination. Lastly, the project anticipated the potential coalitions and incentives to help gain political and financial support to assist Salton Sea's stakeholders.
- *Specific Role:* Determined multi-effect distillation with thermal vapor compression was the best desalination method to restore the Salton Sea salinity level.

### EPA People, Prosperity, Planet (P3) Grant

Aug. 2011-May 2012

#### Microbial Desalination Fuel Cell as a Sustainable Technology for Renewable Water and Power (SU836030), Co-Investigator, UC Irvine

- Worked in an interdisciplinary team to develop a microbial desalination fuel cell (MDFC) as a pre-treatment to the RO system for seawater desalination.
- *Specific Role:* Supervised undergraduate students for the scalability analysis of MDFC for seawater desalination plants using MATLAB software.
- Website: <http://jianglab.eng.uci.edu/epap3/>

### Researcher Assistant, Civil & Environmental Engineering, UC Irvine

Sept. 2008- Jan. 2016

- *Ph.D. Research:* Characterized the role of QS in marine biofilm production and the effect of QS inhibitors on membrane biofouling for seawater desalination.
  - Carried out high-pressure RO and FO membrane experimental studies in Murdoch University in Western Australia in March and August 2013.
  - Supervised a chemical engineering undergraduate student to investigate biofilm response to QS inhibitors using a crystal violet microtiter plate assay.
- *B.S./M.S. Research:* Characterized biofilm development on a flat sheet membrane by developing a bench-scale biofilm detector system operated in a dead-end filtration mode. Demonstrated periodic hyperosmotic shocks were an effective strategy to reduce biofouling.

## **Industry Experience**

---

### **Engineering Intern, GHD, Irvine CA**

December 2013-May 2014

- Assisted in monitoring a pretreatment pilot operation for Carlsbad Desalination plant including a two-week algal simulation run.
- Sampled various locations of the pilot to analyze water quality of feed water, pre-treated water, and RO permeate stream.

### **Engineering Assistant**

March 2007-Sep. 2009

### **TechCom International Corporation, Irvine, CA**

- Provided assistance in performing Instrumentation & Controls loop uncertainty analysis for nuclear power generation industry.

## **Academic Experience**

---

### **CEE 160 Guest Lecturer, Civil & Environmental Engineering, UC Irvine**

May 22, 2015

- Lectured on RO membrane technology and membrane desalination unit process.

### **CEE 169 Teaching Assistant, Civil & Environmental Engineering, UC Irvine**

Fall 2014

- Lead laboratory sections for Environmental Microbiology for Engineers.
- Course description: Fundamental and applied principles of microbiology. Structures and functions of microorganisms, the microbiology of water, wastewater and soil used in environmental engineering, and the impact of microorganisms on human and environmental health.

### **CEE 160 Teaching Assistant, Civil & Environmental Engineering, UC Irvine**

Spring 2014

- Lead discussion sections for Introduction to Environmental Engineering.
- Lectured on desalination technologies and membrane desalination unit processes.
- Course description: Introduction to environmental processes in air and water, mass balances, and transport phenomena. Fundamentals of water quality engineering including water and wastewater treatment.

### **CEE 160 Reader, Civil & Environmental Engineering, UC Irvine**

Spring 2013

- Graded exams and a design project for Introduction to Environmental Engineering.
- The course description is same as the above for CEE 160.

### **CEE 167 Reader, Civil & Environmental Engineering, UC Irvine**

Winter 2013

- Graded exams and lab reports and assisted in applying i-clicker technology for Coastal Ecology.
- Course description: Examines the ecological processes of the coastal environment. Investigates the causes of coastal ecosystem degradation and strategies to restore the ecosystem balance or prevent further coastal ecosystem health degradation.

### **Graduate Student Representative**

Sep. 2011-March 2012

### **Civil and Environmental Engineering, UC Irvine**

- Created and distributed market surveys at professional conferences and to engineering firms to assess the demand for an online M.S. Environmental Engineering program at UC Irvine.

**CEE 160 Teaching Assistant, Civil & Environmental Engineering, UC Irvine** Spring 2011

- Lead discussion sections for Introduction to Environmental Engineering.
- The course description is the same as above for CEE 160.

---

**Skills**

---

- |                    |   |
|--------------------|---|
| • C++              | • Scanning Electron Microscopy            |
| • MATLAB           | • Confocal Laser Scanning Microscopy      |
| • Pro II           | • Liquid Chromatography-Mass Spectrometry |
| • EES              | • Raman Microscopy                        |
| • Microsoft Office | • Goniometer                              |

---

**Awards/Fellowships**

---

School of Henry Samueli's Academic Year Fellowship, UC Irvine	Academic Year 2014- 2015
2014 Affordable Desalination Collaboration (ADC) Fellowship, AMTA	Summer 2014
2014 Thomas R. Camp Scholarship, AWWA & CDM Smith	Summer 2014
Summer Graduate Research Fellowship, Civil & Environmental Engineering, UC Irvine	Summer 2014; 2013; 2012; 2011
Winter Graduate Research Fellowship, Civil & Environmental Engineering, UC Irvine	Winter 2011
Undergraduate Research Opportunities Program Grant/Fellowship (UROP), UC Irvine	Fall 2009- Spring 2010
Summer Undergraduate Research Program Grant/Fellowship, UC Irvine	Summer 2009
UROP Grant/Fellowship, UC Irvine	Fall 2008- Spring 2009

---

**Publications**

---

L. Katebian, S.C. Jiang, Marine bacterial biofilm formation and its responses to periodic hyperosmotic stress on a flat sheet membrane for seawater desalination pretreatment, *J. Mem. Sci.* 425-426 (2013) 182–189.

L. Katebian, E. Gomez, L. Skillman, D. Lim G. Ho, S.C. Jiang, Inhibiting Quorum Sensing Pathways to Mitigate RO Membrane Biofouling for Seawater Desalination, *Desalination*. (*Accepted*)

---

**Conference Publication**

---

L. Katebian, E. Gomez, L. Skillman, D. Lim G. Ho, S.C. Jiang, Mitigating Seawater Desalination RO Membrane using Quorum Sensing Inhibitors, AMTA-AWWA Membrane Technology Conference, Orlando, Florida, March 2015.

---

**Presentations**

---

Oral Presentations L. Katebian, S.C. Jiang, Mitigating Seawater Desalination RO Membrane Biofouling using Quorum Sensing Inhibitors, AMTA-AWWA Membrane Technology Conference, Orlando, Florida, March 2015

L. Katebian, S.C. Jiang, Quorum Sensing Inhibitors to Prevent Seawater Desalination Membrane Biofouling, Water Reuse and Desalination Conference, Las Vegas, Nevada, May 2014

L. Katebian, S.C. Jiang, Seawater Desalination Membrane Biofouling Presentations Prevention using Quorum Sensing Inhibitors, Graduate Student Symposium, UC Irvine, Nov. 2013

L. Katebian, S.C. Jiang, Inhibiting Membrane Fouling using Quorum Quenchers for Seawater Desalination, Graduate Student Symposium, UC Irvine, Dec. 2012

L. Katebian, S.C. Jiang, Preventing Membrane Fouling, Graduate Student Symposium, UC Irvine, Dec. 2011

L. Katebian, S.C. Jiang, Preventing Membrane Fouling by Osmosis Stress, IWA on Natural Organic Matter, Costa Mesa, CA, July 2011

Expo L. Tseng, J.C. Gellers, L. Jiang, M. Jeung, L. Katebian, K. Lim, H. Wang, E. Glenn, S. Huang, X. Huang, A. Karman; T. Tu; Y. Wu, S.C. Jiang, Microbial Desalination Fuel Cell as a Sustainable Technology for Renewable Water and Power, EPA P3 Expo, Washington, DC, April 2012

Poster Presentations L. Katebian, S.C. Jiang, The Effectiveness of Osmosis Stress on the Removal of Biofilm, American Society for Microbiology, San Diego, CA, May 2010

L. Katebian, S.C. Jiang, Effectiveness of Osmotic Shock on Marine Biofilm removal, UROP Symposium, UC Irvine, May 2010

L. Katebian, S.C. Jiang, Marine Biofilm Removal using Osmosis Stress, Symposium, UC Irvine, May 2009

### **Professional Societies & Organizations**

---

American Water Works

Academy of Environmental Engineering Scientists & Professors

American Membrane Technology Association

International Desalination Association



## **ABSTRACT OF DISSERTATION**

Mitigating Seawater Desalination Membrane Biofouling Using Quorum Sensing Inhibitors

By

Leda Katebian

Doctor of Philosophy in Engineering

University of California, Irvine 2016

Professor Sunny Jiang, Chair

Coastal seawater desalination using reverse osmosis (RO) membranes has the potential to alleviate water stress in arid regions. However, membrane biofouling, caused by bacterial biofilm formation, is a significant challenge for seawater desalination plants. Biofilm formation is regulated by quorum sensing (QS) pathways where bacteria secrete auto-inducer molecules to communicate with neighboring bacteria to activate biofilm formation. This research investigated the role of the QS system and the effect of QS inhibiting (QSI) compounds on marine biofilm production and membrane biofouling. This study revealed that four different marine bacteria isolated from fouled RO membranes in a desalination plant produced two low molecular weight auto-inducer 1 (AI-1) QS molecules. Vanillin and cinnamaldehyde were then identified as the most effective QSI compounds with reduction of marine biofilm formed by RO membrane biofouling isolates and native uncultured seawater bacterial communities by more than 79% and 70%, respectively in a microtiter plate assay. Further investigation into the anti-biofouling capabilities of vanillin and cinnamaldehyde in a cross-flow membrane bio-monitoring system indicated that vanillin in the bulk fluid (1200 mg/L) significantly reduced extracellular polysaccharides (>40%) and dead cells (>20%) on the RO membrane surface. In order to

improve the membrane in-situ anti-biofouling potential, vanillin and cinnamaldehyde were physically adsorbed onto various RO membrane surfaces. The addition of the QSI layer on the RO membrane surface significantly altered the membrane surface contact angle along with a less than 16% reduction in pure water permeability, but there was no significant change in salt rejection compared to unmodified membranes. Under biofouling conditions consisting of four mixed marine bacterial species in a high pressure RO system, QSI modified membranes experienced a minimal loss in permeate flux compared to unmodified membranes. Extracellular polysaccharide production, live cells, and dead cells were significantly suppressed on vanillin and cinnamaldehyde modified membrane surfaces by more than 15%, 58%, and 61%, respectively. These findings indicate that QSIs have the potential to suppress marine biofilm formation and membrane biofouling for seawater desalination.

## CHAPTER 1. INTRODUCTION

### 1.1. Background

Brackish and seawater desalination have been regarded as an effective way to relieve water stress in arid regions by producing drinking water [4]. Desalination using reverse osmosis (RO) technology accounts for approximately 50% of the global desalination capacity due to the recent advancement in thin-film composite membranes [4]. RO desalination will likely continue to expand as a result of increased water shortages stemming from climate change and rapid population growth.

However, desalination plants are plagued by RO membrane biofouling, which lowers water production and raises energy consumption. In the Middle East, it is estimated that approximately 70% of the seawater RO membrane desalination plants endure membrane biofouling [5]. Biofouling is caused by bacterial biofilm, which is a complex matrix of live and dead bacteria and their metabolic products including extracellular polysaccharides (EPS), lipids, and proteins.

Pretreatment processes meant to reduce the biofouling propensity of the feed water to protect the RO unit have not been successful in preventing membrane biofilm because a very small number of bacteria that escape the pretreatment process attach and form biofilm on the membrane surface. Membrane cleaning processes are inefficient to restore membrane performance for long periods of time since degraded organic matter stimulates the growth of surviving bacteria on the membrane surface. Frequent cleanings reduce membrane life span because aggressive chemical cleaning agents degrade the polyamide RO membrane surface.

The focus of biofouling control has more recently moved towards membrane surface modification [6]. Past research has extensively explored incorporating antimicrobial nanomaterials (i.e. silver or titanium oxide (TiO<sub>2</sub>)) onto RO membrane surfaces [6, 7]. However, the long-term retention of nanoparticles on RO membranes needs to be improved as indicated by the loss of antibacterial activity under RO operating conditions [6]. Furthermore, Lee *et al.* [6] demonstrated that antimicrobial nanomaterial incorporation onto RO membranes was not able to uproot natural biofilm formation on the membrane surface.

## **1.2. Research Motivation**

Recent progress in bacteriology has identified the important role of quorum sensing (QS) pathways for bacterial communication, which initiates biofilm development. A recent study reported that 60% of bacterial species contributing to biofilm formation on fouled RO membranes produced QS molecules [8]. During QS, bacteria communicate with each other by synthesizing and secreting signaling molecules that accumulate to a threshold level based on the bacterial population density [9]. After the threshold is reached, the signaling molecule binds to the appropriate transcription regulator and either activates or represses target genes to trigger biofilm development [9].

Inhibition of QS molecules and their communication pathways has gained attention due to the potential for universal control of biofilm production at a cellular level. Recent studies demonstrated that QS inhibiting (QSIs) compounds suppress QS pathways by either degrading the QS signaling molecule, blocking the QS signal production, or blocking QS signal reception [10, 11]. Several studies have applied QSIs to control bacterial biofilm formation [12-21]. For example, acylase I enzyme, a QSI that breaks down a QS molecule, was immobilized onto a nanofiltration membrane and effectively hindered mixed species membrane biofouling in a

submerged membrane bioreactor [20]. In a lab-scale continuous cross-flow nanofiltration system subjected to biofouling under constant pressure, the permeate flux for the QSI-immobilized nanofiltration membrane reduced by 10%, whereas the unmodified membrane decreased by 60% [19]. Another study demonstrated that a furanone-modified polymer demonstrated good antimicrobial and inhibition of cell-adhesion for various single and mixed bacterial cultures [21].

Although inhibition of QS pathways have been demonstrated to be a promising approach to reduce biofilm, further investigation into the precise effect of QSI on bacterial growth, biofilm attachment, and polysaccharide production associated with seawater desalination membrane biofouling are required. Furthermore, the effectiveness and stability of QSI-modified RO membranes in seawater systems have not been investigated.

### **1.3. Hypothesis & Objectives**

The hypothesis driving this research was that QSI compounds suppress marine biofilm formation, and consequently seawater desalination membrane biofouling by inhibiting QS molecules responsible for bacterial communication.

The overall goal of this research was to understand the theoretical function of QSIs in biofilm development and the QSI's stability on modified membrane surfaces. The first objective of this work was to study the role of the QS system in marine biofilm production (Chapter 3). The next objective was to identify the most effective QSIs to reduce marine biofilm formation and seawater desalination membrane biofouling (Chapter 3). Lastly, this work explored the anti-biofouling potential of QSI compounds incorporated onto the surface of RO membranes for seawater desalination (Chapter 4).

## CHAPTER 2. LITERATURE REVIEW

### 2.1. The Demand for Alternative Water Treatment Processes

Water scarcity is becoming a global concern as it is projected that two-thirds of the world's population will be living in water stressed regions by 2025 due to climate change, rapid population growth, and industrialization [22, 23]. Alternative water treatment processes such as desalination, wastewater reclamation, and water reuse are gaining attention to meet the increasing water demand by delivering varying qualities of purified water for human consumption.

Desalination produces high quality drinking water by removing contaminants (i.e. salt) from brackish water and seawater. By 2013, there were over 17,000 desalination plants in operation worldwide serving over 200 million people [24]. Water reclamation, another alternative water treatment technology, treats secondary sewage effluent to harvest purified water that can be applied in landscape and agricultural irrigation, toilet flushing, and cooling towers. Water reuse further processes reclaimed wastewater to produce highly purified water that is then blended into a groundwater basin. The blended water serves a dual purpose to protect a groundwater basin from seawater intrusion and then to be drawn as a source for drinking water treatment. In California alone, wastewater is recycled at more than 300 locations for uses ranging from irrigation to groundwater recharge [25]. Water reuse and desalination rely mainly on a semi-permeable reverse osmosis (RO) membrane to separate contaminants (i.e. bacteria, suspended solids, and dissolved solids) from these nonconventional water sources.

## 2.2. Current State of RO Membrane Technology

During the RO process, an artificial hydrostatic pressure is applied to the side with the higher concentration of dissolved solids (i.e. sodium, chloride, calcium, etc.) to facilitate the movement of water opposite to the natural flow of osmosis (Figure 2.1) through a semi-permeable membrane [26]. RO membranes are also able to separate dissolved solids from a feed water source based on surface charge. Membrane surfaces are typically negatively charged to repel negatively

charged ions in the feed water while positively charged ions are rejected to maintain the neutral water charge on both sides of the membrane [27, 28]. The RO membrane generally achieves salt rejections greater than 99% with a nominal pore size of  $0.0001\ \mu\text{m}$  [28, 29].

RO membranes are most commonly configured in a spiral wound module (Figure 2.2) and operated in cross-flow mode to produce a high rate of purified water [30-33]. Spiral wound configuration consists of layers of flat-sheet RO membranes, feed spacers, and permeate spacers wrapped around a permeate collection tube, which increases membrane surface area to enhance purified water production rates [31]. During cross-flow filtration in a spiral wound module, the pressurized feed water enters the element axially, guided by feed spacers where a portion of the feed water will radially permeate through the membrane and into the permeate spacers to be transferred to the permeate collection tube as depicted in Figure 2.2 [30, 32]. The rest of the feed

## RO Membrane Process

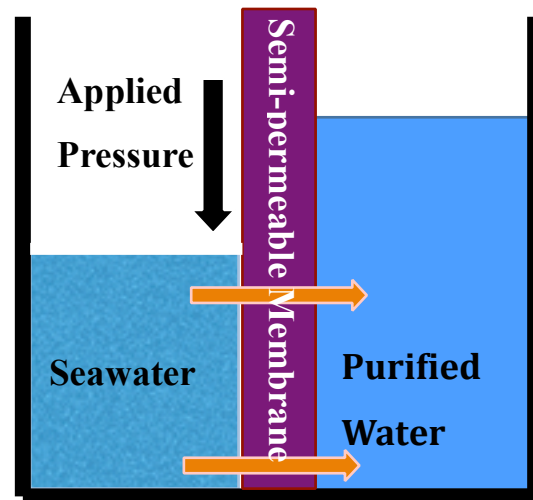


**Figure 2.1.** In reverse osmosis, the applied pressure to the concentrated feed water side (i.e. seawater) overcomes the natural osmotic pressure gradient to drive the flow of water through the semi-permeable RO membrane.

water continues to flow axially and exits as the waste (concentrate) stream. The feed spacers direct the flow of water and promote fluid agitation to effectively shear off accumulated contaminants on the membrane surface [30, 34]. The spiral-wound configuration is inexpensive, has low replacement costs, and can be easily scaled-up [31-34].

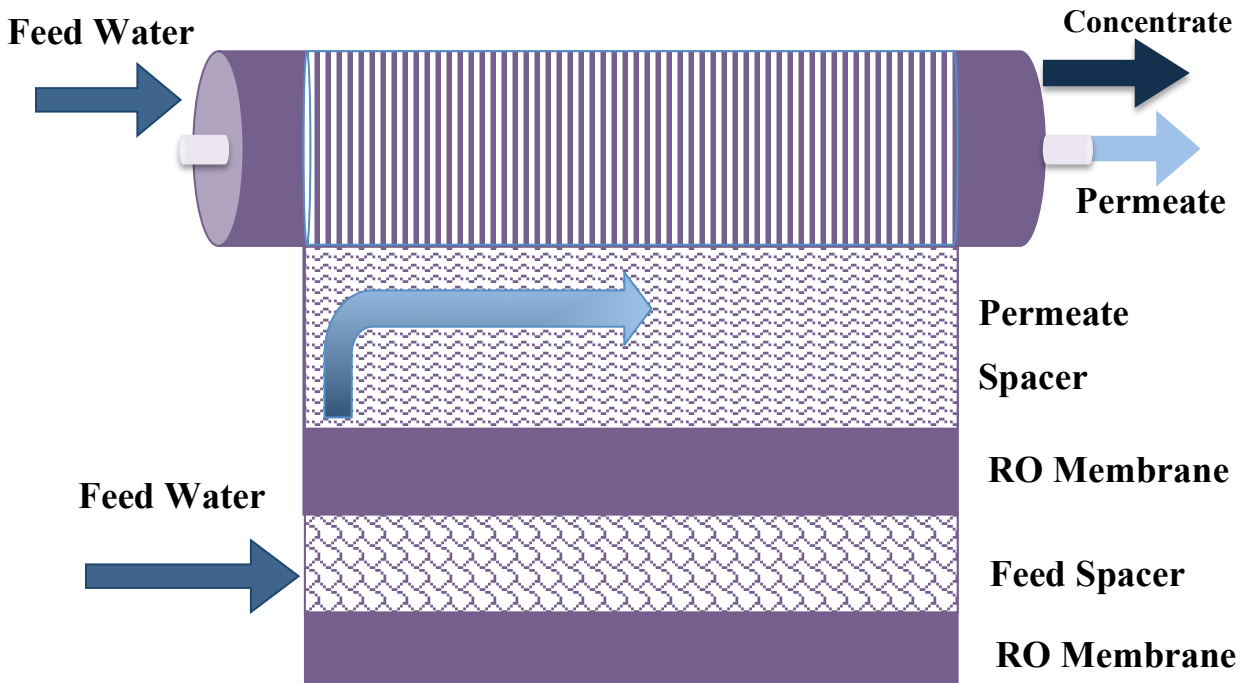


**Figure 2.2.** RO spiral wound module.

Currently, the thin film composite (TFC) polyamide membrane dominates the RO market for the water treatment industry. TFC membranes comprise of an ultra-thin aromatic polyamide barrier layer, usually 0.2  $\mu\text{m}$  thick (Figure 2.3) [35]. This active layer is supported by a micro-porous polysulfone interlayer, about 40-50  $\mu\text{m}$  thick and a polyester structural support, usually 120-150  $\mu\text{m}$  thick (Figure 2.3) [35]. The micro-porous interlayer allows the ultra-thin layer to withstand high-pressure compaction while the ultra-thin barrier layer reduces resistance in permeate transport to improve permeate water flux [35]. Therefore, TFC RO membranes achieve high permeate flux and salt rejection rates.



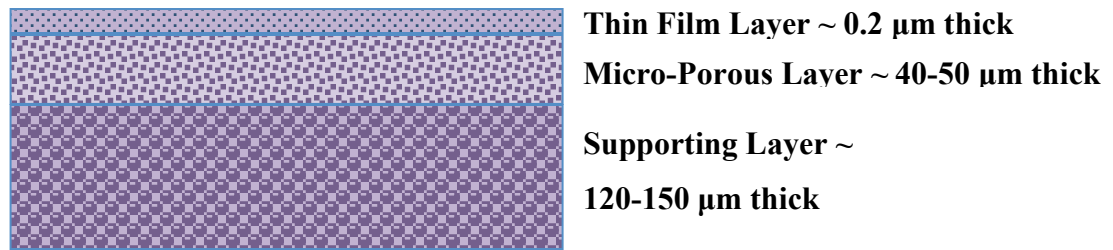


**Figure 2.3.** Cross-section of the thin film composite polyamide RO membrane.

However, membranes are still subjected to fouling, defined as the deposition and accumulation of undesirable materials such as minerals, organics, and bacteria onto membrane surfaces [29, 36]. During a fouling event, the applied pressure in a RO system compresses the fouling layer, which reduces the ability of the cross-flow velocity to effectively shear off particles that accumulate on the membrane surface [29, 37]. As a result, the permeate flux declines, which raises operational pressure and energy demand to maintain the initial flux rate [29, 37, 38]. Energy loss stemming from RO membrane fouling has been estimated to account for up to 50% of the total energy required for seawater desalination plants [39].

Membrane cleaning processes use a proprietary mixture of chemical cleaning agents to decompose the fouling layer in order to restore membrane permeability [40-42]. Although, cleaning only partially restores the membrane performance for a limited time as dissolved minerals and salts continue to deposit and accumulate onto the membrane surface. In addition, surviving bacteria on the membrane surface continue to grow due to readily available degraded organic matter in the surrounding environment. Repeated cleanings also degrade the polyamide thin film, which lowers the membrane life span [43]. Therefore, the RO membrane anti-fouling potential still needs to be improved.

The goal of this section is to review membrane properties affecting the fouling rate and to present a future perspective on the new generation of membranes with enhanced anti-fouling capabilities for alternative water treatment processes. This section focuses on biological

properties and applications in membrane development with respect to RO membranes as opposed to past review papers that focus on nanoparticle and carbon nanotube membrane development [6, 44, 45].

### 2.3. Membrane Fouling with Specific Emphasis on Organic Fouling/Biofouling

In industrial water applications, the main goal of the pretreatment process is to protect the RO membrane by reducing the fouling propensity of feed water. However, only minimal amounts of foulants that escape the pre-treatment process are sufficient enough to cause membrane fouling. Fouling can be classified into the following categories: scaling, organic fouling, and biofouling.

Scaling occurs due to deposition and precipitation of sparingly soluble salts and minerals such as calcium carbonate, silica, and barium sulfate on the membrane surface that form a scale layer when the concentration of the soluble components exceeds the solubility limit as depicted in Figure 2.4

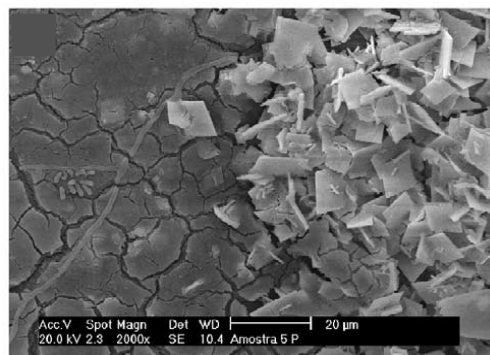


**Figure 2.4.** Scaling caused by crystalline barium sulfate on a RO membrane surface [3].

[3, 46]. Generally, scaling initially appears on the final RO membrane unit as it is exposed to the highest concentration of dissolved solids [47]. Scaling may result in physical membrane damage if the sharp edged crystals (i.e. barium sulfate) cut the polyamide thin film layer (Figure 2.4) [48]. The scale layer also provides an additional resistance barrier to filtration by creating a compact cake layer that blocks membrane pores (Figure 2.4) [49]. Operating at lower water recoveries or regulating pH using acidic chemicals or anti-scalants before the RO unit greatly reduces the possibility of a scaling event occurring [50].

Organic fouling occurs due to the deposition of a complex mixture of particulate and soluble organic compounds known as natural organic matter (NOM) on the membrane surface [47]. Dissolved organic matter (DOM), a major component of NOM, consists of humic substances, polysaccharides, proteins, and amino acids [51]. Organic fouling alters the membrane structure by blocking pores through colloidal NOM and creating a gel-like layer that covers the membrane surface similar to scaling, and likewise can be partially reversed through cleaning methods [47]. However, NOM can also cause irreversible damage by narrowing membrane pores through adsorption onto pore walls, which can only be counteracted to a degree with aggressive chemical cleaning methods [52, 53]. The rate of organic fouling is highly dependent on feed water characteristics and hydrodynamics of the RO system [54-56].

Biofouling occurs through bacterial biofilm formation on membrane surfaces. Membrane biofilm development results from the attachment and aggregation of bacterial species and its metabolic products, including proteins and extracellular polysaccharides (EPS) [57-59]. Biofilm formation happens in the following steps: bacterial attachment to the surface, microcolony formation, maturation, and cell detachment as depicted in Figure 2.5 [1]. Cell attachment is controlled by numerous parameters

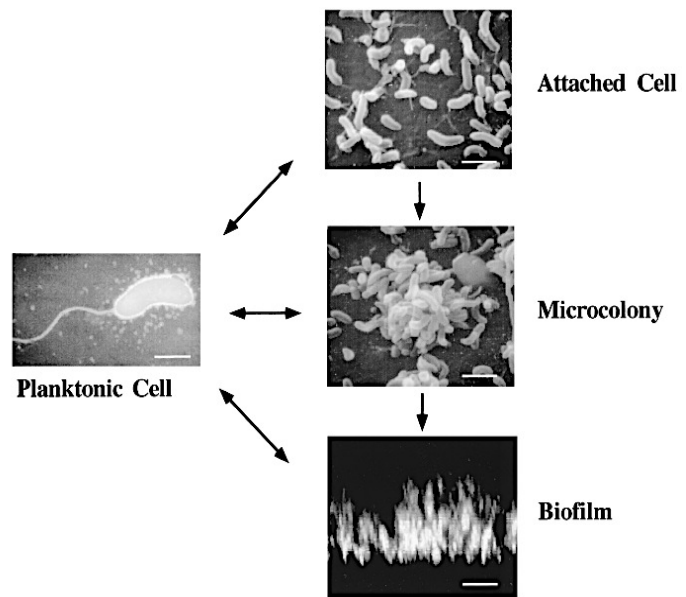


**Figure 2.5.** Stages of biofilm formation [1].

from feed water characteristics to membrane properties to hydrodynamics of the RO system [60]. EPS further affects the extent of cell attachment and acts as a diffusion barrier to protect bacteria

by creating a three-dimensional matrix [61-63]. This matrix consists of approximately 90% of dry mass and only 10% of bacterial cells [59]. Microcolonies, the aggregation of attached cells, are considered the basic unit of the biofilm structure (Figure 2.5). Water channels separate microcolonies and allow for nutrient and oxygen transport within the matrix [64]. Then, biofilm maturation is associated with a decrease in the convective flow and transport of anti-microbial agents that causes increased bacterial resistance to chemical cleaning methods (Figure 2.5) [65, 66]. When nutrient levels are marginal, the bacteria associated with the biofilm either detach and reinitiate biofilm formation on new locations of the membrane surface or leave the surface and return to planktonic mode [67, 68].

#### **2.4. Membrane Properties Affecting the Fouling Rate**

Surface roughness, hydrophobicity, and electrostatic charge significantly affect the membrane fouling rate [60, 69, 70]. As surface roughness increases, the fouling rate intensifies because there is a greater possibility that foulant particles will be trapped by the rougher surface [71-73]. Although, a smoother membrane surface experiences a decrease in permeate flux because there is less effective membrane area to produce purified water [71-73]. The leading TFC RO membranes in the industry have a rough surface with a higher water permeability rate at the expense of developing colloidal and bacterial fouling [71, 72].

Membranes should be developed and selected based on the hydrophobicity and electrostatic property of the major foulants in the feed water. Past studies have demonstrated that a more hydrophilic surface reduced hydrophobic foulant deposition from proteins and polysaccharides by producing a pure water layer over the membrane surface [74, 75]. Additionally, the greater the electrostatic repulsive forces, or the similar the charges between the membrane surface and the foulant are, the less likely a fouling event will occur. Consequently,

studies have demonstrated that the zeta potential, or the mean surface charge of the membrane, will impact the fouling rate depending on the charge of the major foulants and the membrane surface charge distribution [72, 76, 77].

Steric repulsion also reduces membrane fouling due to the addition of multiple polymer chains on the membrane surface, which changes the foulant geometry and reactivity. For example, binding long-chain hydrophilic polymers onto the membrane surface will result in less volume for the hydrophobic foulants (i.e. proteins) to adsorb onto the membrane surface [78].

## 2.5. Antifouling effort with Membrane Materials

Incorporating biological compounds as new membrane materials have been gaining attention in order to improve water permeability, salt rejection, and anti-fouling capabilities [12, 13, 79-82].

### 2.5.1. Biomimetic membrane

Cell membranes are a composite filter, comprised of selective proteins integrated into a lipid bilayer that have the ability to transport either water or specific

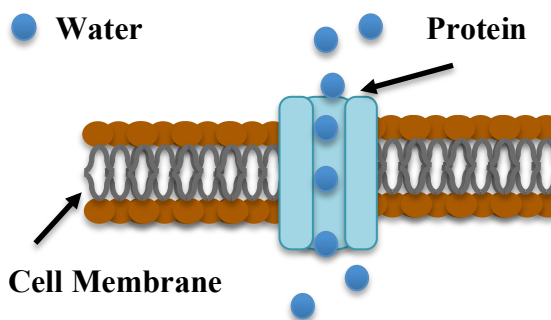


**Figure 2.6.** Water transport in a cell membrane with a selective protein (i.e. aquaporin).

macromolecules or ions at extremely high rates as demonstrated in Figure 2.6 [80]. Aquaporins are a type of protein in these cell membranes that have six membrane-spanning domains with charged particles that form pores for water transport and solute rejection [12, 79]. These membranes achieve water permeability rates at approximately an order of magnitude higher than conventional RO membranes by transporting water through narrow pores [80, 81]. Thus, aquaporins have garnered attention as new membrane materials for water treatment applications.

The first biomimetic membranes consisted of a triblock copolymer embedded with aquaporin Z, isolated from the cell membranes of *Escherichia coli* (*E. coli*) bacteria and various plants [79, 82]. These studies found that the rate of aquaporin integration was highly dependent on membrane characteristics and defects in the polymer [13, 79, 80, 82]. Zhong *et al.* [83] then successfully incorporated the aquaporin Z embedded triblock copolymer onto a cellulose acetate membrane. The study demonstrated that pure water permeability and salt rejection rates increased as the amount of aquaporin Z embedded into the triblock copolymer increased [83]. Additionally, water permeability and salt rejection rates of the aquaporin cellulose acetate membrane were reasonable for water reuse applications.

Zhao *et al.* [84] and Li *et al.* [85] created a TFC and hollow fiber aquaporin Z membrane, respectively. Both studies demonstrated that the pure water permeability increased over 40% for the aquaporin membranes compared to commercially available brackish and seawater RO membranes operating at a pressure of 72.5 psi [84, 85]. The salt rejection rates also increased from commercially available brackish (96%) and seawater (90%) RO membranes to aquaporin TFC (98%) and hollow fiber (96%) membranes operated at 72.5 psi with a sodium chloride solution (200-500ppm) [84, 85].

Li *et al.* [85] further found that embedded aquaporin was relatively stable on hollow fiber membranes after a 40-hour period consisting of four 45 minute-periods of organic fouling (8.6 mM NaCl, 100 ppm bovine serum albumin (BSA), 2mM calcium) with 15-minute periods of cleaning (30mM sodium dodecyl sulfate (SDS, pH 8-9)). As the permeate flux increased from 20 to 35 L/m<sup>2</sup>/H for each period of fouling and cleaning, the aquaporin membrane experienced greater fouling as indicated by the increased trans-membrane pressure [85]. However, water permeability and salt rejection were relatively maintained over the 40-hour period.

These previous research studies have proved that aquaporins can be integrated successfully onto various membrane surfaces. The majority of this research has focused on improving water permeability and salt rejection properties of the aquaporin membrane without exploring the anti-fouling potential especially in relation to membrane bacterial colonization and biofouling. Additional research will be required to determine the long-term stability and functionality of aquaporin biomimetic membranes, especially in RO mode under high-pressure conditions.

### ***2.5.2 Quorum Sensing and Quorum Sensing Inhibition in Biofilm***

Quorum sensing (QS) and inhibition of QS pathways are gaining attention to control biofilm formation at a cellular level. Past research has identified several QS inhibitors (QSIs) for biofilm prevention relating to the clinical field [86-88]. This section investigated the QS pathways and QSI compounds relating to seawater desalination and wastewater treatment.

#### ***2.5.2.1. Quorum Sensing Pathways***

Past studies revealed that gram-negative ( $G^-$ ) and gram-positive ( $G^+$ ) bacteria communicate through QS pathways to regulate a number of target genes including biofilm development and maturation. During QS, bacteria attached to a surface communicate with each other by secreting signaling molecules, known as auto-inducers [9]. As the bacterial population density increases, these signaling molecules accumulate to a threshold level [9]. After the threshold is reached, the signaling molecule binds to the appropriate transcription regulator and either initiates or suppresses target genes to activate biofilm development [9]. Since the majority of bacteria isolated from seawater desalination and wastewater treatment plants are  $G^-$  bacteria,

QS pathways for  $G^+$  intraspecies communication were not explored. The pathways for interspecies and  $G^-$  intraspecies communication are presented in Figure 2.7.

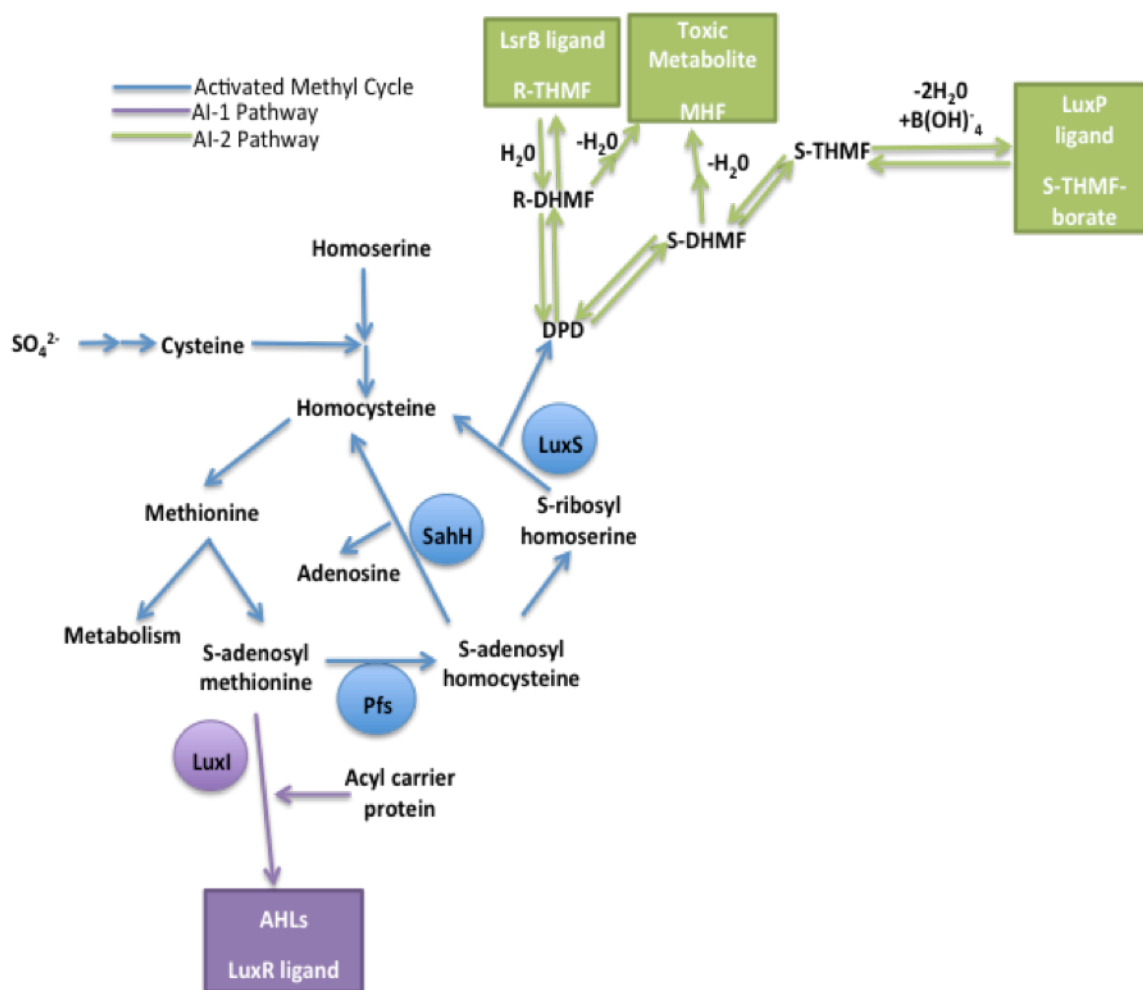


**Figure 2.7.** The steps occurring in the AI-1 (purple) and AI-2 (green) QS pathways responsible for  $G^-$  and  $G^+$  and  $G^-$  bacterial communication, respectively. These pathways are branched off of the activated methyl cycle (blue), which synthesizes amino acids.

#### 2.5.2.2. Auto-inducer type 1 signaling system

The auto-inducer type 1 (AI-1) signaling system potentially plays a significant role in seawater desalination membrane biofouling because the dominant bacteria present in the seawater intake and on RO membrane surfaces belong to the  $G^-$   $\gamma$ -Proteobacteria class [37, 89, 90]. In wastewater treatment, it has been previously noted that  $G^-$  bacteria are present in the



activated sludge process as well as on RO and nanofiltration membranes [91-94]. In the AI-1 QS pathway, G<sup>-</sup> bacterial communication is controlled by N-acyl-homoserine lactone (AHL) QS signaling compounds.

In this pathway, the LuxI family of proteins synthesizes the AHL molecules by linking and lactonizing the methionine moiety from S-adenosylmethionine (SAM) to a particular set of fatty acyl chains carried on acyl-acyl carrier proteins as shown in Figure 2.7 [74, 95, 96]. These

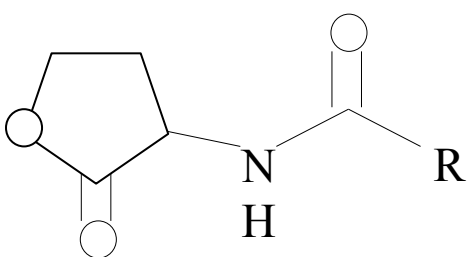


**Figure 2.8.** Chemical structure of the AHL molecule in the AI-1 QS pathway.

AHL molecules differ in degree of saturation, number of oxygen substitutions, and N-acyl chain length, which varies between 4 to 18 carbons bonded to a lactone ring through an amide bond (Figure 2.8) [97]. The AHL

signaling molecules are able to diffuse freely into and out of the cell until a threshold level is reached, which is detected by the LuxR proteins residing in the cell cytoplasm [95, 98]. Once the threshold level is reached, AHL-LuxR complex forms and activates transcription of the lux operon (Figure 2.7) [95, 99]. The AI-1 signaling system plays a significant role in intraspecies communication due to the high degree of specialization between the AHL-LuxR complex. Table 2.1 and Table 2.2 summarize the previously identified AHL signaling molecules that regulate wastewater and marine bacterial biofilm formation.

<b>Table 2.1.</b> AHL Signaling System for Biofilm Regulation in Wastewater Bacterial Isolates		
<b>Bacteria genus</b>	<b>Specific AHL Signaling Molecule</b>	<b>Ref.</b>
<i>Acinetobacter</i>	3 HO-C12-HSL	[100, 101]
<i>Pseudomonas</i>	C4-HSL; 3OC12-HSL	[102-104]
<i>Nitrobacter</i>	-	[105]

<b>Table 2.1.</b> AHL Signaling System for Biofilm Regulation in Wastewater Bacterial Isolates		
<b>Bacteria genus</b>	<b>Specific AHL Signaling Molecule</b>	<b>Ref.</b>
<i>Nitrosomonas</i>	C6-HSL; C8-HSL; C10-HSL; 3OH-C6-HSL	[106, 107]
<i>Vibrio</i>	C4-HSL; C6-HSL; 3OH-C4-HSL	[95, 105, 108, 109]
<i>Xanthomonas</i>	-	[110, 111]

<b>Table 2.2.</b> AHL Signaling System for Biofilm Regulation in Marine Bacterial Isolates		
<b>Bacteria genus</b>	<b>Specific AHL Signaling Molecule</b>	<b>Ref.</b>
<i>Alteromonas</i>	C4-HSL; C6-HSL	[53, 54]
<i>Aeromonas</i>	C4-HSL; C6-HSL	[112, 113]
<i>Ochrobactrum</i>	C4-HSL; C6-HSL	[53, 54]
<i>Pseudomonas</i>	C4-HSL	[95]
<i>Pseudoalteromonas</i>	-	[114]
<i>Shewanella</i>	C4-HSL; C6-HSL	[108, 114]
<i>Thalassomonas</i>	-	[114, 115]
<i>Vibrio</i>	C4-HSL; C6-HSL; 3OH-C4-HSL	[95, 108, 109]

### 2.5.2.3. Auto-inducer type 2 signaling system

The auto-inducer 2 (AI-2) signaling system is a universal QS pathway responsible for interspecies communication between  $G^+$  and  $G^-$  bacteria. A LuxS protein converts S-ribosyl homocysteine (SRH) to yield homocysteine in the activated methyl cycle as well as 4,5-dihydroxy-2,3-pentanedione (DPD) (Figure 2.7). DPD spontaneously undergoes cyclization to form numerous compounds, including the family of AI-2 QS molecules, (2R,4S)-2-methyl-2,3,3,4-tetrahydroxytetrahydrofuran (R-THMF) (Figure 2.9C), 4-hydroxy-5-methyl-3(2H)

furanone (MHF) (Figure 2.9B), and S-THMF-borate, a furanosyl borate diester (Figure 2.9A).

These signaling molecules are then transported to the supernatant from the cytoplasm.

The detection of this auto-inducer is based on the specific AI-2 derived

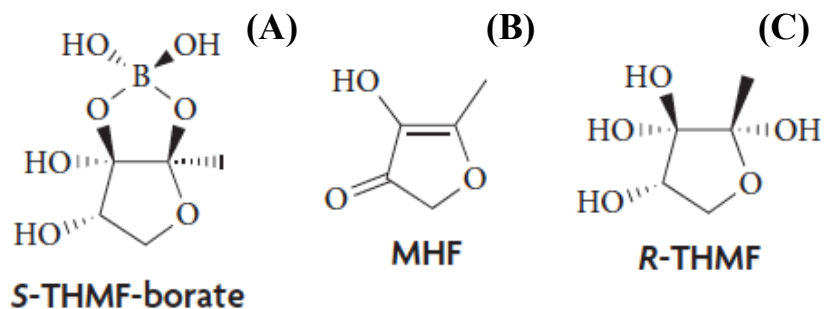


**Figure 2.9.** Chemical structure of the family of AI-2 QS molecules including S-THMF-borate, the furanosyl borate diester (A), MHF (B), and R-THMF (C)[2].

molecule responsible for QS, which varies in certain bacterial species. For instance, LuxP, a periplasmic binding protein belonging to the bacterial species, *Vibrio harveyi* detects S-THMF-borate (Figure 2.7) [2, 120, 121]. Once S-THMF-borate binds to LuxP, the complex interacts with LuxQ, a membrane-bound histidine protein kinase, which triggers a dephosphorylation cascade to activate transcription of the lux operon. LsrB, another periplasmic binding protein, serves as the detector and receptor for the signaling compound, R-THMF, (Figure 2.7) which is found in *Salmonella enterica* and *E. coli* [2, 122].

Since biofilm associated with fouled membranes is generally composed of mixed bacterial species in all water treatment applications, it is imperative to understand the AI-2 signaling system and the signaling

<b>Table 2.3.</b> AI-2 Signaling System in Marine and Wastewater Bacterial Isolates	
<b>Bacteria genus</b>	<b>Ref.</b>
<i>Bacillus</i>	[70]
<i>Escherichia</i>	[116]
<i>Salmonella</i>	[117]
<i>Vibrio</i>	[118, 119]

molecules produced by each bacterial species. Table 2.3 summarizes the previous research characterizing AI-2 production for both marine and wastewater bacterial biofilms.

#### 2.5.2.4. Interfering with QS Signals

Suppressing QS pathways is a potential method to prevent biofilm growth and membrane biofouling. There are various naturally occurring and synthetic QSI compounds that disrupt QS pathways by modifying the signaling molecule or suppressing the signal production (inhibiting synthase proteins) or reducing the ability of the signaling molecule to bind to the transcription regulator (inhibiting the binding or kinase proteins) [10, 11].

QS degradation enzymes found in numerous bacteria and mammals, including AHL-lactonase, AHL-acylase, and acylase I, have been shown to degrade the AHL QS signaling compound by breaking down the lactone and acyl chain [36, 123-125]. The porcine kidney acylase I enzyme has been shown to reduce mixed bacterial biofouling in membrane bioreactors for wastewater treatment [17, 20]. Kim *et al.* [14] further demonstrated that porcine kidney acylase I immobilized on a membrane surface reduced biofilm formation formed by *Pseudomonas aeruginosa* bacterial strain.

QS signal competitors, the focus of this research, consist of a range of natural and synthetic compounds that inhibit either QS signal production or reception. For instance, kojic acid and vanillin, commonly used in the cosmetic and food industries were identified as AI-1 QS inhibitors [18, 126-129]. These compounds were found to suppress or modify the AHL molecule in the AI-1 QS system using a LuxR based bioreporter strain [18, 126-129]. Vanillin has been shown to further modify the AI-1 AHL's structure to hinder the AHL's ability to bind to the appropriate receptor protein [16, 126]. Cinnamaldehyde, another food flavoring agent and synthetic brominated furanone compounds were revealed to disrupt both the AI-1 and AI-2 QS systems by reducing the DNA binding ability of the receptor protein, LuxR [130-132]. Additionally, brominated furanone compounds have been demonstrated to suppress the AI-2 LuxS protein [133].

The QSI's ability to inhibit QS molecules produced by the AI-1 and AI-2 pathways have been researched extensively especially in the medical field [14, 16, 17, 20, 21, 126, 134]. However, the role of the QS system and the QSI's potential to mitigate biofilm formation and membrane biofouling for alternative water treatment processes such as seawater desalination and wastewater treatment still needs to be evaluated.

### **CHAPTER 3. INHIBITING QS PATHWAYS TO MITIGATE SEAWATER DESALINATION RO MEMBRANE BIOFOULING**

\*A modified version of this chapter has been accepted to be a publication in *Desalination* Journal.

#### **Abstract**

Bacterial biofilm formation, the main cause of membrane biofouling, is a crucial issue for membrane separation. Biofilm development is controlled by quorum sensing (QS) systems where bacteria produce auto-inducers to communicate with neighboring bacteria. This study identified that several marine bacteria isolated from a desalination plant produced two low molecular weight auto-inducer 1 (AI-1) signaling molecules. AI-1 production in the mixed culture of the four different biofilm-forming marine bacteria was greater than in the individual bacterial cultures. The QS inhibiting compounds, vanillin and cinnamaldehyde at 1200 mg/L significantly inhibited biofilm formed by these marine bacteria by more than 79% and 70%, respectively in a microtiter plate assay. Anti-biofilm capabilities of vanillin and cinnamaldehyde were further evaluated in a reverse osmosis membrane bio-monitoring system using mixed bacterial cultures and native uncultured bacterial communities in natural seawater. Confocal microscopy demonstrated that vanillin (1200 mg/L) significantly inhibited extracellular polysaccharide production and dead cells on the membrane surface by more than 40% and 20%, respectively.

### 3.1. Introduction

The amount of people residing in regions with insufficient water resources is estimated to rise from one fifth of the global population to two thirds due to population growth and climate change [22]. Alternative water treatment processes such as coastal seawater desalination and water reuse using reverse osmosis (RO) membranes have the potential to meet this demand by producing high quality purified water.

However, biofouling remains a significant challenge in membrane separation because it causes a reduction in membrane flux and an increase in operational pressure [29, 37, 38]. For seawater desalination plants, energy loss stemming from membrane biofouling has been estimated to be up to 50% of the total energy required [39]. Biofouling consists of the attachment and subsequent growth of bacteria on the membrane surface, which secretes bacterial metabolic products including extracellular polysaccharides (EPS) [57-59]. Only less than 0.01% of the  $10^6$ /mL of natural marine bacteria that escape the pretreatment process are sufficient enough to cause RO membrane biofouling.

Typical cleaning processes for membrane biofouling use a proprietary assortment of chemical cleaning compounds to break down the biofouling layer in order to regenerate membrane permeability [40-42]. However, cleaning only partially restores the RO membrane performance for a limited time because degraded organic matter in the surrounding environment further stimulates the growth of surviving bacteria. Moreover, the remaining bacteria may develop resistance to chemical cleaning agents [86]. As a result, the increase in the frequency of membrane cleanings creates an increase in operational difficulty, a decrease in membrane life span, and raises plant operational and maintenance costs [43].

A potential method to control biofouling is to prevent biofilm formation by blocking bacterial communication in quorum sensing (QS) pathways. Bacteria utilize these pathways to control biofilm development and maturation. During QS, bacteria synthesize and secrete auto-inducers or signaling molecules to “communicate” with each other [9]. These auto-inducers accumulate to a threshold concentration based on the local bacterial population density [9]. After the threshold is reached, signaling molecules diffuse through cell membranes to bind to the appropriate transcription regulator in neighboring bacteria to initiate biofilm development [9]. One or more of these QS pathways may be present in bacterial species to regulate a number of specific genes [135-138].

The auto-inducer 1 (AI-1) QS system produces acyl-homoserine lactone (AHL) to regulate gram-negative ( $G^-$ ) bacterial communication whereas the auto-inducer 2 (AI-2) yields a variety of signaling molecules to govern multi-species communication. In the well-studied AI-1 system, the LuxI protein initiates AHL synthesis with the LuxR protein acting as a receptor [97]. The type of AHL molecule produced is dependent on the specific bacterial species of interest. AHLs comprise of a N-acyl chain length, varying from 4 to 18 carbons bonded to a lactone ring through an amide bond [97]. In the AI-2 system, the LuxS protein synthesizes 4,5-dihydroxy-2,3-pentanedione (DPD), which spontaneously rearranges to produce the family of AI-2 QS molecules, comprising of 4-hydroxy-5-methyl-3(2H) furanone (MHF), (2R,4S)-2-methyl-2,3,3,4-tetrahydroxytetrahydrofuran (R-THMF), and S-THMF-borate, a furanosyl borate diester [105, 139]. The detection of these auto-inducers is based on the specific AI-2 derived molecule responsible for QS, which varies in different bacterial species.

There are various naturally occurring and synthetic QS inhibiting compounds (QSIs) that disrupt QS pathways by either degrading the signaling molecule or blocking signal production or



outcompeting the signaling molecule from binding to the receptor protein [10, 11]. Kojic acid, used in the cosmetic industry, and vanillin, a commonly added food-flavoring agent were identified as AI-1 QS inhibitors because both inhibit or alter the AHL molecule using a LuxR based bioreporter strain [18, 126-129]. Vanillin has further been shown to modify the AHL's structure to impede the AHL from binding to the receptor protein [16, 126]. Cinnamaldehyde, another food flavoring agent and synthetic brominated furanone compounds were revealed to disrupt both the AI-1 and AI-2 QS systems by hindering the DNA binding ability of the receptor protein, LuxR [130-132]. Additionally, brominated furanones have been shown to suppress the AI-2 LuxS protein [133]. Although the QSIs' ability to interfere with QS pathways has been researched extensively using bio-reporter strains or model bacterial systems for clinical and other environmental applications [14, 17, 18, 140-144], the QSIs' potential to mitigate marine biofilm formation and seawater desalination RO membrane biofouling needs to be evaluated. This research investigated the role of QS system in desalination membrane biofouling by examining QS production in natural bacterial isolates from biofouled seawater RO membranes. Based on the type of QS produced, several commercially available and inexpensive QSIs were selected to determine the QSI's effect on single and mixed species marine biofilm formation in a static environment. The anti-biofilm capabilities of the most effective QSIs were further evaluated in a membrane bio-monitoring system operated in cross-flow mode using native marine bacterial communities. The biofouled membranes were then examined under fluorescent microscopy to understand the biofilm structure with and without treatment by QSI.

## 3.2. Materials & Methods

### 3.2.1. *Bacterial Strains and Seawater Bacterial Community*

A diverse group of bacteria, isolated from fouled cartridge filters and RO membranes at Carlsbad Desalination pilot plant in California (CA) and Perth Desalination plant in Western Australia were selected to characterize QS molecule production and to study biofilm formation in the presence of QSI. The four Carlsbad bacterial strains, B1 and B3 were determined to be *Shewanella sp.* while B2 and B4 were determined to be *Alteromonas sp.* in a previous study [90]. The four Australian isolates were identified as *Paracoccus sp.* (RO28), *Mycrobacterium sp.* (RO16), *Burkholderia ambifaria* (RO32), and *Bizionia sp.* (C10) by 16S rDNA sequencing [Dr. Lucy Skillman, unpublished results]. In addition, bacterial communities in natural seawater collected from Southern CA coastal sites at Dana Point, Long Beach, and Newport Beach were used without cultivation and isolation. The fresh seawater was unaltered and used directly in biofouling experiments to simulate the desalination fouling condition.

### 3.2.2. *Quorum Sensing Inhibitors*

The four QSIs selected to investigate biofilm inhibition in this study were cinnamaldehyde (CNMA), kojic acid (KJ), vanillin (VA), and a brominated furanone compound (F-30). The selection was based on: 1) the target QS molecule for biofilm inhibition (AI-1 or AI-2); 2) prior demonstration of biofilm reduction in model bacterial system; 3) commercial availability; 4) nontoxic to humans; and 5) inexpensive to manufacture. CNMA (Sigma-Aldrich) was diluted in methanol and used in testing concentrations ranging from 10 to 2400 mg/L. The brominated furanone compound, F-30 also known as (5Z)-4-bromo-5-(bromomethylene)-2(5H)-furanone (Sigma-Aldrich) was dissolved in dimethyl sulfoxide (DMSO) and added to bacterial cultures or

natural seawater to experimental concentrations between 10 and 30 mg/L. KJ (Sigma-Aldrich) and VA (Sigma-Aldrich) were both dissolved in deionized (DI) water and used in testing concentrations ranging from 10 to 2400 mg/L. The solvents used to dissolve each QSI were used as the control for all experiments.

### **3.2.3. *Identification of Bacterial AI-1 QS Molecule Production***

AI-1 production among marine bacteria isolated from biofouled membranes was investigated because AI-1 is commonly reported among *G<sup>-</sup>* bacteria and all QSIs tested in this study were able to interfere with AI-1 QS pathway. AI-1 AHL extraction was modified based on a previous study [145]. Briefly, four bacterial isolates (B1, B2, B3, and B4) from the Carlsbad desalination pilot plant in California (CA) were inoculated into an artificial seawater medium (ASWJP) with 2.5 g/L peptone, 0.5 g/L yeast (ASWJP+1/2PY) and incubated for 24 h on a shaker at 21°C [38, 146]. A 1:100 dilution was made from the bacterial cultures into ASWJP with 1.25 g/L peptone and 0.25 g/L yeast (ASWJP + 1/4PY). The sub-cultures were incubated for 6 h on a shaker at 21°C until bacteria reached exponential growth phase. The optical cell density was recorded at a wavelength of 600 nm (BioPhotometer, Eppendorf). The supernatants from cell cultures were collected after pelleting cells by centrifugation at 4°C at 5,500 g (Centrifuge, Eppendorf) for 20 min. Bacterial pellets were re-suspended in ASWJP and cell pelleted by centrifugation again to collect the supernatant. The combined supernatant from both centrifugations were extracted three times by liquid-liquid extraction with half volume HPLC-grade dichloromethane [145]. Excess water was removed by adding anhydrous magnesium sulfate to dichloromethane extracts. After removal of anhydrous magnesium sulfate by filtration, dichloromethane was evaporated using a speed vacuum concentrator at 30°C (Refrigerated

CentriVap Concentrator, LABCONCO). The extracts were dissolved in 1 ml of 1:1 of DI water : acetonitrile (HPLC-grade) and stored at -20°C until analysis. N-butyryl-L-homoserine lactone (C4-HSL, Cayman Chemical) and N-hexanoyl-homoserine lactone (C6-HSL, Cayman Chemical) were used as the extraction control standards and were taken through the same extraction steps as described above.

The AHL concentration of each extract was analyzed using Acquity UPLC (ultra pure liquid chromatography) system (Waters) coupled to a Quattro Premier XE triple quadrupole mass spectrometer (MS/MS) (Waters) run in positive-ion mode. For the UPLC system, 10 µl of each sample was injected into the 2.1 x 50 mm C<sub>18</sub> reversed phase column (Acquity BEH) at a flow rate of 0.3 ml/min with mobile phases consisting of water with 2% acetonitrile and 0.2% acetic acid and a gradient of 0.5%–95% acetonitrile in 0.2% acetic acid.

#### **3.2.4. *Effect of QSI on Biofilm Production***

The QSI effect on single species marine biofilm growth was analyzed using the Carlsbad and Perth isolates (eight total). Individually, each bacterial isolate was inoculated into ASWJP + 1/2PY then incubated for 48 h at 21°C on a shaker. The enriched bacterial culture was diluted 100 times with ASWJP + 1/4PY. Testing concentrations of each QSI were added to the diluted culture while equal volume of QSI solvents (methanol, DMSO, or DI H<sub>2</sub>O) were added to the control samples. An aliquot (200 µL) of each treatment and their respective control samples were transferred to a 96-well microtiter plate (Biosciences Discovery Labware) in 8 replications. Microtiter plates were incubated in the dark for 24 h at 21°C until bacteria reached exponential growth phase.

In order to ascertain the effects of the QSI on biofilm formation within a competitive community interaction, a mixture of the four enriched Carlsbad bacterial strains were diluted (1:100) with ASWJP + 1/4PY and treated by QSI. The mixed culture of the Carlsbad isolates was also diluted with the same ratio in 0.45  $\mu\text{m}$  filtered seawater (Millipore) from Newport Beach, CA. The filtered seawater was amended with 0.5 g/L peptone to accelerate the biofouling progress. Samples treated with QSI and controls were set up similar to the single species biofilm assay. The microtiter plates were incubated in the dark for 48 h at 21°C for cells to achieve exponential growth phase.

Lastly, uncultured natural marine bacterial communities in unaltered seawater from three locations along the Southern CA coast were investigated to observe the QSI's effect on reduction of marine biofilm in desalination plants. Peptone (0.5 g/L) was added to seawater to expedite the biofouling process. QSI treatments and controls assays were set up the same as for single and mixed species. Microtiter plates were covered to prevent light penetration and incubated for 78h at 21°C. Since the natural marine bacterial community was not cultured, a longer incubation time was required for bacteria to reach exponential growth phase.

At the end of each incubation time, bacterial growth was measured using optical density at 550 nm absorbance (Spectramax 2, Molecular Devices). Biofilm density on microtiter plates was assessed using a crystal violet protocol [147]. Briefly, suspended cells and medium in each well were gently removed and rinsed with PBS (phosphate-buffered saline, pH 7.4). Methanol (99%) was added to each well for 15 min before removal. Biofilm attached to the well were stained using 100  $\mu\text{L}$  of 0.5% crystal violet for 20 minutes followed by a DI water rinse. The bonded crystal violet was released using 33% acetic acid [38, 147]. The crystal violet concentration, which is indicative of biofilm density, was measured at 590 nm absorbance [147]. A statistically

significant difference between the QSI treated and control biofilm was determined using a two-tailed t-test with a 95% confidence level. Normalized biofilm growth results were expressed using the ratio of biofilm density in QSI treated samples to control samples. The responses of single species biofilm and mixed species biofilm were presented in notched boxplots to show the medium and variation between the tests with a 95% confidence level.

### 3.2.5. *RO Membrane Biofilm Reduction*

The QSI's effect on bacterial biofilm formation on a flat sheet RO membrane surface (SWC5, Hydranautics) was examined using a bio-monitoring system

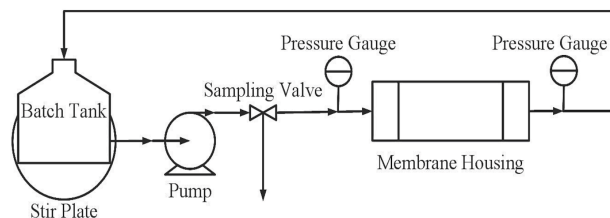


**Figure 3.1.** RO membrane bio-monitoring schematic.

(Figure 3.1). First, each Carlsbad bacterial isolate (B1, B2, B3, and B4) was inoculated into ASWJP + 1/2PY and incubated for 48 h at 21°C on a shaker. The feed tank was inoculated with an equal portion of each of the four bacterial cultures in a 1:100 dilution using 0.45 µm filtered seawater from Newport Beach, CA. The bacterial seeded seawater samples were amended with 0.5 g/L peptone and selective QSI or QSI solvent as a control. The feed tanks were covered from light and mixed continuously on a stir plate. A cross-flow of 180 L/m<sup>2</sup>/h was set using a peristaltic pump (Masterflex) for both treatment and control RO membrane systems. The membrane was placed in a membrane housing with a 0.87 mm thick nylon membrane spacer to promote fluid agitation. The system was run in recirculation mode without permeation as described in previous studies [148, 149] because the effects of permeation on biofouling were not significant for a comparison between treatment and control membrane biofouling. Cell density within the batch tank was assessed using OD<sub>600</sub> (Biophotometer, Eppendorf) at every 6-8

h up to 42 h. Feed and effluent pressures were recorded, and the cross flow rate was measured manually. At the end of the experiment, membranes were collected for biofilm analysis.

In addition to the seeding study using mixed bacterial isolates, the desalination fouling condition was simulated using uncultured natural bacterial community in seawater collected from Dana Point, CA. Similarly to the microtiter plate biofilm study, unaltered seawater was supplemented with peptone (0.5 g/L) and treated by selective QSIs. A control was step up in parallel by adding equal volumes of the QSI solvents to the feed tank.

### **3.2.6. *Biofilm Quantification by Confocal Laser Scanning Microscopy (CLSM)***

Membrane samples collected from the bio-monitoring system were cut into 2 x 5 cm coupons and analyzed for biofilm thickness and live and dead cell counts using CLSM (Zeiss LSM 700). Live cells were stained green with STYO 9 and dead cells were stained red with propidium iodide for 30 min (FilmTracer<sup>TM</sup> LIVE/DEAD<sup>®</sup> Biofilm Viability Kit, Invitrogen). Live and dead cells were imaged at excitation/emission wavelengths of 480/500 and 490/635 nm, respectively. Five locations along the length of the membrane were examined for a better assessment of live and dead cells.

Additionally, EPS on a selective number of coupons were stained for 30 min using ConA lectin (Concanavalin A Conjugates, Invitrogen), which binds to  $\alpha$ -mannopyranosyl and  $\alpha$ -glucopyranosyl residues [150]. The membranes were then analyzed using excitation/emission wavelengths of 555/580 nm at three different locations along the length of the membrane coupons to obtain a better distribution of EPS.

COMSTAT 2 software was used to determine EPS, live cell, and dead cell biomass and thickness under standard automatic thresholding and connected volume filtering methods [34,

151]. The biofilm biomass was calculated as the number of pixels in all images of the z-stack multiplied by the voxel size and divided by the substratum area of the image stack [34, 151]. The biofilm thickness was determined by locating the highest point above each pixel in the bottom layer containing biomass [34, 151]. MATLAB and Microsoft Excel were used to create notched boxplots and to conduct two-tailed t-tests with a 95% confidence level to determine significant differences between the QSI-treated and control biofilm.

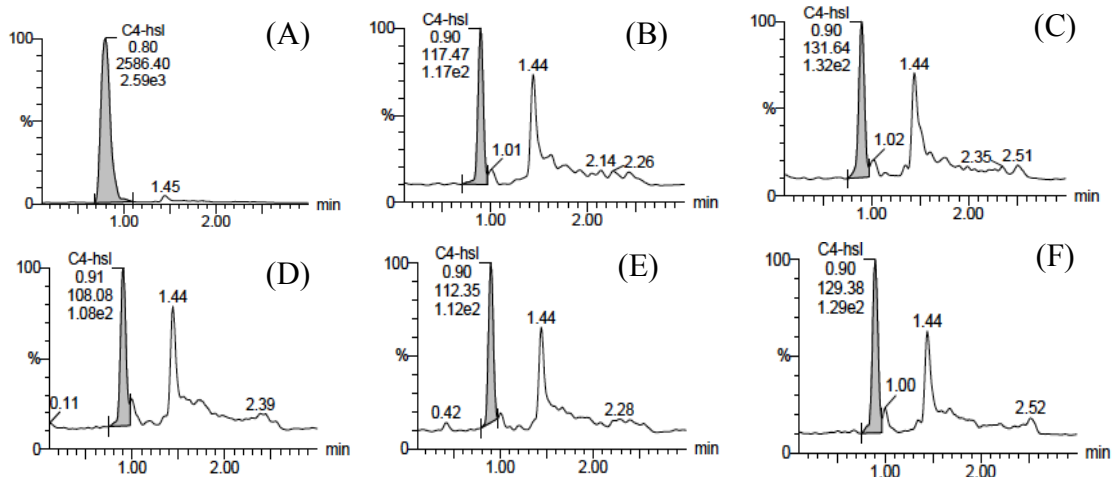


**Figure 3.2.** UPLC-MS/MS Chromatograms of C4-HSL standard (A), and extracts from single species bacterial cultures, B1 (B) and B2 (C), B3 (D), B4 (E) and mixed culture of B1, B2, B3, and B4 (F). The shaded peak indicated the quantity of C4-HSL.

### 3.3. Results

#### 3.2.1. Bacterial AHL Production

UPLC-MS/MS detected C4-HSL, the AI-1 molecule in all cell supernatants of the Carlsbad bacterial isolates, B1, B2, B3, and B4 (Figure 3.2B, C, D, & E). Optimal C4-HSL production was found in the early exponential phase of cell growth (~6 h after sub-culture) where the OD<sub>600</sub> reached between 0.7 and 1.0. The mixed bacterial culture, containing all four isolates produced the highest relative concentration of C4-HSL (Figure 3.2F). C6-HSL was also detected in trace amounts in the exponential growth phase of B1, B2, B3, and B4 cultures as well



as in a mixed culture of these isolates (data not shown). In comparison to C6-HSL, C4-HSL production was relatively higher in both single and mixed cell cultures. Both AHL concentrations were significantly lower or nearly undetectable in the supernatants of overnight cultures. The results indicated that AHL production is dependent on bacterial species and bacterial growth phase.

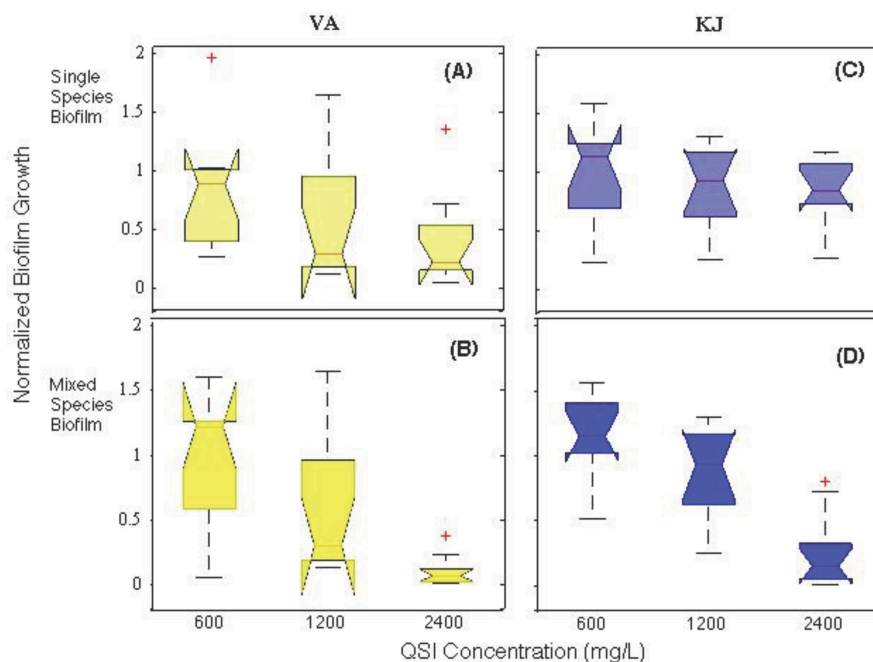


**Figure 3.3.** Normalized biofilm growth in samples treated with the AI-1 inhibitors, VA (A, B) and KJ (C, D) shown as the ratio of the QSI treated to control biofilm growth at different QSI concentrations. Single species marine bacterial biofilm (A, C) comprised of isolates from Carlsbad Desalination Plant, CA (B1, B2, B3, and B4) and Perth Desalination Plant, Western Australia (RO16, RO28, RO32, and C10). Mixed species biofilm (B, D) used the mixture of bacterial isolates from Carlsbad, CA or uncultured native seawater marine bacterial communities from Long Beach, Newport Beach, and Dana Point, CA.

### 3.2.2. *Effect of QSI on Biofilm Growth*

Normalized biofilm growth (the ratio of the QSI treated to control biofilm) in samples treated with the AI-1 inhibitors (VA and KJ) and AI-1/AI-2 inhibitors (F-30 and CNMA) are

shown in Figure 3.3 and 3.4, respectively. The microtiter plate assay results indicated the anti-biofilm capability of each QSI varied, ranging from 5 to 95% with a number of outliers (Figures 3 & 4). Overall, testing concentrations of less than 600 mg/L of VA, KJ, and CNMA did not have a reduction effect on biofilm growth while concentrations below 30 mg/L of F-30 did have an effect.

VA at concentrations above 1200 mg/L substantially reduced biofilm formed by five of the single bacterial isolates tested, ranging from 79.9 to 87.5% (Figure 3.3A). The other three isolates B1, B3, and RO32 showed an increase in biofilm production as noted by the upper range in the boxplot variance in Figure 3A. VA at the same concentration also exhibited significant mixed species biofilm reduction for the four Carlsbad bacterial isolates and native uncultured seawater bacterial communities, ranging from 69.8% to 94.8% (Figure 3.3B). In comparison, KJ at 1200 mg/L was less effective at inhibiting single species biofilm formation and in some cases encouraged biofilm production. Only at the highest concentration (2400 mg/L) was there significant biofilm reduction for the RO28 strain as indicated by the lowest whisker point on the boxplot (Figure 3.3C). Similar responses to KJ were also observed for mixed species bacterial biofilm (Figure 3.3D).

The anti-biofilm formation effects of the AI-1/AI-2 inhibitors (F-30 and CNMA) improved from single species to mixed bacterial communities (Figure 3.4). F-30 at 30 mg/L decreased mixed species biofilm production between 85.7% and 96.3%, whereas CNMA at 1200 mg/L reduced mixed species biofilm between 70.7% and 90.8% (Figure 3.4B,D). The only exception was for a Newport Beach sample, where biofilm production increased in the presence of 20 mg/L of F-30 as indicated by the outlier in Figure 4B. Individual bacterial strains responded to CNMA at concentrations above 1200 mg/L differently as shown by the large range for the normalized biofilm growth with an outlier in the upper range (Figure 3.4C).

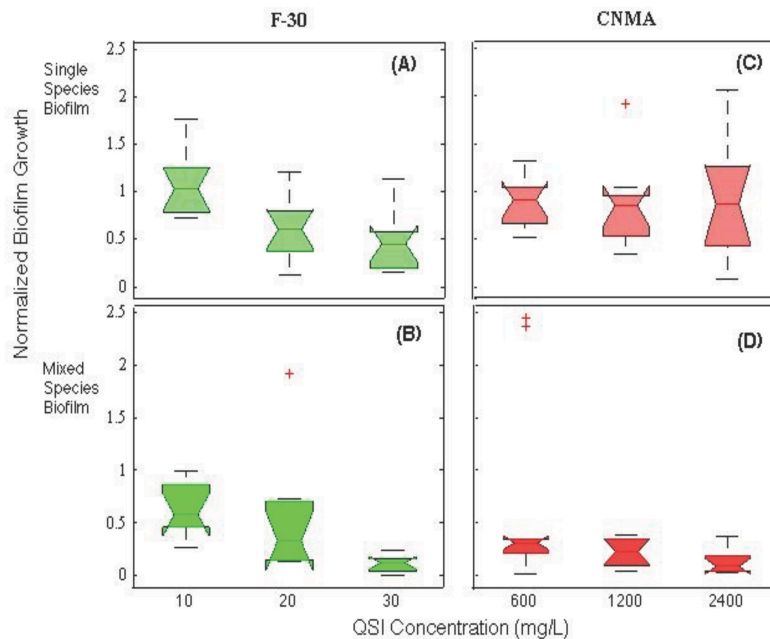


**Figure 3.4.** Normalized biofilm growth in samples treated with the AI-1/AI-2 inhibitors, F-30 (A, B) and CNMA (C, D) shown as the ratio of the QSI treated to control biofilm growth at different QSI concentrations. Single species marine bacterial biofilm (A, C) comprised of isolates from desalination plants in Carlsbad, CA (B1, B2, B3, and B4) and Perth, Western Australia (RO16, RO28, RO32, and C10). Mixed species biofilm (B, D) used the mixture of bacterial isolates from Carlsbad, CA or uncultured native seawater marine bacterial communities from Long Beach, Newport Beach, and Dana Point, CA.

VA was chosen as the AI-1 and CNMA as the AI-1/AI-2 system inhibitors for the subsequent membrane biofouling study. The dose of 1200 mg/L was selected for both QSIs due to median inhibition of biofilm. Although F-30 exhibited excellent biofilm reduction capabilities, it was not selected to move forward with because of toxicity concerns with similar brominated furanone compounds, which arise as disinfection by-products in drinking water systems [152, 153].

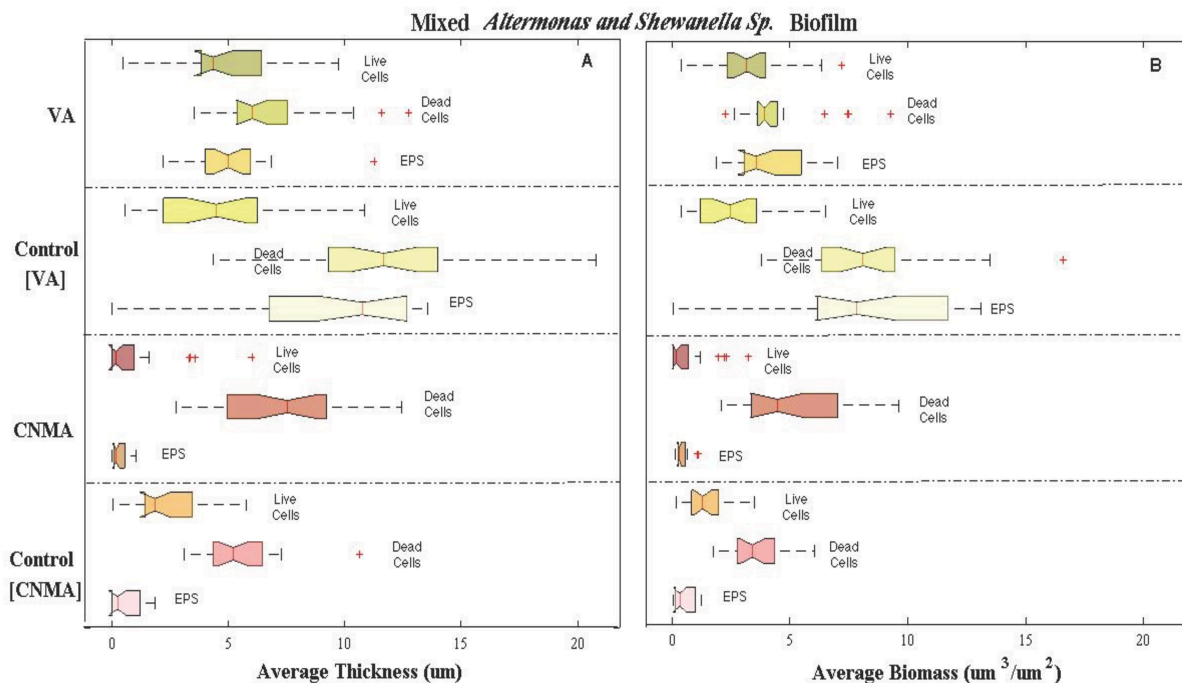


**Figure 3.5.** RO membrane biofilm formed from four mixed species bacterial isolates from Carlsbad, CA (B1, B2, B3 and B4). Samples were subjected to VA (top), CNMA (bottom), and their respective controls (methanol and DI water). The effectiveness of VA and CNMA to reduce marine biofilm were evaluated by comparing average biofilm thickness (A) and biomass (B) in EPS, dead cells and live cells for QSI treated samples and controls.

### 3.2.3. QSI Effect on RO Membrane Biofilm Reduction

Figure 3.5 shows the average membrane biofilm thickness and biomass in VA and CNMA treated mixed bacterial biofilm from Carlsbad and their respective controls. VA significantly reduced membrane EPS and dead cell thickness and biomass between 42% and 51%. However, there was no considerable difference in live cell biomass and thickness. In comparison, there were no significant differences observed in CNMA treated and its control membranes for all biofilm parameters tested, which may be due to the effect of methanol used as the control on membrane biofilm. In these experiments, methanol without QSI also reduced membrane biofilm biomass and thickness in comparison to DI water treated biofilm (used as control for VA) for all parameters tested (Figure 3.5). Therefore, the effect of CNMA on membrane biofilm reduction was inconclusive.

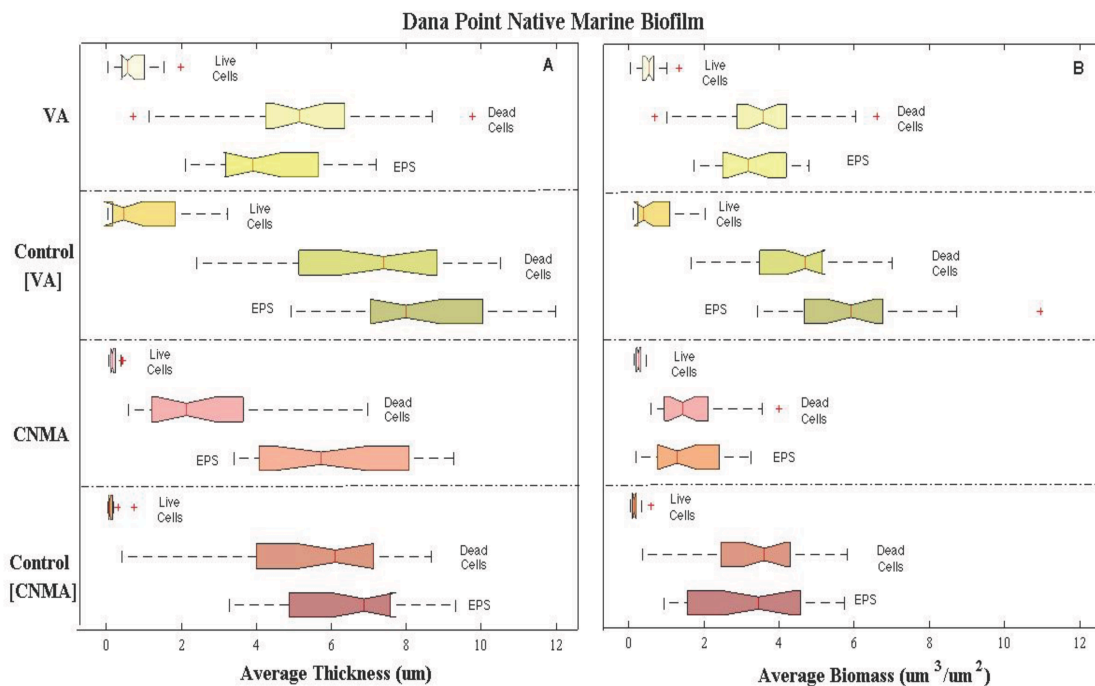


**Figure 3.6.** RO membrane biofilm formed by native marine bacterial community from Dana Point, CA. Samples were treated by VA (top), CNMA, (bottom), and their respective controls (methanol and DI water). The effectiveness of CNMA and VA to reduce marine biofilm were evaluated by comparing average biofilm thickness (A) and biomass (B) in EPS, dead cells and live cells for QSI treated samples and controls.

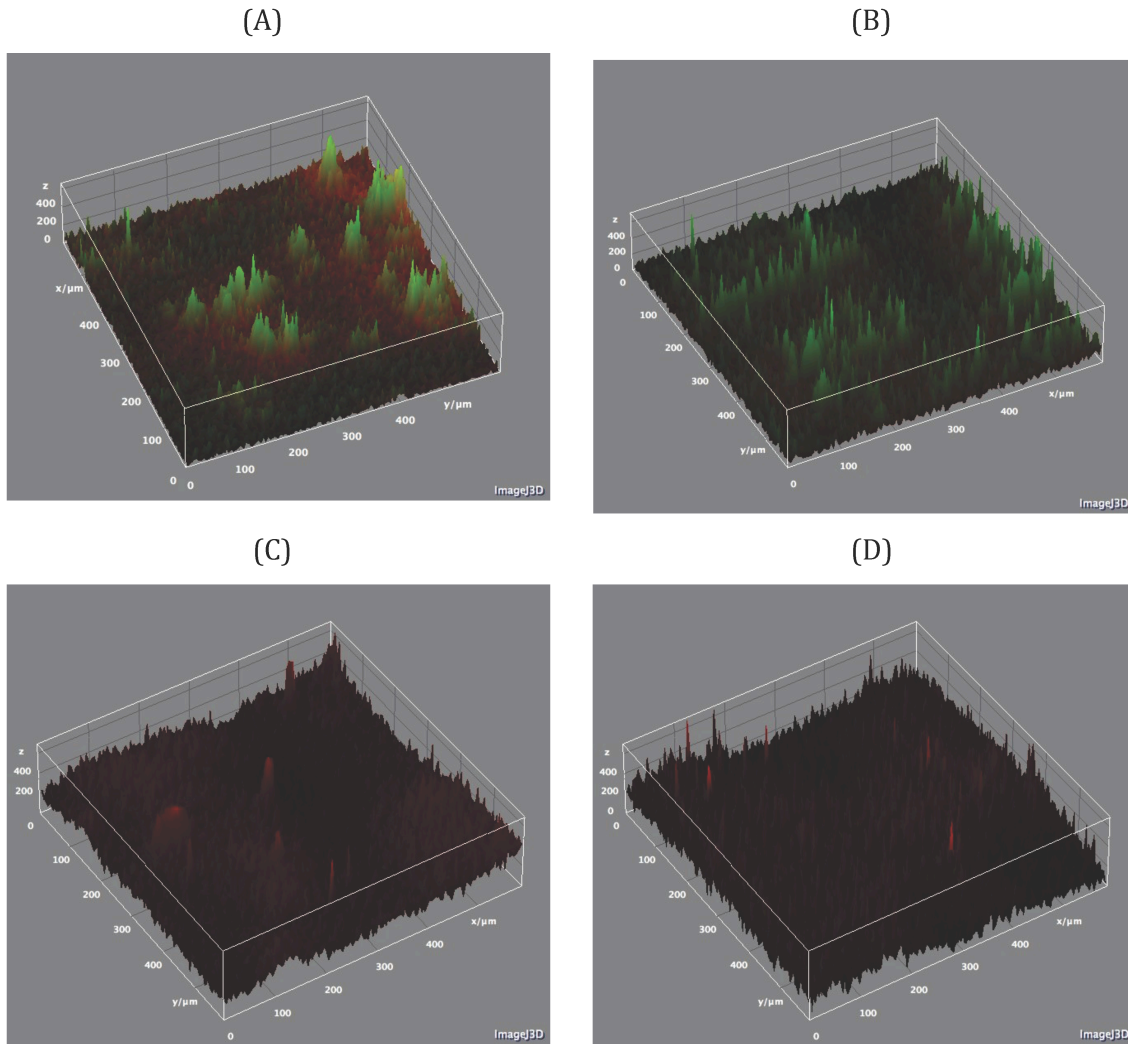


**Figure 3.7.** CSLM 3-D images of control (A, C) and VA treated (B, D) RO membranes that were subjected to biofouling by Dana Point natural bacterial community. Images were captured 48 hours after the initiation of the experiment. Attached live and dead bacterial cells on the control and the VA treated RO membrane are shown in image (A) and (B), respectively. EPS on the control and the VA treated RO membrane is shown in image (C) and (D), respectively. The x-axis and y-axis of the image shows EPS or live and dead cells along the membrane surface. The z-axis measures the fluorescence intensity of EPS or live and dead cells.

Similar observations for the effect of VA and CNMA on membrane biofilm reduction were made for the Dana Point native seawater bacterial community (Figure 3.6). The 3D images acquired by CSLM in Figure 3.7 illustrate the spatial distribution of Dana Point biofilm with and without treatment by VA. Both control and VA treated samples have uneven distribution of

bacterial cells and EPS along the membrane surface. The decrease in dead cells and EPS were visible for samples treated by VA (Figure 3.7B,D). The decrease in EPS was further evident using COMSTAT2 analysis where biomass and thickness were significantly reduced by 46% and 49%, respectively (Figure 3.6). Similar to Carlsbad mixed isolates, there was no significant difference in live cell biomass and thickness (Figure 3.6). Overall VA, the AI-1 system inhibitor, consistently and effectively reduced RO membrane EPS production and dead cells for both the mixed isolates and native bacterial communities.

### **3.4. Discussion**

Understanding bacterial communication pathways and inhibition of their QS molecules potentially holds the key to prevent biofilm formation and ultimately membrane biofouling. This research worked towards this goal by quantifying the production of AHL molecules among a mixed culture of RO membrane biofouling bacterial isolates as well as demonstrating the relationship between the phase of bacterial growth and the rate of QS molecule production. This study further identified the most effective QSIs that are potentially suitable for water treatment technology by comparing the anti-biofouling effects of several commercially available and inexpensive QSIs. Lastly, this research was the first to demonstrate the effectiveness of QSI in a membrane system for biofilm reduction formed by native marine bacterial communities.

The bacterial isolates used in this study are part of the dominant group of bacteria present on fouled RO membrane surfaces for seawater desalination, which is a good representation of the behavior of marine biofouling community [37, 38, 89, 154]. The crystal violet assay results of native marine bacterial communities were mostly consistent with individual isolates' response to QSI treatment. However, the individual isolates also displayed variability in biofilm reduction in

response to different QSIs, suggesting multiple QSIs should be applied simultaneously to block multiple QS pathways for effective biofouling reduction.

Characterizing QS production in single or mixed bacterial species is essential for selecting an appropriate QSI because the QSI's anti-biofilm capability is dependent on the type and concentration of QS signaling compounds present. We have shown that C4-HSL and C6-HSL were produced in single species *Alteromonas sp.* and *Shewanella sp.* biofilm, which was consistent with past studies [155, 156]. We have further demonstrated that co-cultivation of four different species in the same culture always produced a higher C4-HSL concentration than any of the individual cultures under the same growth conditions. Therefore, the variability in biofilm reduction in the QSI crystal violet microtiter plate screening was attributed to type and concentration of the QS compound secreted, which varied from single isolates to mixed isolates to native bacterial communities. The AHL quantification results among randomly selected isolates also indicate that AI-1 QS pathway is universally present in the majority of seawater desalination fouling bacteria.

Through comparing four different QSIs in the crystal violet assay, VA was demonstrated to be the most effective because the majority of single and mixed bacterial biofilm communities were significantly inhibited (>69.8%). In addition, VA significantly suppressed EPS secretion on RO membrane surfaces, which is likely to offer long-term benefits in preventing permeate flux decline since EPS has been attributed to reducing efficiency of convective process [157, 158]. VA treatment did not significantly change the live cell biomass on RO membrane surfaces, indicating the reduction of EPS was not due to the lethal effect of VA on bacteria. The effectiveness of VA was attributed to its ability to interfere with bacterial AHL without the need to diffuse into the cell membrane. The scavenging of AHL in cell suspension effectively reduced



the level of AHL and its binding to the transcription regulator to trigger biofilm production. This mechanism was more effective in comparison with QSIs that require diffusion into the cell membrane as a competitor to the auto-inducer binding site [16, 126].

CNMA, the second most effective QSI identified in the crystal violet assay, significantly reduced biofilm formation at 1200 mg/L in microtiter plates. However, there were no consistencies in the effect of CNMA on membrane biofilm reduction for native bacterial communities. The efficiency of CNMA to inhibit biofilm formation may rely on its diffusion through the cell membrane to inhibit the AI-1 and AI-2 molecules from binding to the appropriate receptor protein [130, 131]. The interactions between CNMA, marine bacteria, and membrane surface require further investigation to understand the complexity.

These findings also imply that the QSI's anti-biofilm capability is dependent not only on the bacterial species present and QS production but also on the hydrodynamic and substrate surface properties. The magnitude of biofilm reduction by VA and CNMA decreased from the microtiter plate to the RO membrane surface. This was potentially due to the change from static to dynamic water conditions and increased surface area on the RO membrane surface, which altered bacterial attachment efficiency. On the larger RO membrane surface, the observed bacterial attachment and growth were uneven as found in this and past research [159], which hindered the ability of QSI to reach all bacteria. The surface characteristics such as hydrophobicity and surface roughness have been known to play an important role in bacterial attachment [160]. Bacteria were less likely to attach and grow on the smooth polystyrene microtiter plate than the rough polyamide membrane surface.

For both the microtiter plate and the RO membrane biofouling studies, the QSI concentration required in the bulk fluid was high and needed a constant dose to suppress biofilm

because the QSI was only effective against their respective QS pathway before biofilm formation was activated. The environmental impacts associated with discharge of QSI with concentrate reject have not been studied although both VA and CNMA are non-toxic to humans as food additives at the concentrations similar to those tested in this study. However, the requirement of a continuous dose of QSI in the intake water at a high concentration would be in practical as an approach for biofouling prevention in desalination industry. Incorporation and immobilization of QSI onto the RO membrane surface should be considered in future studies to potentially enhance in-situ membrane anti-biofouling capability. Another approach to improve biofilm inhibition may be to combine multiple QSIs because not all marine bacteria responded to a single type of QSI as shown in the crystal violet assay.

### **3.5. Conclusions**

This study confirmed the production of two low molecular weight AHLs, C4-HSL and C6-HSL among single and mixed marine biofouling bacterial isolates. It further demonstrated that a mixed culture of bacterial isolates always produced a higher C4-HSL concentration than any of the individual cultures under the same growth conditions, suggesting the importance of interspecies interactions in AHL production. The microtiter plate assay identified VA and CNMA as the best candidates to reduce marine biofilm formation. VA was further shown to effectively suppress EPS production for various marine bacterial communities on the RO membrane surface. The findings indicate that QSIs have the potential to alleviate seawater desalination membrane bacterial fouling and reduce operational costs.

## **CHAPTER 4. QSI MODIFIED RO MEMBRANES FOR BIOFOULING PREVENTION IN SEAWATER DESALINATION**

### **Abstract**

Quorum sensing (QS) pathways regulate bacterial communication to activate biofilm development, which is the main source of membrane biofouling. Recent studies have identified the important role of QS inhibiting (QSI) compounds to disrupt QS pathways and ultimately biofilm production. This study physically adsorbed the QSIs, vanillin and cinnamaldehyde onto various RO membrane surfaces to enhance the membrane in-situ anti-biofouling potential. The QSI layer on the RO membrane surface significantly altered the membrane surface contact angle to reflect the property of the QSI along with less than a 16% reduction in pure water permeability and no significant change in salt rejection. QSI modified membranes subjected to biofouling conditions in a high-pressure RO system experienced a minimal loss in permeate flux compared to unmodified membranes. The QSI modified membranes significantly suppressed extracellular polysaccharide production (>15%), live bacteria (>58%), and dead bacteria (>61%) consisting of a mixed culture of four different biofilm forming marine bacterial isolates on the membrane surface.

#### **4.1.Introduction**

Non-conventional water treatment technologies such as water reuse and seawater desalination rely on thin-film composite (TFC) reverse osmosis (RO) membranes to produce high quality drinking water. TFC membranes consist of an ultra-thin polyamide layer (0.2  $\mu\text{m}$  thick) supported by a micro-porous polysulfone intermediate layer (40-50  $\mu\text{m}$  thick), and a polyester structural support (120-150  $\mu\text{m}$ ) [35]. TFC membranes achieve high permeate flux and salt rejection due to the micro-porous intermediate layer that allows the ultra-thin layer to withstand high-pressure compaction as well as the ultra-thin layer that decreases resistance in permeate transport [28-30, 35].

However, biofouling compromises membrane integrity and remains a major challenge for the membrane industry. Biofouling is product of the deposition and aggregation of bacteria and their metabolic products on the membrane surface [57-59]. During a fouling event in the RO system, the applied pressure compacts the fouling layer, which reduces the ability of the cross-flow velocity to efficiently shear off particles that accumulate on the membrane surface [29, 37]. As a result, the permeate flux declines, which raises operational pressure and energy demand to maintain the original flux conditions [29, 37, 38]. Membrane cleaning processes have been known to be inefficient to restore membrane performance for long periods of time because 1) degraded organic matter in the surrounding environment becomes readily available and stimulates the growth of surviving bacteria on the membrane surface; 2) surviving bacteria may develop a tolerance to chemical cleaning agents; and 3) frequent cleanings degrade the polyamide thin film over time [40-42, 161].

Suppressing bacterial communication pathways, known as quorum sensing (QS) offers a potential approach to inhibit biofilm formation at a biological level. The QS inhibiting agents, cinnamaldehyde (CNMA) and vanillin (VA) are both known to inhibit gram-negative bacterial biofilm formation, which are the predominant biofoulant species on fouled RO membranes in seawater desalination plants [16, 18, 90, 130, 131]. CNMA has been shown to further suppress the bacterial QS pathway responsible for communication between gram-negative and gram-positive bacteria [130-132], which may have broader impacts on biofilm formation. CNMA and VA in the bulk fluid have been demonstrated to effectively reduce marine biofilm production, but biofilm formation on the membrane surface still persists as shown in Section 0. Additionally, QSIs are only effective prior to biofilm formation being activated. Therefore, a constant QSI dose is required, which may be impractical for scale up design and environmental impacts associated with QSI discharge in the waste are unknown. The goal of this research was to incorporate CNMA and VA onto the surface of various RO membranes to lower the membrane potential towards bacterial colonization and biofilm growth. This work further investigated changes to membrane surface and performance under QSI incorporation. The anti-biofouling capabilities of the QSI modified membranes were examined in a well-controlled high-pressure RO system using a mixture of four RO membrane biofouling isolates. Biofilm development on QSI modified and unmodified membranes were examined and compared using confocal microscopy. QSI incorporation and retention on the membrane surface was observed under Raman microscopy.

## 4.2.Methods

### 4.2.1. QSI Compounds

CNMA was diluted in methanol and VA was dissolved in deionized water (DI H<sub>2</sub>O) to a concentration of 1200 mg/L, which was previously determined to be effective to reduce marine biofilm formation in the bulk fluid using a microtiter plate assay and RO membrane bio-monitoring system (Section 3.2.2 & 3.2.3).

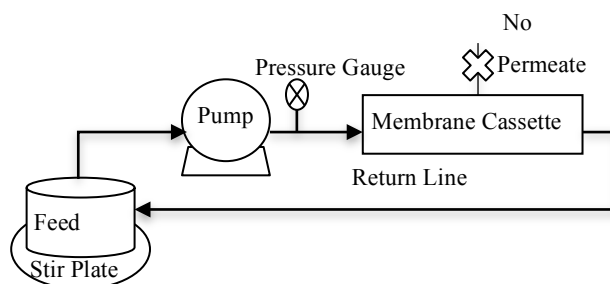


**Figure 4.1.** Set-up for QSI deposition onto the thin film surface of the RO membrane.

### 4.2.2. QSI Modified RO Membranes

Either QSI was incorporated onto the leading commercially available seawater grade polyamide RO membranes, SW30XLE (Dow) and SWC5 (Hydranautics) to ensure consistent QSI deposition following previous approaches [162-164]. The unmodified RO membrane was placed into a cross-flow cell (Figure 4.1) to expose the thin film surface to the QSI solution (1200 mg/L) for 24, 48, and 72 h at a cross-flow rate of 0.005 cm/s with re-circulation and no permeation. Afterwards, the membrane was rinsed with DI H<sub>2</sub>O to remove accumulated particles on the membrane surface and stored in DI H<sub>2</sub>O at 4°C until further analysis.

### 4.2.3. QSI Presence on RO membranes Detected by Raman Microscopy

The presence and stability of either QSI on the membrane surface was determined by Raman *In vivo* microscopy (Renishaw). The Raman spectra of the unmodified RO membrane surfaces and the QSIs, VA (powder) and CNMA (liquid) in their natural state were acquired to determine the QSI signal peaks on the modified RO membrane surfaces. Samples were placed directly under the diode laser to excite the sample at 532nm (visible light range) under 50,000 magnifications. Spectrums were collected

under 3 mW of laser power and 2s exposure time at five random locations for each sample. The baseline was corrected for all spectrums using WIRE 3.4 software (Reinshaw). The maximum amount of QSI deposited onto the membrane surfaces was determined based on significant differences in the expected QSI signal peak areas from 24 to 72 h using a two-tailed T-test with a 95% confidence level in Microsoft Excel.

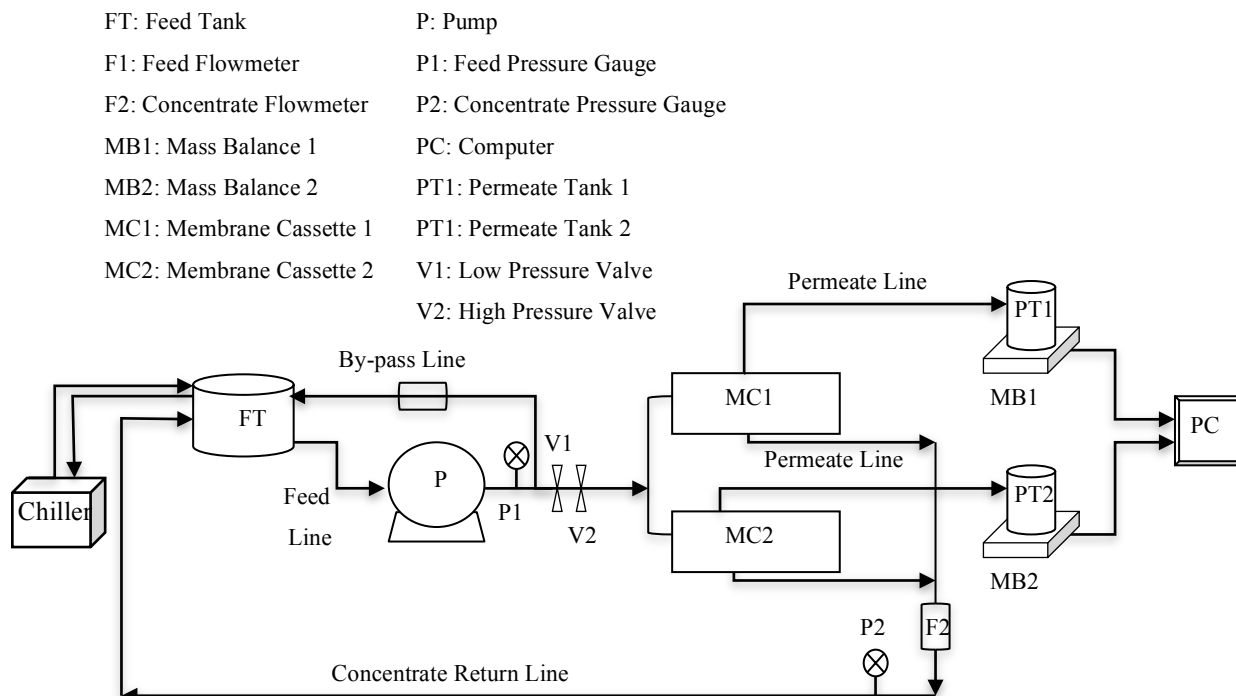


**Figure 4.2.** High pressure RO system schematic.

#### **4.2.4. Membrane Performance and Surface Property Characterization**

The QSI-RO membrane permeability and salt rejection rates were investigated in a high pressure RO flow cell (Figure 4.2) similar to past methods [165]. The QSI-RO membrane was placed in a high-pressure cassette holder (CF402, Sterlitech) with DI H<sub>2</sub>O as the feed solution at 25°C. The starting pressure was set to 450 psi with a cross-flow velocity of 15 cm/s for membrane compaction and equalization. Afterwards, the flux rate was monitored for 60 minutes using a digital balance to continuously record the permeate weight. At the end of the permeability test, the membrane salt rejection rate was carried out with 50mM of sodium

chloride solution in the feed tank. After the system reached steady-state conditions, conductivity measurements were taken of the permeate and feed streams to calculate the salt rejection rate.

The hydrophilicity of the QSI-RO membrane was tested using the sessile drop contact angle method with a Goniometer (Rame-Hart) as presented in previous studies [72, 166, 167]. DI H<sub>2</sub>O (1  $\mu$ L) was placed in ten random locations on each membrane sample and an image was acquired of the water droplet. The left and right contact angle were measured using Image J's LB-ASADA plugin program. The results of the QSI-RO membrane testing parameters were compared with an unmodified RO membrane under the same testing conditions.

#### ***4.2.5. QSI-RO Membrane Anti-Biofouling Capability***

The anti-biofouling capabilities of the QSI modified and unmodified RO membranes were examined in the high pressure RO system (Figure 4.2). The bacterial strains, *Alteromonas sp.* (B2 and B4) and *Shewanella sp.* (B1 and B3), isolated from fouled RO membranes at a desalination pilot plant in Carlsbad, California (CA) were separately inoculated into artificial seawater with 0.5g/L peptone and 0.25 g/L yeast (ASWJP + 1/2PY) [146, 168]. The bacterial strains were then incubated on a shaker for 24 h at 21°C. Either the QSI modified or unmodified membranes were placed into two high pressure cassette holders with ASWJP as the feed solution at the operational parameters of 450 psi, 15 cm/s, and 25 °C. After overnight stabilization, minimal amounts of peptone (0.31 g/L) and yeast (0.06 g/L) were added to the feed tank to accelerate the fouling rate. An equal portion of each of the four bacterial cultures were diluted (1:100) in the feed tank. The system continued to run at the same low operating conditions in order to develop a thick biofilm layer within a 24 h period. The drip permeate flux rate was continuously monitored during the experimental period while the concentrate stream was re-



circulated back to the feed tank. Cell density within the feed tank was periodically taken using an optical density of 600nm (OD<sub>600</sub>, Biophotometer, Eppendorf). At the end of the experiment, the biofouled membranes were removed to assess membrane biofilm formation. QSI retention on membrane surfaces was further investigated under Raman microscopy to determine if there were any significant differences in the QSI signal peak areas between the maximum deposited and biofouled QSI membranes using the two-tailed T-test with a 95% confidence level in Microsoft Excel.

#### ***4.2.6. Membrane Biofilm Characterization***

Biofilm development was analyzed on biofouled membrane samples using Confocal Laser Scanning Microscopy (CLSM, Zeiss LSM 700). Live and dead cells were stained with SYTO9 (green) and propidium iodide (red), respectively (FilmTracer<sup>TM</sup> LIVE/DEAD<sup>®</sup> Biofilm Viability Kit, Invitrogen). EPS was characterized on separate membrane samples using ConA lectin (Concanavalin A Conjugates, Invitrogen) [150]. EPS, live cells, and dead cells were imaged at twenty locations along the length of the membrane using excitation/emission wavelengths of 555/580, 480/500, and 555/580 nm, respectively. Biomass and thickness of EPS, live cells, and dead cells were further analyzed using COMTSTAT 2 under standard automatic thresholding and connected volume filtering [151, 169]. Significant differences between biofilm biomass and thickness on QSI modified and unmodified RO membranes were determined using notched boxplots in MATLAB and two-tailed T-tests with a 95% confidence in Microsoft Excel.

## 4.3.Result

### 4.3.1. QSI Deposited RO Membranes and Stability

Raman spectroscopy (Figure 4.3, 4.4) revealed that the polyamide thin film RO membranes, SWC5 and SW30XLE have major spectral peaks located at a Raman shift of 790, 1074, 1148, 1587, and 1608  $\text{cm}^{-1}$ , which was previously determined to be associated with the polyamide functional groups [170]. QSI (CNMA and VA) deposited RO membranes have the characteristic polyamide peaks at shifts corresponding to 790, 1074, 1148, 1587, and 1608  $\text{cm}^{-1}$  as well (Figure 4.3 & 4.4).

Additionally, CNMA deposited RO membranes have significant peak formation at 1002, 1251, 1597, 1628, and 1677  $\text{cm}^{-1}$ , which was consistent with peaks belonging to CNMA in its natural state (liquid) as depicted in Figure 4.3A,C. Past research has further identified that these peaks belong to C-H, C=O, and C=C bonds on the aldehyde and benzene functional groups of CNMA [171, 172].

Similar to CNMA, VA incorporated membranes and VA in its natural state (powder) shared a major peak at a Raman shift of 1677  $\text{cm}^{-1}$  with minor peak formations located at 999 and 1253  $\text{cm}^{-1}$  (Figure 4.4A,C) [171, 173, 174]. A major peak was observed at a Raman shift of 1628  $\text{cm}^{-1}$  for VA deposited membranes, which did not correspond to either VA or the polyamide thin film (Figure 4.4A,C).

Raman spectroscopy further determined that the maximum amount of both QSIs deposited onto the membrane surface occurred within 24 and 48 h for SWC5 and SW30XLE membranes, respectively based on the significantly greater QSI signal peak areas at those time periods (Figure 4.3B,D & 4.4B,D).

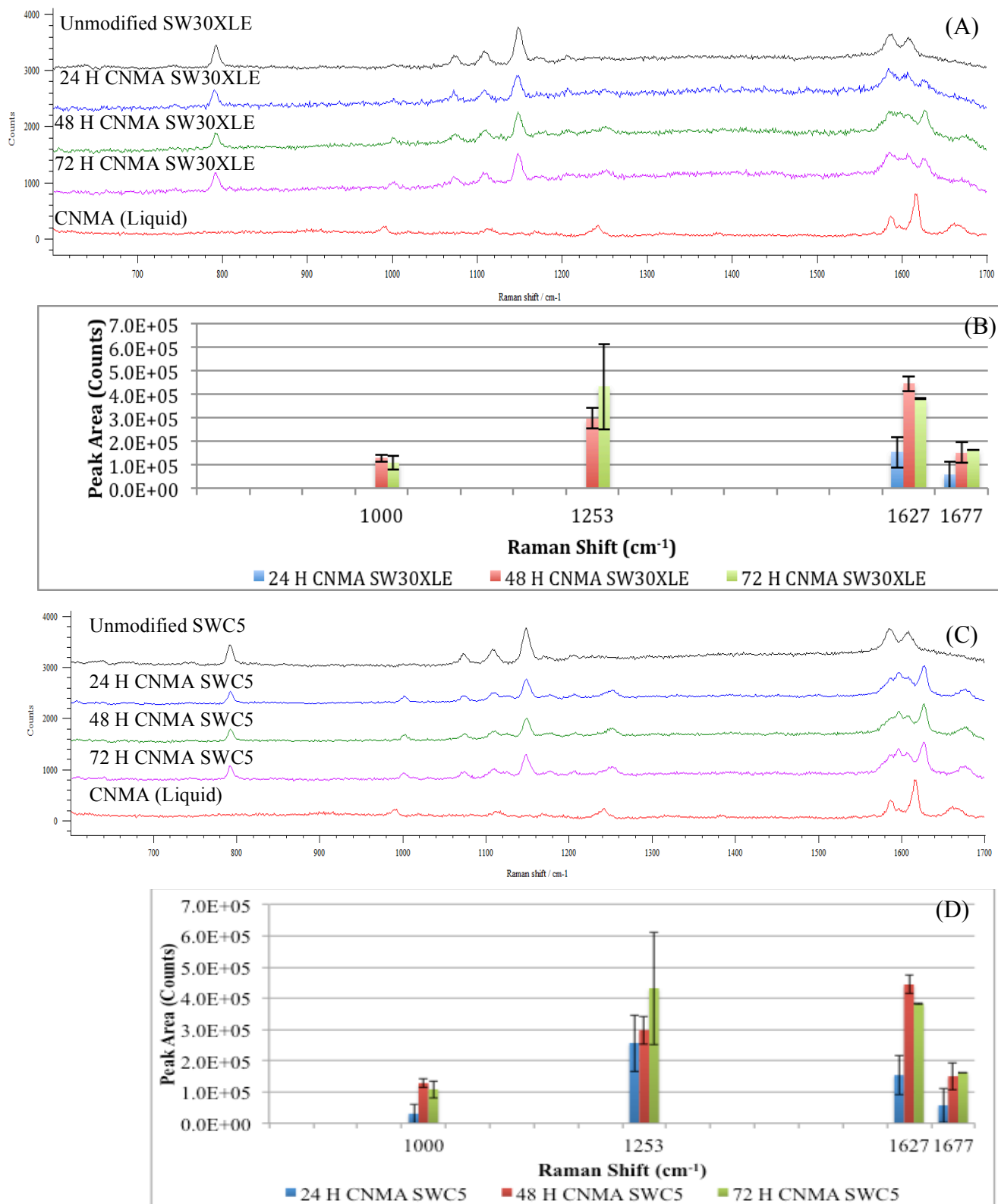


**Figure 4.3.** Characterization of CNMA deposited Dow SW30XLE (A,B) and Hydranautics SWC5 (C,D) RO membranes. CNMA peaks associated with the CNMA RO membrane were revealed based on the Raman spectra for the CNMA modified and unmodified membranes and CNMA in its natural state as a liquid (A,C). The time period for the maximum amount of CNMA incorporated onto the membrane surface was determined based on the QSI peak areas (1000, 1253, 1627, and 1677 cm<sup>-1</sup>) at 24, 48, and 72 h (B,D).

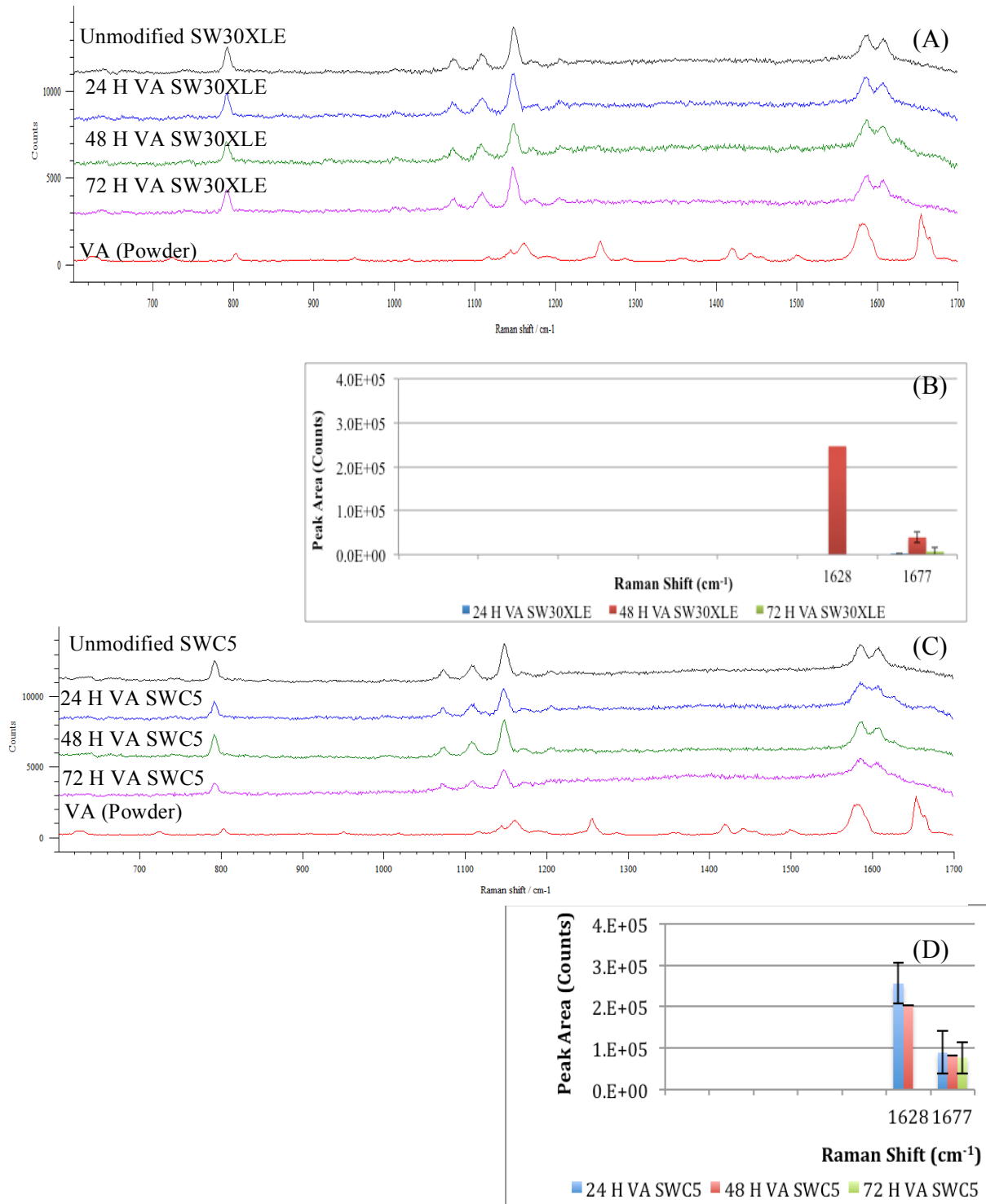


**Figure 4.4.** Surface characterization for VA deposited Dow SW30XLE and Hydranautics SWC5 RO membrane. VA peaks were identified based on the Raman spectra for the VA modified and unmodified membranes and VA in its natural state (A,C). The time at which the maximum amount of VA was deposited onto the membrane was based on the QSI peak areas (1628 and 1677 cm<sup>-1</sup>) at 24, 48, and 72 h (B,D).

### 4.3.2. QSI-RO Membrane Performance and Surface Property

The pure water permeate flux (Figure 4.5A) for QSI modified and unmodified RO membranes were evaluated at an operating pressure of 450 psi and a cross-flow velocity of 15 cm/s. CNMA RO membranes experienced between 12% and 16% reduction in pure water permeate flux compared to unmodified RO membranes (Figure 4.5A). In comparison to unmodified membranes, VA SWC5 membranes experienced minimal changes in permeate flux while VA SW30XLE membranes exhibited a 10% reduction in permeate flux (Figure 4.5A). In addition, no significant difference in the salt rejection between QSI and unmodified RO membranes were observed (Figure 4.5B).

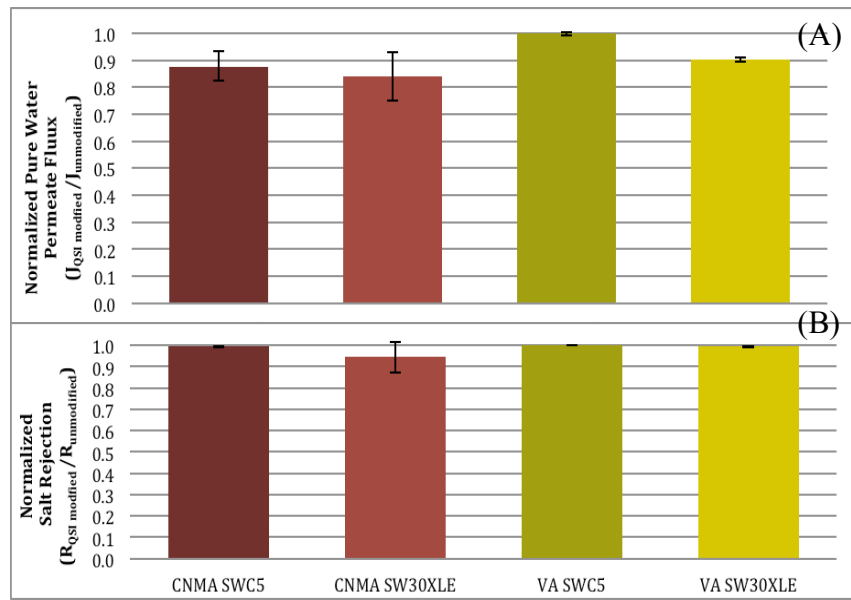


**Figure 4.5.** QSI modified RO membrane performance. Normalized pure water permeate flux (A) and salt rejection rates (B) were calculated by the ratio of QSI RO membrane to unmodified membrane performance.

Figure 4.6 revealed that QSI modified membranes retained its hydrophilic nature from unmodified membranes. Prior QSI incorporation, the unmodified SW30XLE ( $35.66^{\circ} \pm 2.52$ ) membrane was significantly more hydrophilic

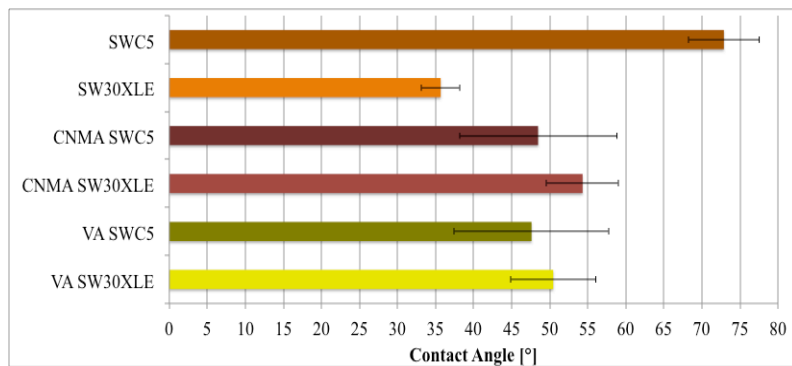


**Figure 4.6.** Contact angle measurements for the unmodified SWC5 (Hydranautics) and SW30XLE (Dow) membranes as well as the CNMA and VA deposited SWC5 and SW30XLE membranes.

than the SWC5 membrane ( $72.89^\circ \pm 4.63$ ) (Figure 4.6). The contact angle for CNMA and VA SWC5 membranes significantly decreased to  $48.47^\circ \pm 10.36$  and  $47.61^\circ \pm 10.15$  while the CNMA and VA SW30XLE membranes increased to  $54.32^\circ \pm 4.73$  and  $50.46^\circ \pm 5.59$  (Figure 4.6).

#### 4.3.3. QSI-RO Membrane Biofilm Formation

QSI and unmodified SWC5 and SW30XLE membranes experienced different trends in permeate flux over the biofouling period (Figure 4.7). The permeate flux for CNMA and VA deposited SWC5 RO membranes were similar to the unmodified SWC5 membrane permeate flux over the biofouling period (Figure 4.7A). For CNMA and VA SW30XLE membranes, the

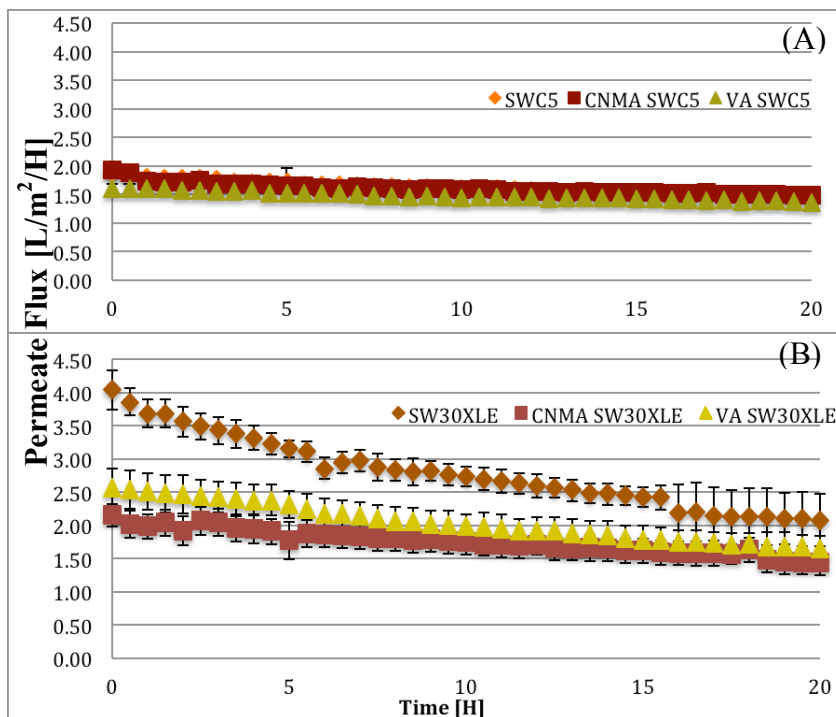


**Figure 4.7.** Permeate flux over the biofouling period for QSI (CNMA and VA) modified and unmodified RO membranes, SWC5 (A) and SW30XLE (B).

starting permeate flux was reduced by 40% compared to the unmodified membrane (Figure 4.7B). However, both QSI deposited SW30XLE membranes experienced less decline in permeate flux over the biofouling period compared to the unmodified SW30XLE membrane (Figure 4.7B).

CNMA deposited SWC5 and SW30XLE membranes experienced similar permeate flux over the biofouling period (Figure 4.7A,B). CSLM further revealed that CNMA deposited membranes have similar trends in reduction of biofilm formation compared to unmodified

membranes (Figure 4.8). CNMA SWC5 membranes experienced a 61.93% and 75.12% significant decrease in live cell biomass and thickness with a 33.64% and 28.91% reduction in dead cell biomass and thickness (Figure 4.8A,B). CNMA SW30XLE membranes have a 59.18% reduction in live cell thickness along with a significant decrease in dead cells biomass at 27.71% and thickness at 29.43% (Figure 4.7A,B). Additionally, CNMA SWC5 and SW30XLE membranes have a 15.53% and 22.80% reduction in EPS thickness, respectively (Figure 4.8B).

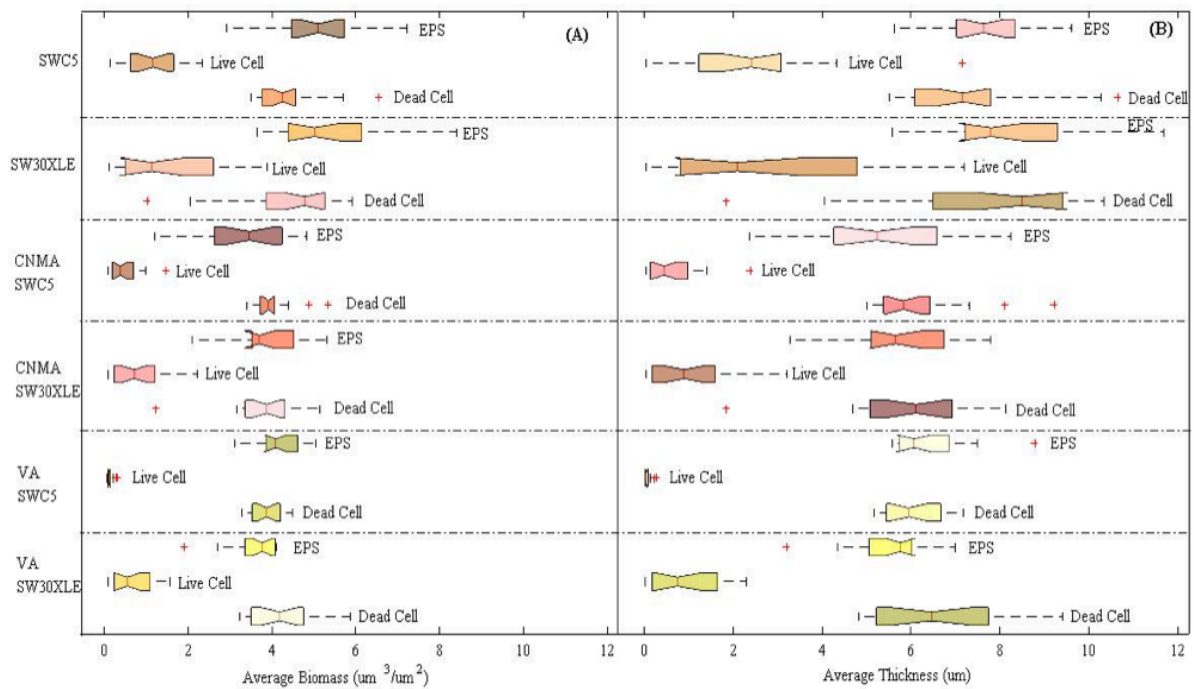


**Figure 4.8.** Biofilm formation on CNMA and VA modified and unmodified RO membranes (Hydranautics SWC5 and Dow SW30XLE) formed by a mixed culture of *Alteromonas sp.* and *Shewanella sp.* bacterial isolates. The effectiveness of QSI deposited RO membranes to reduce membrane biofilm formation was evaluated by comparing EPS, live and dead cell biomass (A) and thickness (B) with unmodified membranes.

However, VA deposited RO membranes experienced different trends in permeate flux (Figure 4.7) as well as biofilm formation (Figure 4.8). The VA modified SWC5 RO membrane experienced a lower starting permeate flux with minimal change over the biofouling period compared to VA SW30XLE (Figure 4.7A,B). VA SWC5 also had a significant reduction in live

and dead cell biomass (90.97% and 97.83%) and thickness (18.79% and 16.41%). The VA SWC5 membrane further experienced a significant reduction in EPS biomass (11.71%) and thickness (17.68%) as presented in Figures 4.8A,B. VA SW30XLE membrane showed a significant reduction in live and dead cell biomass (58.39% & 31.57%) and thickness (67.62% & 32.16%) with no considerable difference in EPS production (Figure 4.8A,B). After the biofouling period, the QSI peaks associated with both VA and CNMA were not significantly retained on the modified membrane surfaces (Figure 4.9).

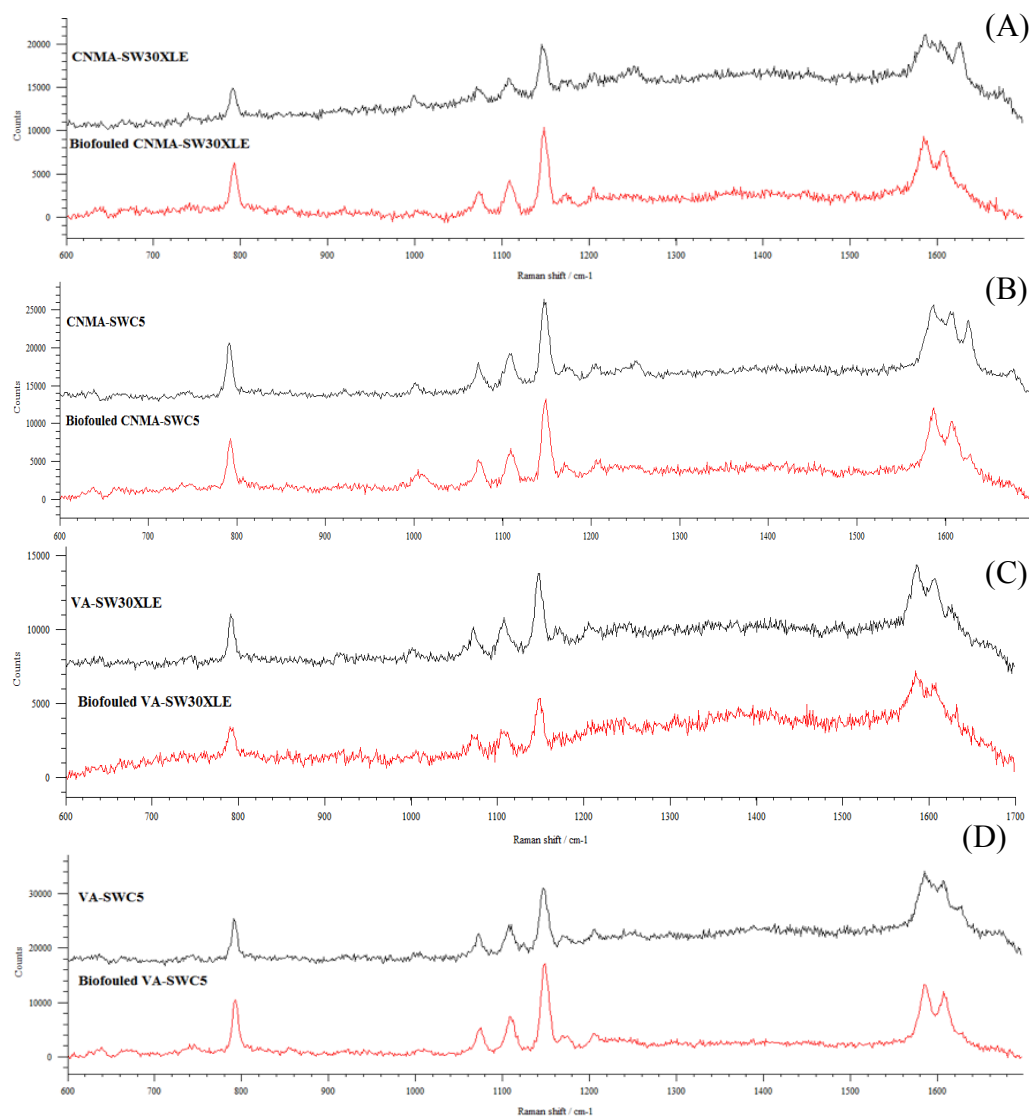


**Figure 4.9.** Raman spectra of the maximum CNMA deposited and biofouled SW30XLE (A) and SWC5 (B) membranes along with the VASW30XLE (C) and SWC5 (D) membranes before and after the biofouling event, respectively. QSI retention on the membrane surface was based on the QSI peak areas for CNMA (1000, 1253, 1627, and 1677  $\text{cm}^{-1}$ ) and VA (1628 and 1677  $\text{cm}^{-1}$ ) before and after the biofouling event. Biofouled QSI RO membranes showed minimal QSI peak formation, which could not be quantified.



#### 4.4. Discussion

This research worked to improve the membrane anti-biofouling potential by successfully incorporating the QSI compounds, CNMA and VA onto the thin film layer of two commercially available RO membrane surfaces. This work further demonstrated that QSI modified membranes significantly suppressed membrane biofilm formation with minimal loss in permeate flux over the biofouling period compared to unmodified membranes.

CNMA and VA deposited primarily through physical adsorption onto the RO membrane surfaces since the majority of peaks on the QSI modified RO membranes belonged to either the unmodified membrane or the QSI in its natural form (Figure 4.3,4.4). A chemical bond potentially formed between VA and the polyamide thin film based on the significant peak formation located at a Raman shift of  $1628\text{ cm}^{-1}$  (Figure 4.4A,C), which was not present on the unmodified membrane surfaces or VA (powder). Past research has shown that this peak correlates to a Schiff base reaction [175] between the aldehyde (VA) and amide (polyamide) functional groups.

QSIs also adsorbed unevenly onto the polyamide thin film surface as illustrated by the large standard deviations in the QSI peak areas (Figure 4.3B, 4.4B) and contact angle measurements (Figure 4.6), which was potentially due to the inherent SWC5 and SW30XLE membrane surface roughness. In addition, there was no significant difference in contact angle measurements between QSI deposited SWC5 and SW30XLE RO membranes because these QSIs have limited water solubility due to the presence of hydrophobic (i.e. benzene) and hydrophilic (i.e. aldehyde) functional groups. Therefore, the QSI layer on the RO membrane surface significantly altered the contact angle to reflect the property of either CNMA or VA (Figure 4.6).

Since QSIs deposited primarily through physical adsorption, the QSI layer on the thin film potentially blocked water transport through membrane pores or narrowed pore walls to slow down water transport as indicated by the reduced pure water permeability for QSI modified membranes (Figure 4.5A). This was further evident by the reduced starting permeate flux (<40%) for QSI modified SW30XLE membranes during the biofouling period (Figure 4.7B). However, there was no significant difference in operational flux between QSI and unmodified SWC5 RO membranes (Figure 4.7A). These results indicate that the choice of membrane for surface modification plays an important role in membrane performance.

Overall, QSI deposited RO membranes did not experience a drastic decline in permeate flux over the fouling period compared to the unmodified membranes. This was supported by the fact that QSI deposited membranes consistently had a reduction in live and dead cells compared to unmodified membranes. Furthermore, CNMA modified RO membranes and VA SWC5 suppressed EPS production. The reduction in biofilm could be attributed to either the adsorbed CNMA or VA acting to suppress bacterial communication or the QSI layer creating a physical barrier to hinder bacteria attachment onto the RO membrane surface.

CNMA and VA incorporated RO membranes have the potential to reduce membrane biofouling, but QSIs were not retained on the membrane surface by physical adsorption. Future work should investigate chemically linking QSIs onto the membrane surface to improve QSI stability and water permeability. *Zodrow et al.* [176] covalently linked biodegradable encapsulated CNMA onto a membrane surface, but determined that the low concentration of CNMA released from the membrane surface did not reduce *Escherichia coli* biofilm formation. Thus, the method for QSI incorporation will be key to ensure that the correct QSI concentration is present and that the QSI active site remains unaltered to prevent biofilm formation.

#### 4.5. Conclusions

CNMA and VA physically adsorbed onto RO membrane surfaces with a maximum deposition time of 24 and 48 h for SWC5 and SW30XLE membranes, respectively. The addition of a QSI layer onto the thin film membrane surface altered the membrane contact angle and resulted in reduction of pure water permeability with no significant change in salt rejection. During a biofouling event caused by a mixture of *Alteromonas sp.* and *Shewanella sp.* bacterial strains, QSI deposited membranes experienced less decline in permeate flux along with a significant reduction of biofilm formation compared to unmodified membranes. Since QSIs were not retained on the biofouled membrane surfaces, future work should consider chemically bonding QSIs to the membrane surface to improve QSI stability and water permeability.

## CHAPTER 5. SUMMARY, CONCLUSIONS & RECOMMENDATIONS

Understanding and controlling bacterial communication pathways at a biological level potentially holds the key to inhibit biofilm formation and membrane biofouling. This research worked towards this goal by quantifying the production of auto-inducer 1 (AI-1) signaling molecules among a mixed culture of *Alteromonas sp.* (B2 and B4) and *Shewanella sp.* (B1 and B3) bacterial strains, which were isolated from fouled RO membranes at a local desalination plant. This study determined that the mixed bacterial culture always produced a higher amount of AI-1 molecules than single cultures. This work further showed the relationship between the bacterial growth phase and the rate of AI-1 molecule production.

In addition to understanding the AI-1 molecule production among marine bacterial isolates, this research found that cinnamaldehyde (CNMA) and vanillin (VA) were the most effective quorum sensing inhibiting (QSI) compounds to reduce marine biofilm formation by comparing several commercially available and inexpensive QSIs in a microtiter crystal violet plate assay. This research then demonstrated the reduction of membrane biofilm formed by native marine bacterial communities subjected to QSIs administered in the bulk fluid in a membrane system.

The microtiter plate and the RO membrane biofouling studies indicated inhibition of biofilm required a constant and high concentration of QSI in the bulk fluid because the QSI was only effective before the respective quorum sensing (QS) pathway activated biofilm formation. A continuous and high dose of QSI in the intake water or after the pretreatment process is

impractical and expensive. There are also potential concerns associated with the environmental impact of QSI in the concentrate discharge, which have not been studied. Although, both CNMA and VA are non-toxic food additives at similar concentrations to those tested in these studies.

This research further worked to address these concerns by physically adsorbing CNMA or VA onto the polyamide thin film layer of various RO membrane surfaces. The QSI layer on the RO membrane surface changed the membrane surface properties (i.e. contact angle) to reflect the hydrophilicity of the QSIs. Additionally, the QSI modified RO membranes significantly suppressed membrane biofilm formed by the mixed culture of RO membrane biofouling bacterial isolates with minimal loss in permeate flux in a high pressure RO system.

However, QSIs were not retained on the membrane surface after the biofouling period and the addition of the QSI layer lowered the membrane water permeability rates. Therefore, future work should investigate chemically linking QSIs onto the membrane surface to improve QSI stability and water permeability. It will be important to select a method for QSI incorporation that guarantees the correct QSI dose is present on the membrane surface. Moreover, the chemical linking method should not alter the QSI active site required for biofilm inhibition.

## CHAPTER 6. REFERENCES

- [1] P. Watnick, R. Kolter, Biofilm, City of Microbes, *Journal of Bacteriology*, 182 (2000) 2675-2679.
- [2] K.R. Hardie, K. Heurlier, Establishing bacterial communities by 'word of mouth': LuxS and autoinducer 2 in biofilm development, *Nature Reviews Microbiology*, 6 (2008) 635-643.
- [3] R.P. Schneider, L.M. Ferreira, P. Binder, J.R. Ramos, Analysis of foulant layer in all elements of an RO train, *Journal of Membrane Science*, 261 (2005) 152-162.
- [4] L.F. Greenlee, D.F. Lawler, B.D. Freeman, B. Marrot, P. Moulin, Reverse osmosis desalination: Water sources, technology, and today's challenges, *Water Research*, 43 (2009) 2317-2348.
- [5] M. Gamal Khedr, Membrane fouling problems in reverse osmosis desalination plants, *Desalination & Water Reuse*, 10 (2011) 8-17.
- [6] K.P. Lee, T.C. Arnot, D. Mattia, A review of reverse osmosis membrane materials for desalination—development to date and future potential, *Journal of Membrane Science*, 370 (2011) 1-22.
- [7] H. Zhang, G. Wang, D. Chen, X.J. Lv, U.H. Jinghong, Tuning Photoelectrochemical Performances of Ag-TiO<sub>2</sub> Nanocomposites via Reduction/Oxidation of Ag, *Chemistry of Materials*, 20 (2008) 6543-6549.
- [8] S. Kim, S. Lee, S. Hong, Y. Oh, M. Seoul, J. Kweon, T. Kim, Biofouling of reverse osmosis membranes: Microbial quorum sensing and fouling propensity, *Desalination*, 247 (2009) 303-315.
- [9] S. Dobretsov, H.-U. Dahms, H. YiLi, M. Wahl, P.-Y. Qian, The effect of quorum-sensing blockers on the formation of marine microbial communities and larval attachment, *FEMS Microbiology Ecology*, 60 (2007) 177-188.
- [10] M. Hentzer, M. Givskov, L. Eberl, Quorum Sensing in Biofilms: Gossip in Slime City Microbial biofilms, (2004) 118.
- [11] D.M. Roche, J.T. Byers, D.S. Smith, F.G. Glansdorp, D.R. Spring, M. Welch, Communications blackout? Do N-acylhomoserine-lactone-degrading enzymes have any role in quorum sensing?, *Microbiology*, 150 (2004) 2023-2028.
- [12] J.S. Jung, R.V. Bhat, G.M. Preston, W.B. Guggino, J.M. Baraban, P. Agre, Molecular characterization of an aquaporin cDNA from brain: candidate osmoreceptor and regulator of water balance, *Proceedings of the National Academy of Sciences*, 91 (1994) 13052-13056.
- [13] X. Li, R. Wang, C. Tang, A. Vararattanavech, Y. Zhao, J. Torres, T. Fane, Preparation of supported lipid membranes for aquaporin Z incorporation, *Colloids and Surfaces B: Biointerfaces*, 94 (2012) 333-340.
- [14] J.H. Kim, D.C. Choi, K.M. Yeon, S.R. Kim, C.H. Lee, Enzyme-immobilized nanofiltration membrane to mitigate biofouling based on quorum quenching.
- [15] E.B.H. Hume, J. Baveja, B. Muir, T.L. Schubert, N. Kumar, S. Kjelleberg, H.J. Griesser, H. Thissen, R. Read, L.A. Poole-Warren, K. Schindhelm, M.D.P. Willcox, The control of *Staphylococcus epidermidis* biofilm formation and in vivo infection rates by covalently bound furanones, *Biomaterials*, 25 (2004) 5023-5030.

- [16] K. Ponnusamy, S. Kappachery, M. Thekeettle, J. Song, J. Kweon, Anti-biofouling property of vanillin on *Aeromonas hydrophila* initial biofilm on various membrane surfaces, *World Journal of Microbiology and Biotechnology*, (2013) 1-9.
- [17] K.-M. Yeon, W.-S. Cheong, H.-S. Oh, W.-N. Lee, B.-K. Hwang, C.-H. Lee, H. Beyenal, Z. Lewandowski, Quorum Sensing: A New Biofouling Control Paradigm in a Membrane Bioreactor for Advanced Wastewater Treatment, *Environmental Science & Technology*, 43 (2008) 380-385.
- [18] S. Kappachery, D. Paul, J. Yoon, J.H. Kweon, Vanillin, a potential agent to prevent biofouling of reverse osmosis membrane, *Biofouling*, 26 (2010) 667-672.
- [19] J.H. Kim, D.C. Choi, K.M. Yeon, S.R. Kim, C.H. Lee, Enzyme-Immobilized Nanofiltration Membrane To Mitigate Biofouling Based on Quorum Quenching, *Environ Sci Technol*, 45 (2011) 1601-1607.
- [20] W. Jiang, S.Q. Xia, J. Liang, Z.Q. Zhang, S.W. Hermanowicz, Effect of quorum quenching on the reactor performance, biofouling and biomass characteristics in membrane bioreactors, *Water Research*, 47 (2013) 187-196.
- [21] N.P. Gule, O. Bshena, M. de Kwaadsteniet, T.E. Cloete, B. Klumperman, Immobilized Furanone Derivatives as Inhibitors for Adhesion of Bacteria on Modified Poly(styrene-co-maleic anhydride), *Biomacromolecules*, 13 (2012) 3138-3150.
- [22] W.W.A. Programme, The United Nations World Water Development Report 4: Managing Water under Uncertainty and Risk, in, UNESCO, Paris, France 2012.
- [23] I. Tetra Tech, Evaluating Sustainability of Projected Water Demands Under Future Climate Change Scenarios, in, 2010.
- [24] R.G. Raluy, R. Schwantes, V.J. Subiela, B. Peñate, G. Melián, J.R. Betancort, Operational experience of a solar membrane distillation demonstration plant in Pozo Izquierdo-Gran Canaria Island (Spain), *Desalination*, 290 (2012) 1-13.
- [25] L. Wu, X. Guo, K. Hunter, E. Zagory, R. Waters, J. Brown, Studies of salt tolerance of landscape plant species and California native grasses for recycled water irrigation, Slosson report, (2001) 1-14.
- [26] S. Lee, C. Boo, M. Elimelech, S. Hong, Comparison of fouling behavior in forward osmosis (FO) and reverse osmosis (RO), *Journal of Membrane Science*, 365 (2010) 34-39.
- [27] T. Tsuru, M. Urairi, S.-i. Nakao, S. Kimura, Reverse osmosis of single and mixed electrolytes with charged membranes: experiment and analysis, *Journal of chemical engineering of Japan*, 24 (1991) 518-524.
- [28] X.-L. Wang, W.-N. Wang, D.-X. Wang, Experimental investigation on separation performance of nanofiltration membranes for inorganic electrolyte solutions, *Desalination*, 145 (2002) 115-122.
- [29] P.K. Abdul Azis, I. Al-Tisan, N. Sasikumar, Biofouling potential and environmental factors of seawater at a desalination plant intake, *Desalination*, 135 (2001) 69-82.
- [30] G. Belfort, R.H. Davis, A.L. Zydney, The behavior of suspensions and macromolecular solutions in crossflow microfiltration, *Journal of Membrane Science*, 96 (1994) 1-58.
- [31] C. Bartels, M. Hirose, H. Fujioka, Performance advancement in the spiral wound RO/NF element design, *Desalination*, 221 (2008) 207-214.

- [32] V. Polasek, S. Talo, T. Sharif, Conversion from hollow fiber to spiral technology in large seawater RO systems—process design and economics, *Desalination*, 156 (2003) 239-247.
- [33] G. Pearce, Water and wastewater filtration: Membrane module format, *Filtration & separation*, 44 (2007) 31-33.
- [34] J. Schwinge, D. Wiley, A. Fane, Novel spacer design improves observed flux, *Journal of membrane Science*, 229 (2004) 53-61.
- [35] J.E. Cadotte, Reverse osmosis membrane, in, Google Patents, 1977.
- [36] Y.-H. Dong, L.-H. Wang, J.-L. Xu, H.-B. Zhang, X.-F. Zhang, L.-H. Zhang, Quenching quorum-sensing-dependent bacterial infection by an N-acyl homoserine lactonase, *Nature*, 411 (2001) 813-817.
- [37] J. Lee, I.S. Kim, Microbial community in seawater reverse osmosis and rapid diagnosis of membrane biofouling, *Desalination*, 273 (2011) 118-126.
- [38] L. Katebian, S.C. Jiang, Marine bacterial biofilm formation and its responses to periodic hyperosmotic stress on a flat sheet membrane for seawater desalination pretreatment, *Journal of Membrane Science*, 425 (2013) 182-189.
- [39] A. Matin, Z. Khan, S.M.J. Zaidi, M.C. Boyce, Biofouling in reverse osmosis membranes for seawater desalination: Phenomena and prevention, *Desalination*, 281 (2011) 1-16.
- [40] P.A.C. Bonné, J.A.M.H. Hofman, J.P. van der Hoek, Scaling control of RO membranes and direct treatment of surface water, *Desalination*, 132 (2000) 109-119.
- [41] C. Fritzmann, J. Löwenberg, T. Wintgens, T. Melin, State-of-the-art of reverse osmosis desalination, *Desalination*, 216 (2007) 1-76.
- [42] F. Reverberi, A. Gorenflo, Three year operational experience of a spiral-wound SWRO system with a high fouling potential feed water, *Desalination*, 203 (2007) 100-106.
- [43] G.D. Kang, Y.M. Cao, Development of antifouling reverse osmosis membranes for water treatment: A review, *Water Research*, 46 (2012) 584-600.
- [44] S. Avlonitis, W. Hanbury, T. Hodgkiess, Chlorine degradation of aromatic polyamides, *Desalination*, 85 (1992) 321-334.
- [45] T.B. Rasmussen, M. Givskov, Quorum sensing inhibitors: a bargain of effects, *Microbiology*, 152 (2006) 895-904.
- [46] C. Van de Lisdonk, B. Rietman, S. Heijman, G. Sterk, J. Schippers, Prediction of supersaturation and monitoring of scaling in reverse osmosis and nanofiltration membrane systems, *Desalination*, 138 (2001) 259-270.
- [47] E.C.a.E. Drioli, Membranes for Desalination, in: G.M. Andrea Cipollina, Lucio Rizzuti (Ed.) *Seawater Desalination: Conventional and Renewable Energy Processes*, Springer, Berlin, Germany, 2009, pp. 41-76.
- [48] S.F. Boerlage, M.D. Kennedy, G.J. Witkamp, J.P. van der Hoek, J.C. Schippers, BaSO<sub>4</sub> solubility prediction in reverse osmosis membrane systems, *Journal of membrane science*, 159 (1999) 47-59.
- [49] C.J. Gabelich, T.I. Yun, B.M. Coffey, Effects of aluminum sulfate and ferric chloride coagulant residuals on polyamide membrane performance, *Desalination*, 150 (2002) 15-30.



- [50] V. Bonnelye, M.A. Sanz, J.-P. Durand, L. Plasse, F. Gueguen, P. Mazounie, Reverse osmosis on open intake seawater: pre-treatment strategy, *Desalination*, 167 (2004) 191-200.
- [51] A. Zularisam, A. Ismail, R. Salim, Behaviours of natural organic matter in membrane filtration for surface water treatment—a review, *Desalination*, 194 (2006) 211-231.
- [52] A. Asatekin, S. Kang, M. Elimelech, A.M. Mayes, Anti-fouling ultrafiltration membranes containing polyacrylonitrile-graft-poly (ethylene oxide) comb copolymer additives, *Journal of Membrane Science*, 298 (2007) 136-146.
- [53] H. Li, Y. Lin, P. Yu, Y. Luo, L. Hou, FTIR study of fatty acid fouling of reverse osmosis membranes: Effects of pH, ionic strength, calcium, magnesium and temperature, *Separation and Purification Technology*, 77 (2011) 171-178.
- [54] C.Y. Tang, Y.-N. Kwon, J.O. Leckie, Fouling of reverse osmosis and nanofiltration membranes by humic acid—effects of solution composition and hydrodynamic conditions, *Journal of Membrane Science*, 290 (2007) 86-94.
- [55] S. Lee, M. Elimelech, Relating organic fouling of reverse osmosis membranes to intermolecular adhesion forces, *Environmental science & technology*, 40 (2006) 980-987.
- [56] Y. Gu, Y.-N. Wang, J. Wei, C.Y. Tang, Organic fouling of thin-film composite polyamide and cellulose triacetate forward osmosis membranes by oppositely charged macromolecules, *Water research*, 47 (2013) 1867-1874.
- [57] J.W. Costerton, Overview of microbial biofilms, *Journal of Industrial Microbiology & Biotechnology*, 15 (1995) 137-140.
- [58] H.C. Flemming, G. Schaule, T. Griebe, J. Schmitt, A. Tamachkiarowa, Biofouling—the Achilles heel of membrane processes, *Desalination*, 113 (1997) 215-225.
- [59] H.C. Flemming, G. Schaule, Biofouling on membranes - A microbiological approach, *Desalination*, 70 (1988) 95-119.
- [60] R.M. Donlan, Biofilms: microbial life on surfaces, *Emerging Infect Dis*, 8 (2002) 881-890.
- [61] Y. Xiong, Y. Liu, Biological control of microbial attachment: a promising alternative for mitigating membrane biofouling, *Applied Microbiology and Biotechnology*, 86 (2010) 825-837.
- [62] A.L. Lim, R. Bai, Membrane fouling and cleaning in microfiltration of activated sludge wastewater, *Journal of Membrane Science*, 216 (2003) 279-290.
- [63] G. Leslie, R. Schneider, A. Fane, K. Marshall, C. Fell, Fouling of a microfiltration membrane by two Gram-negative bacteria, *Colloids and Surfaces A: Physicochemical and Engineering Aspects*, 73 (1993) 165-178.
- [64] Z. Lewandowski, H. Beyenal, Biofilms: their structure, activity, and effect on membrane filtration, *Water science and technology: a journal of the International Association on Water Pollution Research*, 51 (2005) 181.
- [65] E. Drenkard, Antimicrobial resistance of *Pseudomonas aeruginosa* biofilms, *Microbes Infect*, 5 (2003) 1213-1219.
- [66] G. Geesey, M. Stupy, P. Bremer, The dynamics of biofilms, *International biodeterioration & biodegradation*, 30 (1992) 135-154.
- [67] T. Romeo, When the party is over: a signal for dispersal of *Pseudomonas aeruginosa* biofilms, *J Bacteriol*, 188 (2006) 7325-7327.

- [68] G.A. O'Toole, H.B. Kaplan, R. Kolter, Biofilm formation as microbial development, *Annu Rev Microbiol*, 54 (2000) 49-79.
- [69] M.H. Turakhia, W.G. Characklis, Activity of *Pseudomonas aeruginosa* in biofilms: effect of calcium, *Biotechnol. Bioeng.*, 33 (1989) 406-414.
- [70] C.S. Pereira, A.K. de Regt, P.H. Brito, S.T. Miller, K.B. Xavier, Identification of functional LsrB-like autoinducer-2 receptors, *Journal of bacteriology*, 191 (2009) 6975-6987.
- [71] C.S. Pereira, A.K. de Regt, P.H. Brito, S.T. Miller, K.B. Xavier, Identification of functional LsrB-like autoinducer-2 receptors, *Journal of Bacteriology*, (2009).
- [72] A. Subramani, X. Huang, E.M. Hoek, Direct observation of bacterial deposition onto clean and organic-fouled polyamide membranes, *J Colloid Interface Sci*, 336 (2009) 13-20.
- [73] E.M. Hoek, S. Bhattacharjee, M. Elimelech, Effect of membrane surface roughness on colloid-membrane DLVO interactions, *Langmuir*, 19 (2003) 4836-4847.
- [74] M.R. Parsek, D.L. Val, B.L. Hanzelka, J.E. Cronan, E. Greenberg, Acyl homoserine-lactone quorum-sensing signal generation, *Proceedings of the National Academy of Sciences*, 96 (1999) 4360-4365.
- [75] P. Xu, J.E. Drewes, T.-U. Kim, C. Bellona, G. Amy, Effect of membrane fouling on transport of organic contaminants in NF/RO membrane applications, *Journal of Membrane Science*, 279 (2006) 165-175.
- [76] W. Lee, C.H. Ahn, S. Hong, S. Kim, S. Lee, Y. Baek, J. Yoon, Evaluation of surface properties of reverse osmosis membranes on the initial biofouling stages under no filtration condition, *Journal of Membrane Science*, 351 (2010) 112-122.
- [77] A.E. Childress, M. Elimelech, Relating nanofiltration membrane performance to membrane charge (electrokinetic) characteristics, *Environ. Sci. Technol.*, 34 (2000) 3710-3716.
- [78] P. Wang, K. Tan, E. Kang, K. Neoh, Plasma-induced immobilization of poly (ethylene glycol) onto poly (vinylidene fluoride) microporous membrane, *Journal of Membrane Science*, 195 (2002) 103-114.
- [79] M. Kumar, M. Grzelakowski, J. Zilles, M. Clark, W. Meier, Highly permeable polymeric membranes based on the incorporation of the functional water channel protein Aquaporin Z, *Proceedings of the National Academy of Sciences*, 104 (2007) 20719-20724.
- [80] M. Kumar, M.M. Payne, S.K. Poust, J.L. Zilles, Polymer-based biomimetic membranes for desalination, in: *Biomimetic Membranes for Sensor and Separation Applications*, Springer, 2012, pp. 43-62.
- [81] D.A. Ladner, Effects of bloom-forming algae on fouling of integrated membrane systems in seawater desalination, in, University of Illinois, 2009.
- [82] Y. Kaufman, A. Berman, V. Freger, Supported lipid bilayer membranes for water purification by reverse osmosis, *Langmuir*, 26 (2010) 7388-7395.
- [83] P. Zhong, T.-S. Chung, K. Jeyaseelan, A. Armugam, Aquaporin-embedded biomimetic membranes for nanofiltration, *Journal of Membrane Science*, (2012).
- [84] Y. Zhao, C. Qiu, X. Li, A. Vararattanavech, W. Shen, J. Torres, C. Helix-Nielsen, R. Wang, X. Hu, A.G. Fane, Synthesis of robust and high-performance aquaporin-based biomimetic membranes by interfacial polymerization-membrane preparation and RO performance characterization, *Journal of Membrane Science*, (2012).

- [85] X. Li, S. Chou, R. Wang, L. Shi, W. Fang, G. Chaitra, C.Y. Tang, J. Torres, X. Hu, A.G. Fane, Nature gives the best solution for desalination: Aquaporin-based hollow fiber composite membrane with superior performance, *Journal of Membrane Science*, 494 (2015) 68-77.
- [86] D. Davies, Understanding biofilm resistance to antibacterial agents, *Nature reviews Drug discovery*, 2 (2003) 114-122.
- [87] H. Wu, Z. Song, M. Hentzer, J.B. Andersen, S. Molin, M. Givskov, N. Høiby, Synthetic furanones inhibit quorum-sensing and enhance bacterial clearance in *Pseudomonas aeruginosa* lung infection in mice, *Journal of Antimicrobial Chemotherapy*, 53 (2004) 1054-1061.
- [88] E. Hume, J. Baveja, B. Muir, T. Schubert, N. Kumar, S. Kjelleberg, H. Griesser, H. Thissen, R. Read, L. Poole-Warren, The control of *Staphylococcus epidermidis* biofilm formation and in vivo infection rates by covalently bound furanones, *Biomaterials*, 25 (2004) 5023-5030.
- [89] H. Bae, H. Kim, S. Jeong, S. Lee, Changes in the relative abundance of biofilm-forming bacteria by conventional sand-filtration and microfiltration as pretreatments for seawater reverse osmosis desalination, *Desalination*, 273 (2011) 258-266.
- [90] M. Zhang, S. Jiang, D. Tanuwidjaja, N. Voutchkov, E.M. Hoek, B. Cai, Composition and variability of biofouling organisms in seawater reverse osmosis desalination plants, *Applied and environmental microbiology*, 77 (2011) 4390-4398.
- [91] T. Egli, H.-U. Weilenmann, T. El-Banna, G. Auling, Gram-negative, aerobic, nitrilotriacetate-utilizing bacteria from wastewater and soil, *Systematic and applied microbiology*, 10 (1988) 297-305.
- [92] M. Wagner, R. Amann, P. Kampfer, B. Assmus, A. Hartmann, P. Hutzler, N. Springer, K.-H. Schleifer, Identification and in situ detection of gram-negative filamentous bacteria in activated sludge, *Systematic and applied microbiology*, 17 (1994) 405-417.
- [93] H. Ridgway, A. Kelly, C. Justice, B. Olson, Microbial fouling of reverse-osmosis membranes used in advanced wastewater treatment technology: chemical, bacteriological, and ultrastructural analyses, *Applied and environmental microbiology*, 45 (1983) 1066-1084.
- [94] H. Ivnitsky, I. Katz, D. Minz, G. Volvovic, E. Shimoni, E. Kesselman, R. Semiat, C.G. Dosoretz, Bacterial community composition and structure of biofilms developing on nanofiltration membranes applied to wastewater treatment, *Water research*, 41 (2007) 3924-3935.
- [95] C.M. Waters, B.L. Bassler, Quorum sensing: cell-to-cell communication in bacteria, *Annu. Rev. Cell Dev. Biol.*, 21 (2005) 319-346.
- [96] M.I. Moré, L.D. Finger, J.L. Stryker, C. Fuqua, A. Eberhard, S.C. Winans, Enzymatic synthesis of a quorum-sensing autoinducer through use of defined substrates, *Science*, 272 (1996) 1655-1658.
- [97] I. Ahmad, M.S.A. Khan, F.M. Husain, M. Zahin, M. Singh, Bacterial Quorum Sensing and Its Interference: Methods and Significance, in: *Microbes and Microbial Technology*, Springer, 2011, pp. 127-161.
- [98] J. Engebrecht, K. Nealson, M. Silverman, Bacterial bioluminescence: isolation and genetic analysis of functions from *Vibrio fischeri*, *Cell*, 32 (1983) 773-781.

- [99] A.M. Stevens, K.M. Dolan, E. Greenberg, Synergistic binding of the *Vibrio fischeri* LuxR transcriptional activator domain and RNA polymerase to the lux promoter region, *Proceedings of the National Academy of Sciences*, 91 (1994) 12619-12623.
- [100] R.H. González, A. Nusblat, B. Nudel, Detection and characterization of quorum sensing signal molecules in *Acinetobacter* strains, *Microbiological research*, 155 (2001) 271-277.
- [101] R. González, L. Dijkshoorn, M. Van den Barselaar, C. Nudel, Quorum sensing signal profile of *Acinetobacter* strains from nosocomial and environmental sources, *Rev Argent Microbiol*, 41 (2009) 73-78.
- [102] D.G. Davies, M.R. Parsek, J.P. Pearson, B.H. Iglewski, J.W. Costerton, E.P. Greenberg, The involvement of cell-to-cell signals in the development of a bacterial biofilm, *Science*, 280 (1998) 295-298.
- [103] J.J. Huang, J.-I. Han, L.-H. Zhang, J.R. Leadbetter, Utilization of acyl-homoserine lactone quorum signals for growth by a soil pseudomonad and *Pseudomonas aeruginosa* PAO1, *Applied and environmental microbiology*, 69 (2003) 5941-5949.
- [104] J.P. Pearson, K.M. Gray, L. Passador, K.D. Tucker, A. Eberhard, B.H. Iglewski, E. Greenberg, Structure of the autoinducer required for expression of *Pseudomonas aeruginosa* virulence genes, *Proceedings of the National Academy of Sciences*, 91 (1994) 197-201.
- [105] J.D. Shroat, R. Nerenberg, Monitoring Bacterial Twitter: Does Quorum Sensing Determine the Behavior of Water and Wastewater Treatment Biofilms?, *Environmental Science & Technology*, 46 (2012) 1995-2005.
- [106] E. Burton, H. Read, M. Pellitteri, W. Hickey, Identification of acyl-homoserine lactone signal molecules produced by *Nitrosomonas europaea* strain Schmidt, *Applied and environmental microbiology*, 71 (2005) 4906-4909.
- [107] S. Batchelor, M. Cooper, S. Chhabra, L. Glover, G. Stewart, P. Williams, J. Prosser, Cell density-regulated recovery of starved biofilm populations of ammonia-oxidizing bacteria, *Applied and environmental microbiology*, 63 (1997) 2281-2286.
- [108] C.T. Cuadrado-Silva, L. Castellanos, C. Arévalo-Ferro, O.E. Osorno, Detection of quorum sensing systems of bacteria isolated from fouled marine organisms, *Biochemical Systematics and Ecology*, 46 (2013) 101-107.
- [109] B.K. Hammer, B.L. Bassler, Quorum sensing controls biofilm formation in *Vibrio cholerae*, *Mol Microbiol*, 50 (2003) 101-104.
- [110] H. Ya-Wen, Z. Lian-Hui, Quorum sensing and virulence regulation in *Xanthomonas campestris*, *FEMS Microbiol. Rev.*, 32 (2008) 842-857.
- [111] J.M. Dow, L. Crossman, K. Findlay, Y.-Q. He, J.-X. Feng, J.-L. Tang, Biofilm dispersal in *Xanthomonas campestris* is controlled by cell-cell signaling and is required for full virulence to plants, *Proceedings of the National Academy of Sciences*, 100 (2003) 10995-11000.
- [112] M.J. Lynch, S. Swift, D.F. Kirke, C.W. Keevil, C.E. Dodd, P. Williams, The regulation of biofilm development by quorum sensing in *Aeromonas hydrophila*, *Environmental microbiology*, 4 (2002) 18-28.
- [113] S. Swift, A.V. Karlyshev, L. Fish, E.L. Durant, M.K. Winson, S.R. Chhabra, P. Williams, S. Macintyre, G. Stewart, Quorum sensing in *Aeromonas hydrophila* and *Aeromonas salmonicida*: identification of the LuxRI homologs AhyRI and AsaRI and

- their cognate N-acylhomoserine lactone signal molecules, *Journal of bacteriology*, 179 (1997) 5271-5281.
- [114] Y.L. Huang, J.S. Ki, R.J. Case, P.Y. Qian, Diversity and acyl-homoserine lactone production among subtidal biofilm-forming bacteria, *Aquatic Microbial Ecology*, 52 (2008) 185.
- [115] N.M. Mohamed, E.M. Cicirelli, J. Kan, F. Chen, C. Fuqua, R.T. Hill, Diversity and quorum-sensing signal production of Proteobacteria associated with marine sponges, *Environmental Microbiology*, 10 (2008) 75-86.
- [116] K.B. Xavier, B.L. Bassler, Regulation of uptake and processing of the quorum-sensing autoinducer AI-2 in *Escherichia coli*, *Journal of bacteriology*, 187 (2005) 238-248.
- [117] S.T. Miller, K.B. Xavier, S.R. Campagna, M.E. Taga, M.F. Semmelhack, B.L. Bassler, F.M. Hughson, *Salmonella typhimurium* Recognizes a Chemically Distinct Form of the Bacterial Quorum-Sensing Signal AI-2, *Molecular cell*, 15 (2004) 677-687.
- [118] A.F.G. Barrios, R. Zuo, Y. Hashimoto, L. Yang, W.E. Bentley, T.K. Wood, Autoinducer 2 controls biofilm formation in *Escherichia coli* through a novel motility quorum-sensing regulator (MqsR, B3022), *Journal of Bacteriology*, 188 (2006) 305-316.
- [119] B. Beutler, Z. Jiang, P. Georgel, K. Crozat, B. Croker, S. Rutschmann, X. Du, K. Hoebe, Genetic analysis of host resistance: Toll-like receptor signaling and immunity at large, *Annu. Rev. Immunol.*, 24 (2006) 353-389.
- [120] A. Vendeville, K. Winzer, K. Heurlier, C.M. Tang, K.R. Hardie, Making'sense'of metabolism: autoinducer-2, LuxS and pathogenic bacteria, *Nature Reviews Microbiology*, 3 (2005) 383-396.
- [121] B.L. Bassler, R. Losick, Bacterially speaking, *Cell*, 125 (2006) 237-246.
- [122] M.E. Taga, J.L. Semmelhack, B.L. Bassler, The LuxS-dependent autoinducer AI-2 controls the expression of an ABC transporter that functions in AI-2 uptake in *Salmonella typhimurium*, *Molecular microbiology*, 42 (2001) 777-793.
- [123] Y.H. Dong, L.H. Zhang, Quorum sensing and quorum-quenching enzymes, (2005).
- [124] S. Dobretsov, M. Teplitski, V. Paul, Mini-review: quorum sensing in the marine environment and its relationship to biofouling, *Biofouling*, 25 (2009) 413-427.
- [125] M. Romero, S.P. Diggle, S. Heeb, M. Camara, A. Otero, Quorum quenching activity in *Anabaena* sp. PCC 7120: identification of AiiC, a novel AHL-acylase, *FEMS microbiology letters*, 280 (2008) 73-80.
- [126] K. Ponnusamy, D. Paul, J.H. Kweon, Inhibition of quorum sensing mechanism and *Aeromonas hydrophila* biofilm formation by vanillin, *Environmental Engineering Science*, 26 (2009) 1359-1363.
- [127] T. Katayama, I. Nagai, Chemical significance of the volatile components of spices in the food preservative viewpoint. VI. Structure and antibacterial activity of terpenes, *Nippon Suisan Gakkaishi*, 26 (1960) 29.
- [128] S. Dobretsov, M. Teplitski, M. Bayer, S. Gunasekera, P. Proksch, V.J. Paul, Inhibition of marine biofouling by bacterial quorum sensing inhibitors, *Biofouling*, 27 (2011) 893-905.
- [129] V. Plyuta, J. Zaitseva, E. Lobakova, N. Zagoskina, A. Kuznetsov, I. Khmel, Effect of plant phenolic compounds on biofilm formation by *Pseudomonas aeruginosa*, *Apmis*, 121 (2013) 1073-1081.

- [130] G. Brackman, T. Defoirdt, C. Miyamoto, P. Bossier, S. Van Calenbergh, H. Nelis, T. Coenye, Cinnamaldehyde and cinnamaldehyde derivatives reduce virulence in *Vibrio* spp. by decreasing the DNA-binding activity of the quorum sensing response regulator LuxR, *BMC microbiology*, 8 (2008) 149.
- [131] C. Niu, S. Afre, E. Gilbert, Subinhibitory concentrations of cinnamaldehyde interfere with quorum sensing, *Letters in applied microbiology*, 43 (2006) 489-494.
- [132] T. Defoirdt, C.M. Miyamoto, T.K. Wood, E.A. Meighen, P. Sorgeloos, W. Verstraete, P. Bossier, The natural furanone (5Z)-4-bromo-5-(bromomethylene)-3-butyl-2 (5H)-furanone disrupts quorum sensing-regulated gene expression in *Vibrio harveyi* by decreasing the DNA-binding activity of the transcriptional regulator protein luxR, *Environmental microbiology*, 9 (2007) 2486-2495.
- [133] T. Zang, B.W. Lee, L.M. Cannon, K.A. Ritter, S. Dai, D. Ren, T.K. Wood, Z.S. Zhou, A naturally occurring brominated furanone covalently modifies and inactivates LuxS, *Bioorganic & medicinal chemistry letters*, 19 (2009) 6200-6204.
- [134] K. Ponnusamy, D. Paul, Y.S. Kim, J.H. Kweon, 2(5h)-Furanone: A Prospective Strategy for Biofouling-Control in Membrane Biofilm Bacteria by Quorum Sensing Inhibition, *Brazilian Journal of Microbiology*, 41 (2010) 227-234.
- [135] J.M. Henke, B.L. Bassler, Three Parallel Quorum-Sensing Systems Regulate Gene Expression in *Vibrio harveyi*, *Journal of Bacteriology*, 186 (2004) 6902-6914.
- [136] B.L. Bassler, M. Wright, M.R. Silverman, Multiple signalling systems controlling expression of luminescence in *Vibrio harveyi*: sequence and function of genes encoding a second sensory pathway, *Molecular microbiology*, 13 (1994) 273-286.
- [137] J.M. Henke, B.L. Bassler, Quorum sensing regulates type III secretion in *Vibrio harveyi* and *Vibrio parahaemolyticus*, *Journal of Bacteriology*, 186 (2004) 3794-3805.
- [138] M.B. Miller, K. Skorupski, D.H. Lenz, R.K. Taylor, B.L. Bassler, Parallel Quorum Sensing Systems Converge to Regulate Virulence in *Vibrio cholerae*, *Cell*, 110 (2002) 303-314.
- [139] K.B. Xavier, S.T. Miller, W. Lu, J.H. Kim, J. Rabinowitz, I. Pelczar, M.F. Semmelhack, B.L. Bassler, *ACS Chem. Biol.*, 2 (2007) 128.
- [140] K. Ponnusamy, D. Paul, Y.S. Kim, J.H. Kweon, 2 (5H)-Furanone: a prospective strategy for biofouling-control in membrane biofilm bacteria by quorum sensing inhibition, *Brazilian Journal of Microbiology*, 41 (2010) 227-234.
- [141] W. Jiang, S. Xia, J. Liang, Z. Zhang, S.W. Hermanowicz, Effect of quorum quenching on the reactor performance, biofouling and biomass characteristics in membrane bioreactors, *Water research*, 47 (2013) 187-196.
- [142] T. Defoirdt, R. Crab, T.K. Wood, P. Sorgeloos, W. Verstraete, P. Bossier, Quorum sensing-disrupting brominated furanones protect the gnotobiotic brine shrimp *Artemia franciscana* from pathogenic *Vibrio harveyi*, *Vibrio campbellii*, and *Vibrio parahaemolyticus* isolates, *Applied and environmental microbiology*, 72 (2006) 6419-6423.
- [143] N.P. Gule, O. Bshena, M.I. de Kwaadsteniet, T.E. Cloete, B. Klumperman, Immobilized Furanone Derivatives as Inhibitors for Adhesion of Bacteria on Modified Poly (styrene-co-maleic anhydride), *Biomacromolecules*, 13 (2012) 3138-3150.
- [144] L.K. Vestby, J. Lönn-Stensrud, T. Møretrø, S. Langsrud, A. Aamdal-Scheie, T. Benneche, L.L. Nesse, A synthetic furanone potentiates the effect of disinfectants on *Salmonella* in biofilm, *Journal of Applied Microbiology*, 108 (2010) 771-778.

- [145] D. Morin, B. Grasland, K. Vallée-Réhel, C. Dufau, D. Haras, On-line high-performance liquid chromatography–mass spectrometric detection and quantification of N-acylhomoserine lactones, quorum sensing signal molecules, in the presence of biological matrices, *Journal of Chromatography A*, 1002 (2003) 79-92.
- [146] J.H. Paul, Use of Hoechst dyes 33258 and 33342 for enumeration of attached and planktonic bacteria, *Applied and environmental microbiology*, 43 (1982) 939-944.
- [147] S. Stepanovic, D. Vukovic, I. Dakic, B. Savic, M. Svabic-Vlahovic, A modified microtiter-plate test for quantification of staphylococcal biofilm formation, *J Microbiol Meth*, 40 (2000) 175-179.
- [148] J. Vrouwenvelder, J. Van Paassen, L. Wessels, A. Van Dam, S. Bakker, The membrane fouling simulator: a practical tool for fouling prediction and control, *Journal of Membrane Science*, 281 (2006) 316-324.
- [149] E. Cornelissen, J. Vrouwenvelder, S. Heijman, X. Viallefont, D. Van Der Kooij, L. Wessels, Periodic air/water cleaning for control of biofouling in spiral wound membrane elements, *Journal of Membrane Science*, 287 (2007) 94-101.
- [150] M. Herzberg, M. Elimelech, Physiology and genetic traits of reverse osmosis membrane biofilms: a case study with *Pseudomonas aeruginosa*, *Isme J*, 2 (2008) 180-194.
- [151] A. Heydorn, A.T. Nielsen, M. Hentzer, C. Sternberg, M. Givskov, B.K. Ersboll, S. Molin, Quantification of biofilm structures by the novel computer program COMSTAT, *Microbiol-Uk*, 146 (2000) 2395-2407.
- [152] G.A. Boorman, Drinking water disinfection byproducts: review and approach to toxicity evaluation, *Environmental Health Perspectives*, 107 (1999) 207.
- [153] S.D. Richardson, M.J. Plewa, E.D. Wagner, R. Schoeny, D.M. DeMarini, Occurrence, genotoxicity, and carcinogenicity of regulated and emerging disinfection by-products in drinking water: a review and roadmap for research, *Mutation Research/Reviews in Mutation Research*, 636 (2007) 178-242.
- [154] Y. Chun, P.T. Ha, L. Powell, J. Lee, D. Kim, D. Choi, R.W. Lovitt, I.S. Kim, S.S. Mitra, I.S. Chang, Exploring microbial communities and differences of cartridge filters (CFs) and reverse osmosis (RO) membranes for seawater desalination processes, *Desalination*, 298 (2012) 85-92.
- [155] C.T. Cuadrado-Silva, L. Castellanos, C. Arévalo-Ferro, O.E. Osorno, Detection of quorum sensing systems of bacteria isolated from fouled marine organisms, *Biochemical Systematics and Ecology*, 46 (2013) 101-107.
- [156] H. YL, K. JS, C. RJ, Q. P, Diversity and acyl-homoserine lactone production among subtidal biofilm-forming bacteria, *Aquatic Microbial Ecology*, 52 (2008) 185-193.
- [157] H.C. Flemming, Reverse osmosis membrane biofouling, *Exp. Therm. Fluid Sci.*, 14 (1997) 382-391.
- [158] A.C. Fonseca, R.S. Summers, A.R. Greenberg, M.T. Hernandez, Extra-cellular polysaccharides, soluble microbial products, and natural organic matter impact on nanofiltration membranes flux decline, *Environmental science & technology*, 41 (2007) 2491-2497.
- [159] Z. Lewandowski, H. Beyenal, Biofilms: their structure, activity, and effect on membrane filtration, *Water Science & Technology*, 51 (2005) 181-192.
- [160] R.M. Donlan, Biofilms: microbial life on surfaces, *Emerging infectious diseases*, 8 (2002) 881-890.

- [161] D.G. Davies, A.M. Chakrabarty, G.G. Geesey, Exopolysaccharide production in biofilms: substratum activation of alginate gene expression by *Pseudomonas aeruginosa*, *Appl Environ Microbiol*, 59 (1993) 1181-1186.
- [162] S. Azari, L. Zou, Using zwitterionic amino acid L-DOPA to modify the surface of thin film composite polyamide reverse osmosis membranes to increase their fouling resistance, *Journal of Membrane Science*, 401 (2012) 68-75.
- [163] Z.-G. Wang, J.-Q. Wang, Z.-K. Xu, Immobilization of lipase from *Candida rugosa* on electrospun polysulfone nanofibrous membranes by adsorption, *Journal of Molecular Catalysis B: Enzymatic*, 42 (2006) 45-51.
- [164] N. Hilal, M. Khayet, C.J. Wright, *Membrane modification: Technology and applications*, CRC Press, 2012.
- [165] K.R. Zodrow, M.E. Tousley, M. Elimelech, Mitigating biofouling on thin-film composite polyamide membranes using a controlled-release platform, *Journal of Membrane Science*, 453 (2014) 84-91.
- [166] A. Marmur, Equilibrium contact angles: theory and measurement, *Colloids and Surfaces A: Physicochemical and Engineering Aspects*, 116 (1996) 55-61.
- [167] E.M. Vrijenhoek, S. Hong, M. Elimelech, Influence of membrane surface properties on initial rate of colloidal fouling of reverse osmosis and nanofiltration membranes, *J Membrane Sci*, 188 (2001) 115-128.
- [168] M.L. Zhang, S. Jiang, D. Tanuwidjaja, N. Voutchkov, E.M.V. Hoek, B.L. Cai, Composition and Variability of Biofouling Organisms in Seawater Reverse Osmosis Desalination Plants, *Applied and Environmental Microbiology*, 77 (2011) 4390-4398.
- [169] K. Sauer, A.K. Camper, G.D. Ehrlich, J.W. Costerton, D.G. Davies, *Pseudomonas aeruginosa* displays multiple phenotypes during development as a biofilm, *J Bacteriol*, 184 (2002) 1140-1154.
- [170] R. Lamsal, S.G. Harroun, C.L. Brosseau, G.A. Gagnon, Use of surface enhanced Raman spectroscopy for studying fouling on nanofiltration membrane, *Separation and Purification Technology*, 96 (2012) 7-11.
- [171] A.M.M. da Silva, A.M. Amado, P. Ribeiro-Claro, J. Empis, J. Teixeira-Dias,  $\beta$ -Cyclodextrin Complexes of Benzaldehyde, Vanillin and Cinnamaldehyde: A Raman Spectroscopic Study, *Carbohydrate Chemistry*, 14 (1995) 677-684.
- [172] D. Stewart, N. Yahiaoui, G.J. McDougall, K. Myton, C. Marque, A.M. Boudet, J. Haigh, Fourier-transform infrared and Raman spectroscopic evidence for the incorporation of cinnamaldehydes into the lignin of transgenic tobacco (*Nicotiana tabacum* L.) plants with reduced expression of cinnamyl alcohol dehydrogenase, *Planta*, 201 (1997) 311-318.
- [173] R. Aggarwal, L. Farrar, B. Saar, T. Jeys, R. Goodman, Measurement of the Absolute Raman Cross Sections of Diethyl Phthalate, Dimethyl Phthalate, Ethyl Cinnamate, Propylene Carbonate, Tripropyl Phosphate, 1, 3-Cyclohexanedione, 3'-Aminoacetophenone, 3'-Hydroxyacetophenone, Diethyl Acetamidomalonate, Isovanillin, Lactide, Meldrum's Acid, p-Tolyl Sulfoxide, and Vanillin, in, DTIC Document, 2013.
- [174] J. Binoy, I.H. Joe, V. Jayakumar, Changes in the vibrational spectral modes by the nonbonded interactions in the NLO crystal vanillin, *Journal of Raman Spectroscopy*, 36 (2005) 1091-1100.
- [175] G. Socrates, *Infrared and Raman characteristic group frequencies: tables and charts*, John Wiley & Sons, 2004.



- [176] K.R. Zodrow, M.E. Tousley, M. Elimelech, Mitigating biofouling on thin-film composite polyamide membranes using a controlled-release platform, *Journal of Membrane Science*, 453 (2014) 84-91.
- [177] T.-H. Bae, I.-C. Kim, T.-M. Tak, Preparation and characterization of fouling-resistant TiO<sub>2</sub> self-assembled nanocomposite membranes, *Journal of membrane science*, 275 (2006) 1-5.
- [178] T. Peters, J. Van der Tuin, C. Houssin, M. Vorstman, N. Benes, Z. Vroon, A. Holmen, J. Keurentjes, Preparation of zeolite-coated pervaporation membranes for the integration of reaction and separation, *Catalysis today*, 104 (2005) 288-295.

## APPENDIX A. SUPPORTING STUDY: SUPPRESSING RO AND FO MEMBRANE BIOFOULING WITH QUORUM SENSING INHIBITORS

### A.1. Introduction

The goal of this study was to investigate the effectiveness of a quorum sensing inhibiting (QSI) compound to reduce membrane biofilm production in lab scale RO and FO systems. The QSI compound, vanillin was selected since it was previously demonstrated to be an effective inhibitor against single and mixed species biofilm formation (Section 3.3.3.2.2 and 0). This work was conducted at Murdoch University in Western Australia as part of an international collaboration.

### A.2. Methods

#### A.2.1. RO Membrane Biofouling

##### Study

The effectiveness of vanillin to reduce membrane biofilm formation was carried out in a lab scale high pressure RO membrane system (Figure

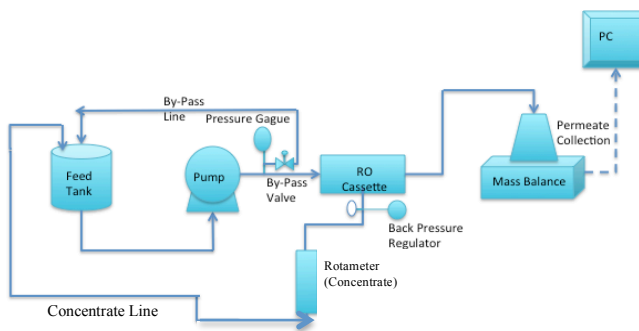
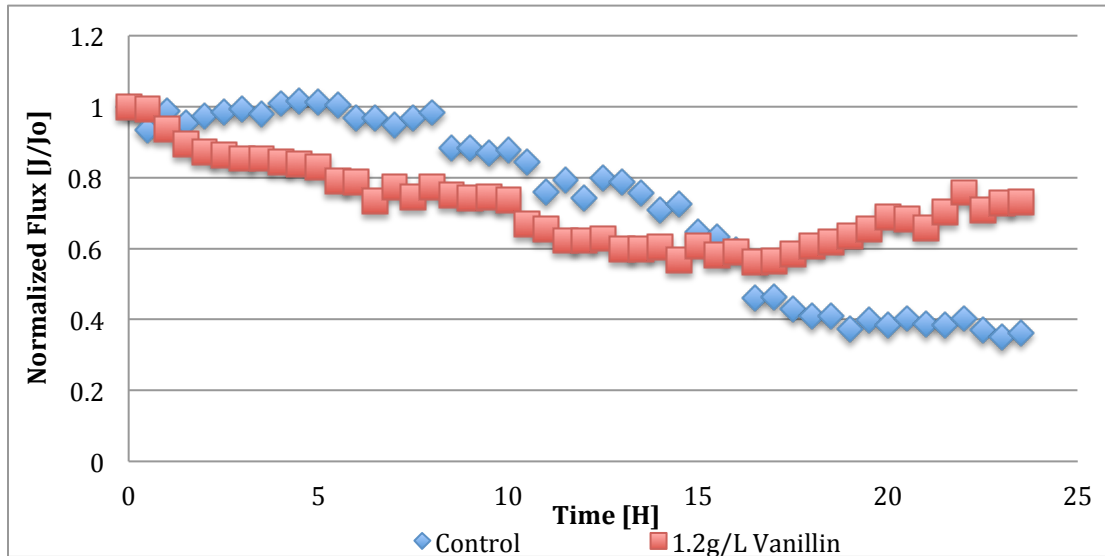


Figure A.1. Bench scale RO membrane system schematic.

A.1). The bacterial isolate, B2 (*Alteromonas sp.*), was chosen as the model foulant because it was found to be the highest biofilm producer among marine bacteria isolated from fouled RO membranes in a desalination plant [38]. The SWC5 RO membrane (Hydranautics) was soaked overnight in deionized water to remove the protective layer

and then placed in a high-pressure cassette holder. The system was stabilized for 24 h with sterile 0.45  $\mu\text{m}$ -filtered seawater from Port Beach in Western Australia at a cross flow velocity of 8.5 cm/s and an operating pressure of 590 psi. The system was run at a lower pressure and cross flow velocity in order to develop a thick biofilm layer within a 24 hour period. An overnight culture of B2 was added to the feed tank along with peptone (0.05 g/L) to accelerate biofilm development in the batch system. Then, the feed reservoir was injected with or without vanillin (1.2 g/L). The system was run in a recirculation mode to bring the concentrate back to the feed reservoir. The drip permeate was collected, weighed, and recorded automatically every minute. Conductivity measurements were taken periodically to ensure the membrane was operating properly during operation. The RO membrane was sacrificed at the end of each experiment for biofilm characterization using confocal microscopy following methods as described in Section 3.2.3.2.6 and 4.2.6.

The FO membrane biofouling system was set-up similar to the RO system except there was no high pressure application and oversaturated NaCl was used as the draw solution. The concentrate was returned back to the feed reservoir while the diluted draw solution was returned back to the draw reservoir. The weight of the draw reservoir was recorded automatically every minute. The FO membrane (HTI) was sacrificed at the end of each experiment for biofilm characterization as well.



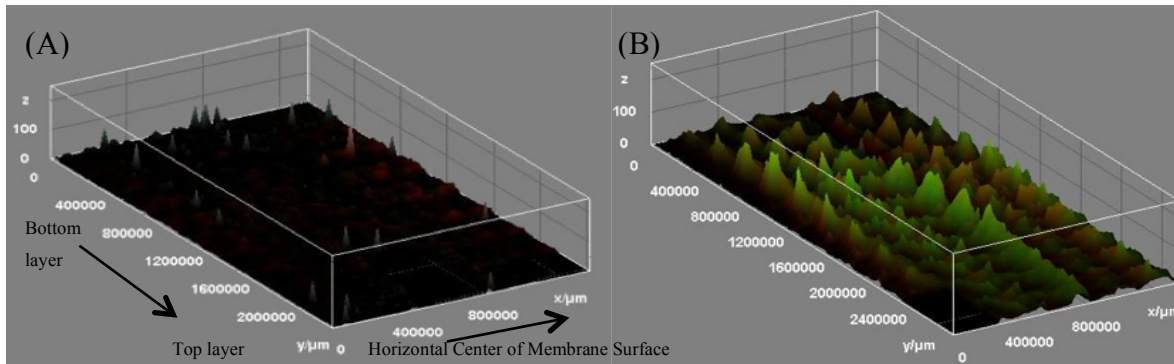
**Figure A.2.** The normalized flux for control and vanillin treated RO membrane biofouling systems. The normalized permeate flux was calculated as the flux over the initial flux.

### A.3. Results

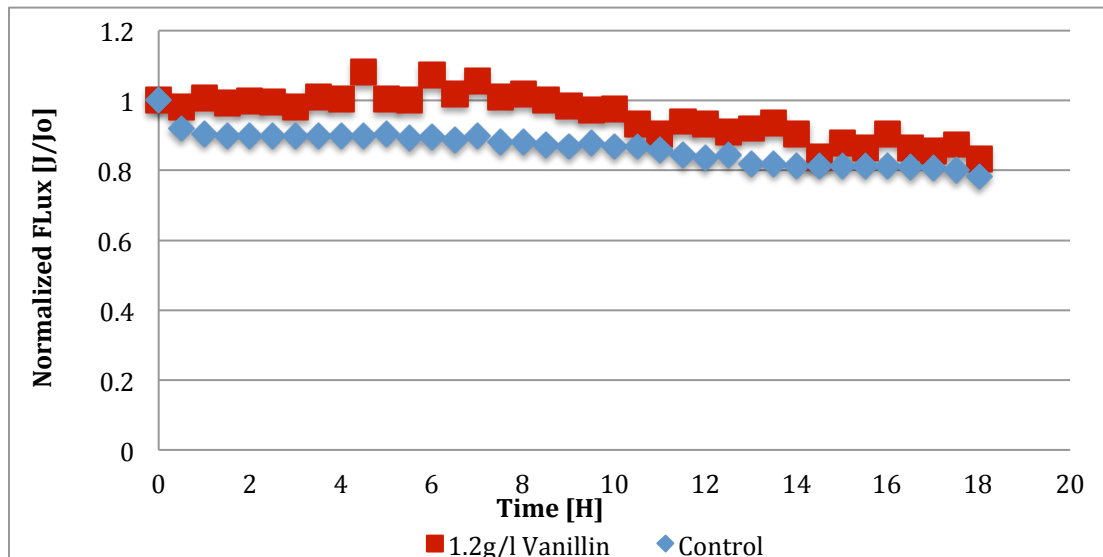
#### A.3.1. Normalized Permeate Flux and RO Membrane Biofilm Formation

Figure A.2 showed the normalized flux for the control and 1.2 g/l vanillin treated RO membrane biofouling systems. Both control and vanillin treated systems experienced severe biofouling around 15 h as indicated by the sharp decline in permeate flux (Figure A.2). The onset of biofouling occurred faster in the vanillin treated system, which could be due to vanillin acting as an organic foulant, which decreased the flux. The increase in permeate flux for the vanillin treated system around 17 h was potentially due to temperature fluctuations and membrane damage as noted by the conductivity readings of the permeate stream (control: 1000  $\mu$ S and vanillin treated: 2500  $\mu$ S systems at 24 h).

Confocal microscopy revealed that there was a 30% reduction of membrane biofilm thickness for the vanillin treated membrane compared to the control (Figure A.3). In addition, there were significantly more dead bacteria and less live bacteria present on the membrane surface than the control membrane. The data showed the effectiveness of vanillin to reduce membrane biofilm formation in a high pressure RO system.



**Figure A.3.** Comparison of membrane biofilm without (A) and with vanillin treatment (B) in high pressure RO system for the lead membrane section. The 3D image is composed of multiple layers of biofilm, which are approximately 1000  $\mu\text{m}$  in height. ImageJ automatically determines the dimensions of the y- and x-axis. The y-axis represents the bottom to top layer of the biofilm and the x-axis refers to bottom biofilm layer along the horizontal center of the membrane surface. The z-axis measures the florescence intensity of the live and dead cells.



**Figure A.4.** Normalized flux for vanillin treated and control FO membrane system. The normalized permeate flux was measured by the flux over the starting permeate flux.

### ***A.3.2. FO Membrane Permeate Flux and Biofilm***

The normalized flux for 1.2g/l vanillin treated and control FO membrane system was depicted in Figure A.4. Both the control and vanillin treated systems did not experience severe biofouling by 20 h as indicated by the relatively stable permeate flux (Figure A.4). This was further evident by the presence of only a thin biofilm layer on both the control and vanillin treated membrane surfaces (data not shown). Therefore, there was no significant difference in membrane biofilm formation between the control and vanillin treated FO systems (data not shown).

### **A.4. Conclusions**

There was no significant difference in normalized permeate flux and membrane biofilm formation between control and vanillin treated FO systems due to a thin biofilm layer. In a high pressure RO system, vanillin reduced membrane *Alteromonas sp.* biofilm formation. Since the onset of fouling occurred faster in the vanillin treated RO system, there is a potential that vanillin at 1.2 g/L acted as an organic foulant. Future work should consider modifying the membrane surface with vanillin to improve the membrane anti-biofouling capability and permeate flux.

## APPENDIX B. SUPPORTING STUDY: THE EFFECTIVENESS OF PHYSICALLY ATTACHED QUORUM SENSING INHIBITORS TO RO AND FO MEMBRANES TO REDUCE BIOFOULING

### B.1 Introduction

Since previous studies have shown that biofilm formation on the membrane surface still persists after being subjected to vanillin in the bulk fluid (Section 0 and A.3.1), the objective of this study was to improve the membrane anti-biofouling potential by incorporating vanillin onto the membrane surface. The experimental studies were conducted at Murdoch University in Western Australia as part of an international collaboration.

### B.2. Methods

#### *B.2.1. QSI Modified RO Membrane Anti-Biofouling Potential*

The lab scale high pressure RO system depicted in Figure B.1 was improved upon from the previous section

(Figure A.1). The *Alteromonas sp.*, B2 was selected as the model foulant as in Section A.2.1. A SWC5 RO membrane (Hydranautics) and FO membrane (HTI) were

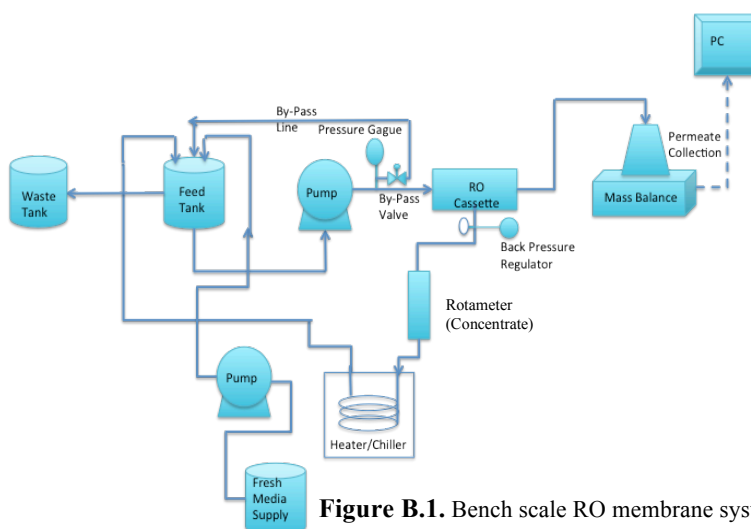


**Figure B.1.** Bench scale RO membrane system.

separately soaked in a solution of 1.2 g/L vanillin overnight to allow sufficient time for

vanillin to be coated onto the membrane surface as done in past studies for nanoparticle integration onto a surface [177, 178]. The physical integration of vanillin onto the surface was noted by the change in color of the active layer on the RO and FO membranes. However, the rate of QSI incorporation was not analyzed.

The next day, the membrane was placed in a high pressure cassette holder (Figure B.1) and stabilized for 24 h with sterile 0.45  $\mu\text{m}$  filtered seawater from Port Beach in Western Australia. Afterwards, overnight culture of the B2 bacterium was diluted into the feed tank (1:100). A chiller was used to maintain the temperature around 25°C during the experimental run. The feed reservoir was amended with 0.313 g/L of peptone and 0.0063 g/L of yeast to accelerate biofilm development. The system was operated at a cross flow velocity of 8.5 cm/s and pressure of 590 psi to develop a thick biofilm layer within a 24 hour period. After 4 h, the baseline bacteria concentration was taken. Every 4 h from that point, bacterial dilutions were performed to dilute back to the baseline bacteria concentration. The conductivity measurements of the feed and permeate tank were taken every 4 h to ensure the membrane was operating properly. The high pressure RO system was run in a recirculation mode. The drip permeate was collected, weighed, and recorded automatically every minute. The RO membrane was sacrificed at the end of each experiment for biofilm characterization using confocal scanning laser microscopy as described in Section 3.2.3.2.6 and 4.2.6.

The FO membrane system was kept very similar to the set up in the previous Section A.2.1. In addition, bacterial dilutions were performed as in the improved RO membrane set up. Conductivity measurements were taken of the draw and feed reservoirs to ensure the membrane was operating properly during the experimental run. The FO



membrane was scarified at the end of each experiment for biofilm characterization as well.

### B.3. Results

#### B.3.1. Flux and Biofilm Characterization for Vanillin Attached RO Membrane

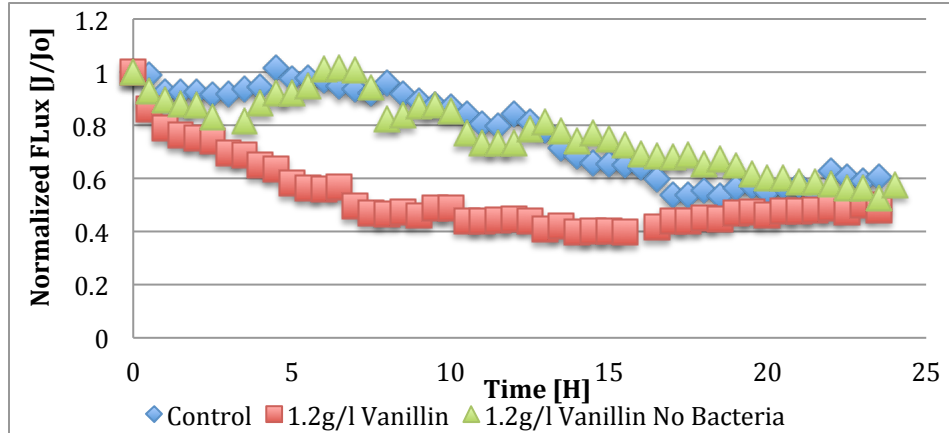


**Figure B.2.** Normalized permeate flux for RO membranes with the following conditions: control, vanillin attached, and vanillin attached without bacteria present in the feed reservoir. Normalized permeate flux was calculated as the permeate flux over the initial flux.

Figure B.2 showed that the normalized flux for the control and vanillin attached RO membranes with seeded bacteria in feed reservoir increased every 4 h due to the fresh media input, which was needed to maintain the bacteria concentration in the feed tank. The control flux experienced a severe decline in permeate flux around 15 h due significant biofilm formation on the membrane surface as indicated by the confocal data in Figure B.3A. The physically attached vanillin membrane without bacterial addition experienced similar trends in permeate flux with the control (Figure B.2). The vanillin incorporated membrane along with B2 seeded in the feed tank experienced a faster onset of fouling than the control or the vanillin attached membrane without B2 as indicated by the flux decline (Figure B.2). This was potentially due to vanillin de-attaching from the membrane surface

under high pressure conditions, which then caused vanillin to act as an organic foulant. The normalized permeate flux for the vanillin attached RO membrane without any bacterial foulant in the system indicated that vanillin on the membrane surface was not stable (Figure B.2).

Confocal data demonstrated that there was a 35% reduction of membrane biofilm thickness for the vanillin attached membrane compared to the control membrane. The 3D images showed that the majority of cells distributed onto the membrane surface were live for both control and vanillin treated membranes in the 24 h period (Figure B.3). In addition, there was a slight increase in live cells distributed on the vanillin attached RO membrane as indicated by the fluorescence intensity (z-axis) in Figure B.3.

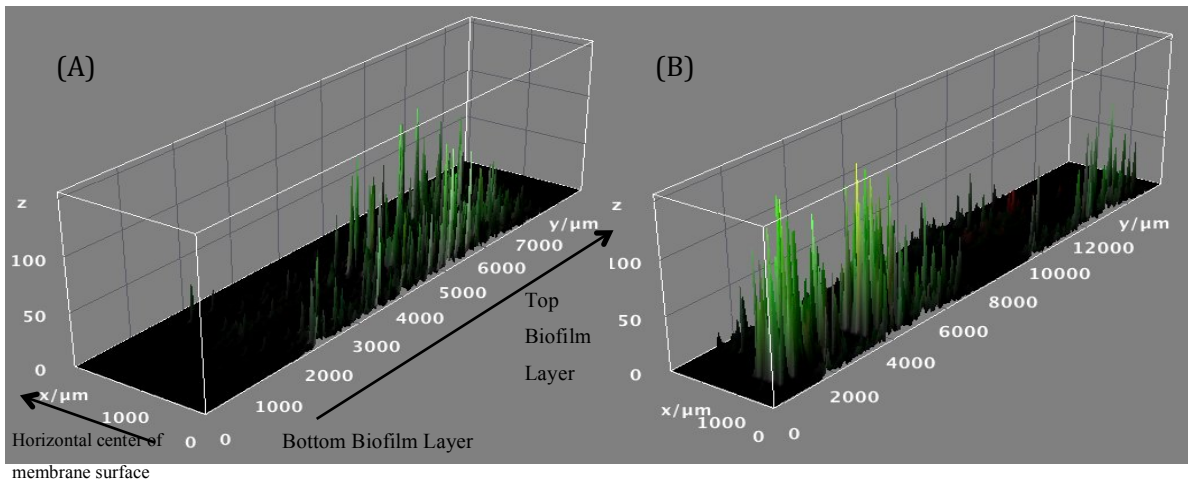


**Figure B.3.** 3D Comparison of single species biofilm formation on the surface of the RO membrane (A) and physically attached vanillin RO membrane (B). The 3D image is composed of multiple layers of biofilm, which are approximately 1000  $\mu\text{m}$  in height. ImageJ automatically determines the dimensions of the y- and x-axis. The y-axis represents the bottom to top layer of the biofilm and the x-axis refers to bottom biofilm layer along the horizontal center of the membrane surface. The z-axis measures the fluorescence intensity of the live and dead cells.

### B.3.2. Flux and Biofilm Characterization for Vanillin Attached FO Membrane

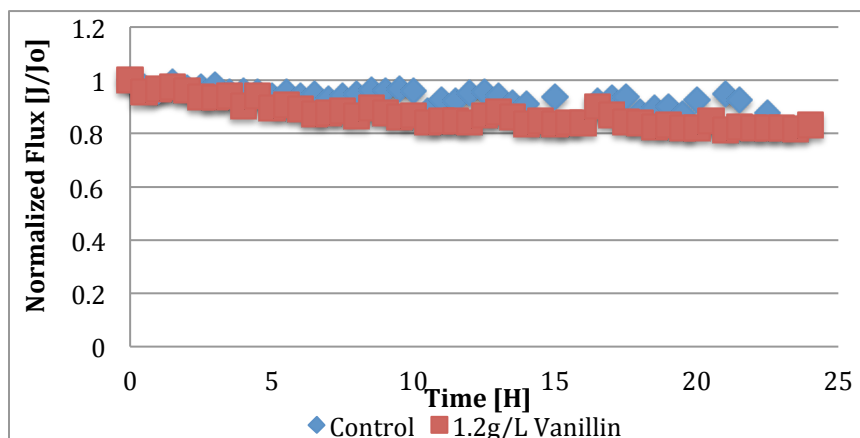
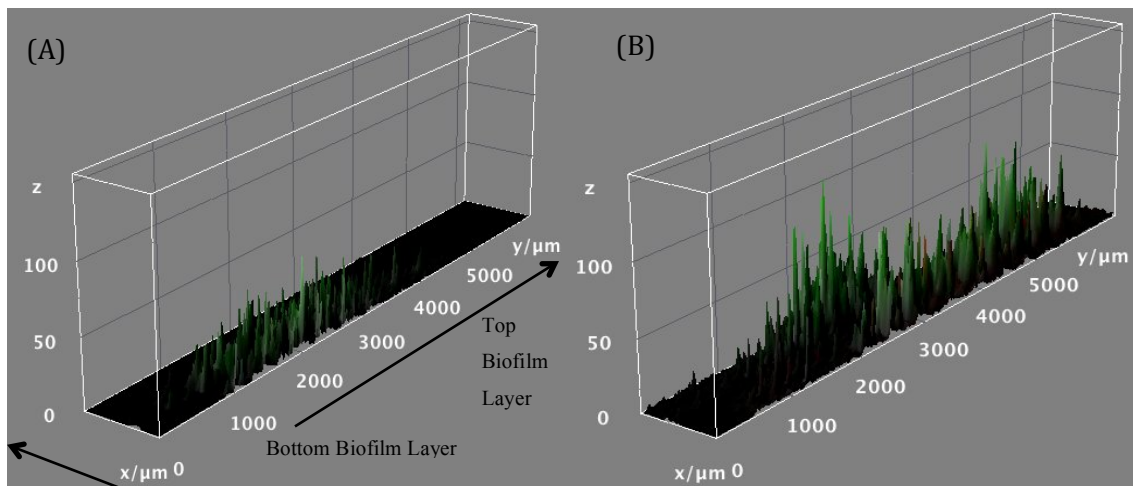


**Figure B.4.** Normalized flux for control and vanillin attached FO membranes. Normalized flux was measured as the permeate flux over the initial flux.

The normalized permeate flux for both the control and physically attached vanillin FO membranes were relatively stable during the experimental period (Figure B.4). Confocal data revealed that the percent of biofilm thickness reduced by approximately 10% for the vanillin incorporated membrane compared to the control. The 3D images displayed the live and dead cell distribution onto the control and vanillin treated FO membrane surfaces for the lead membrane section only (Figure B.5). On the lead membrane section, the vanillin attached membrane had an increase in live cells compared to the control membrane. There were no significant biofilm formation on the middle and tail end of both FO membranes.



Horizontal center of membrane surface

**Figure B.5.** 3D Comparison of biofilm formation on the lead FO membrane (A) and physically attached vanillin FO membrane biofilm (B). The 3D image is composed of multiple layers of biofilm, which are approximately 1000  $\mu\text{m}$  in height. ImageJ automatically determines the dimensions of the y- and x-axis. The y-axis represents the bottom to top layer of the biofilm and the x-axis refers to bottom biofilm layer along the horizontal center of the membrane surface. The z-axis measures the florescence intensity of the live and dead cells.

#### B.4. Conclusions and Recommendations

Overall, the permeate flux over the biofouling period for the control and vanillin attached FO membranes were relatively stable as indicated by the thin layer of biofilm on both membrane surfaces. For both FO and RO systems, vanillin attached membranes experienced an increase in live cells. However in the presence of the high pressure RO system, the vanillin treated RO membrane was not stable as indicated by the permeate flux with and without bacterial addition. Future work should explore chemically linking vanillin to the membrane surface to improve vanillin stability on the RO membrane surface.